on Observation Techniques

from space in support of climate change studies

Pierluigi Silvestrin

pierluigi.silvestrin@esa.int

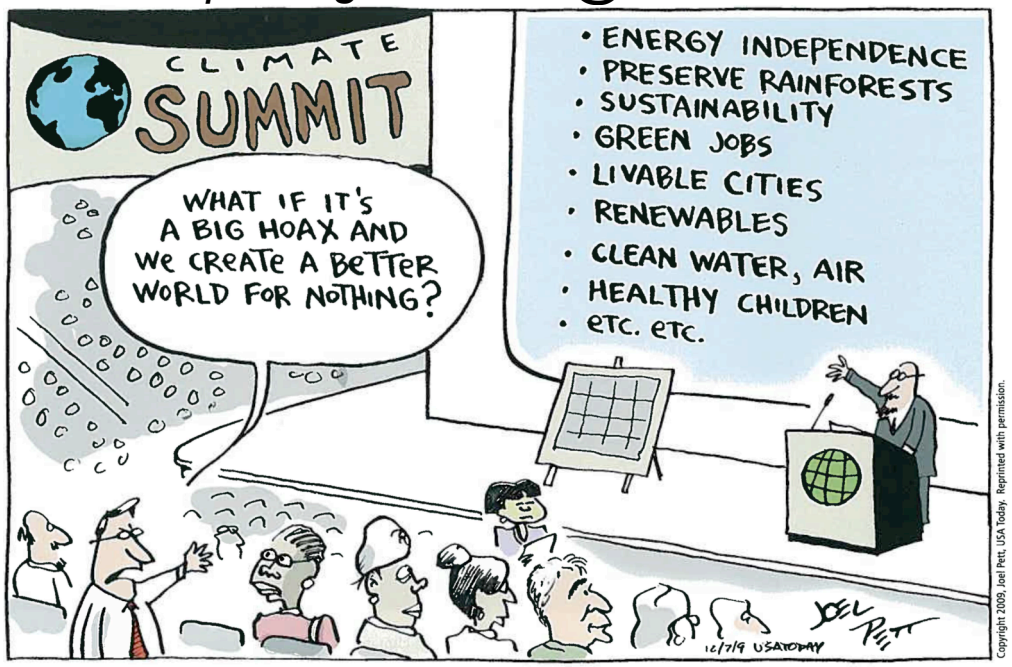

Outline

- general considerations (definitions, principles, geometries,..)
- passive remote sensing:
  - microwave radiometry incl. aperture synthesis
  - a (climate-oriented) example in infrared radiometry
- active remote sensing:
  - atmospheric sounding by occultation of GNSS signals
  - synthetic aperture radars
- other mission examples:
  - optical observations for land, examples specific to biosphere

Some of the EO Challenges (excerpt)

OCEANS – 1 A						
Scientific Challenges		**New Observations**	**Technology Challenges**	**Missions flown / in operation / *under development***	**International Context**	**Missions proposed in EE proposals**
Ocean general circulation	Mesoscale circulation; Western boundary currents	Global absolute sea-level altimetry referenced to high-resolution geoid; high spatial/temporal resolution altimetry; Gravity variations Combination of scatterometer and altimeters GNSS reflectometry	Wide-swath altimeters: ultra-stable interferometric baseline, precise attitude estimation, calibration; on-board processing Constellations of low-cost miniaturised altimeters, High resolution scatterometry GNSSR performance demonstration	Envisat GOCE; *GMES Sentinel-3 altimetry;* *AltiKa, CFOSat (ex-SwimSat);* *Cryosat-2*	Oceansat 3 (India) AltiKa on SARAL Jason-2, *-3, -CS*	EE8 (GNSS-R)
Currents	Spatial patterns in surface currents; Absolute magnitudes and dynamics	Along-track SAR interferometry; SAR Doppler processing	Antenna technology; on-board processing; scan-on-receive and other technologies for wide swath;	Envisat, Jason-2, *-3, -CS*		WATER (EE7 commended by ESAC)
Coastal winds	High spatial resolution coastal winds	High-resolution scatterometry; wide-swath SAR-derived winds	scan-on-receive and other technologies for wide swath; high sensitivity SAR systems; high resolution scatterometry; retrieval algorithms	MetOp ASCAT *Post-EPS SCA* *GMES Sentinel-1*	Oceansat-2, -3 (India)	
Ocean bottom pressure	Barotropic vs. baroclinic circulation components	High-resolution, gravity variations	Laser interferometer; drag-free technologies; high resolution altimetry	GOCE, GRACE, *LISA, LPF*	Jason-2, -3, -CS	(see under solid Earth)

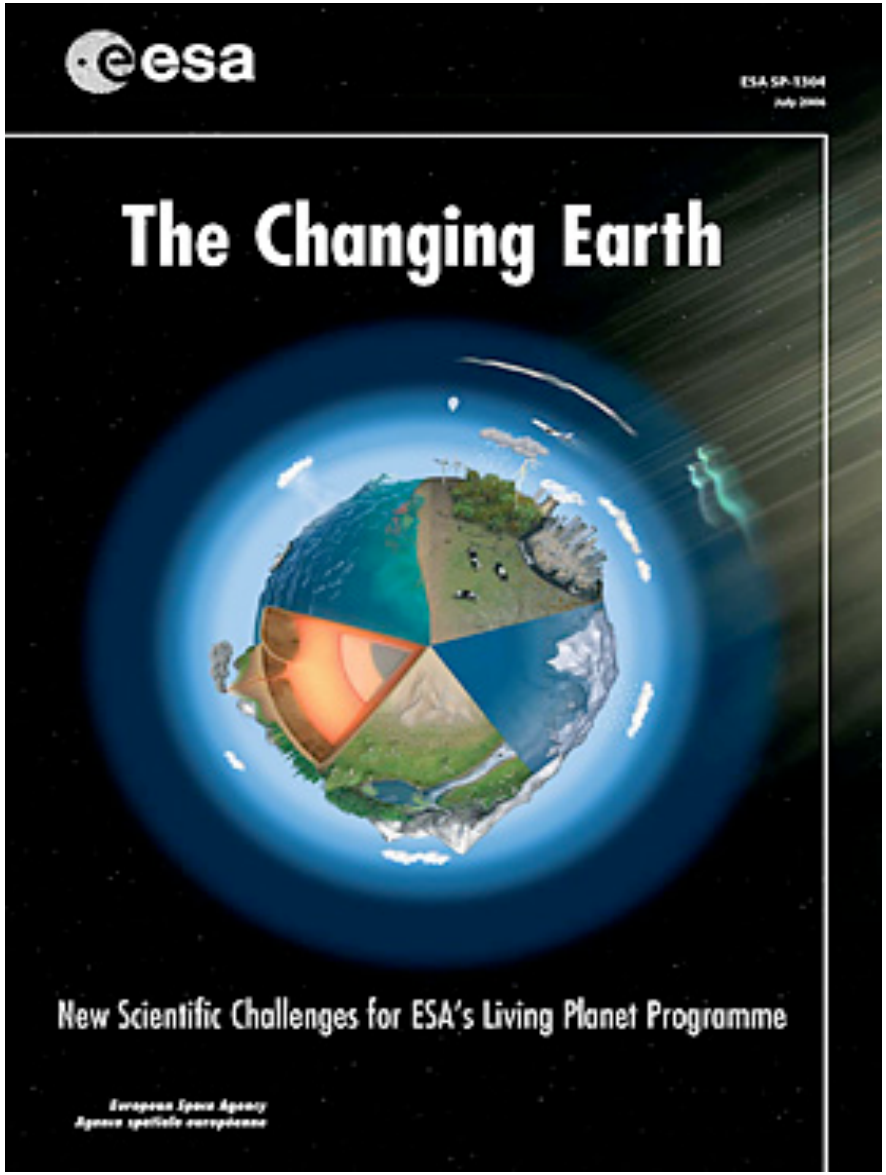

ESA SP-1304 (2006), available from www.esa.int

- **Observing the Earth**
- **Living Planet Programme**
- **Earth Explorers**

Earth Observation and Remote Sensing

Remote sensing:

acquisition of information about an object or phenomenon without being in physical contact with it by detecting and measuring changes that the object or phenomenon imposes on the surrounding electromagnetic or potential field

Role of **potential fields** (gravitation, magnetic) not to be neglected (but not addressed here)

Is all EO carried out through remote sensing (RS)? No, but vast majority is: in-situ space EO sensors, e.g. Swarm's Lagmuir probe, are rare

MODELS AND OBSERVATIONS

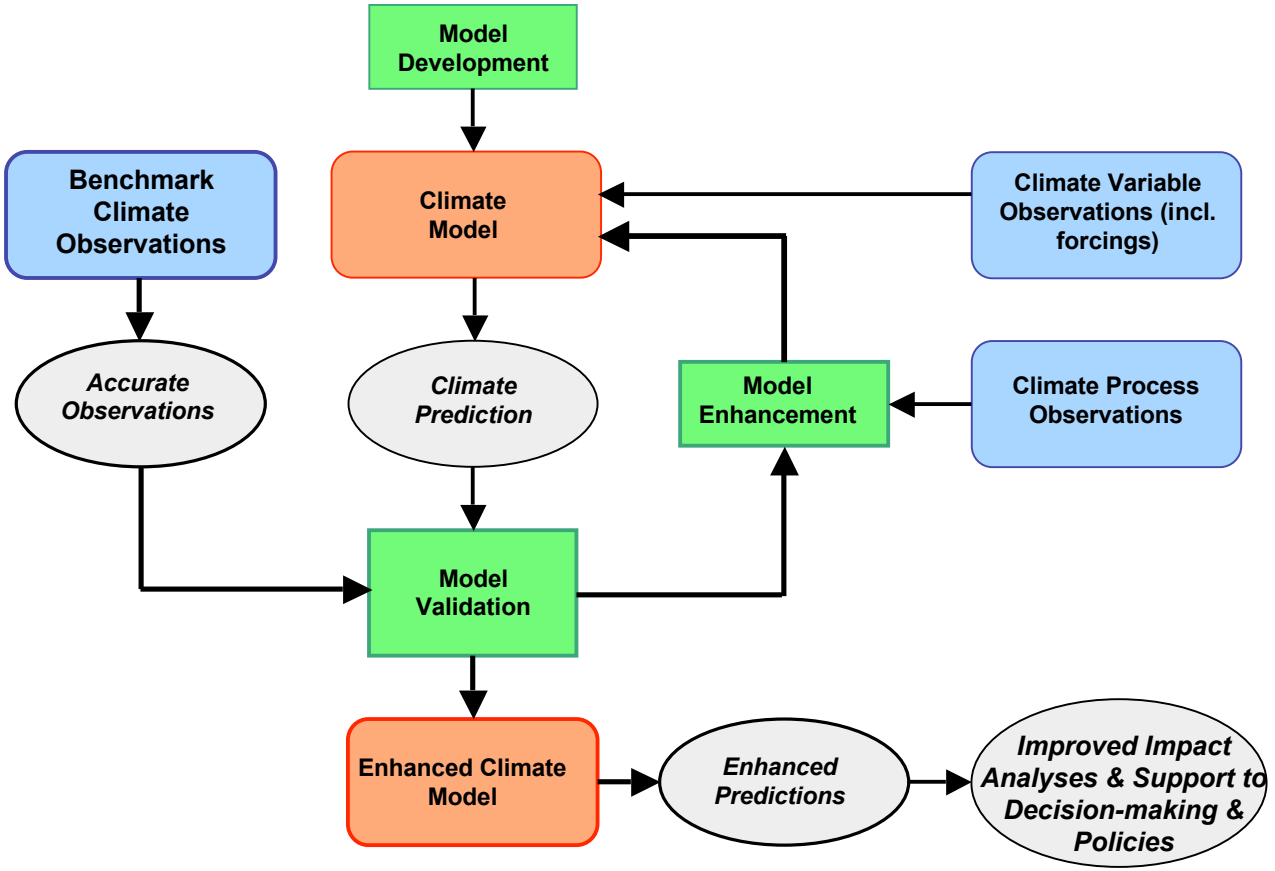

Remote sensing data used to

- develop and improve climate models
- determine climate evolution until today as initial point for predictions
- measure directly key climate change parameters to high, well controlled accuracy (climate benchmarking)

why use Remote Sensing from space?

- only way to observe a wide range of geophysical parameters on a global or quasi-global scale (synoptic view) to good (and characterisable) accuracy in a consistent repeatable manner
- high spatial resolution (up to 3D) and high temporal resolution achievable (though costly to reach simultaneously) over vast areas
- can measure at locations of the Earth system impossible or difficult to access (with all-weather day-night capability for microwave sensing)
- can measure at same time several parameters and in synergy
- can be highly automatic, from acquisition to exploitation
- on a per-measurement basis, usually far less expensive than any other means

some caveats..

- remote sensing measurements are indirect measurements
- observed signal is always affected by more effects than just the one aimed at with the measurement (but often what's noise to one, it's signal to another.. new techniques often prove useful also to 'unplanned' user communities)
- additional assumptions and models are needed for the interpretation of the measurements, e.g. to calibrate sensor, to remove perturbing effects,..
- the area / volume of the intended target of the measurement is often relatively large (representativity issue, e.g. surface heterogeneities)
- validation of remote sensing measurements can be a major task, often not possible in optimal way
- estimation of the errors of the data products can be difficult

example: radar altimetry for ocean circulation and sea level studies

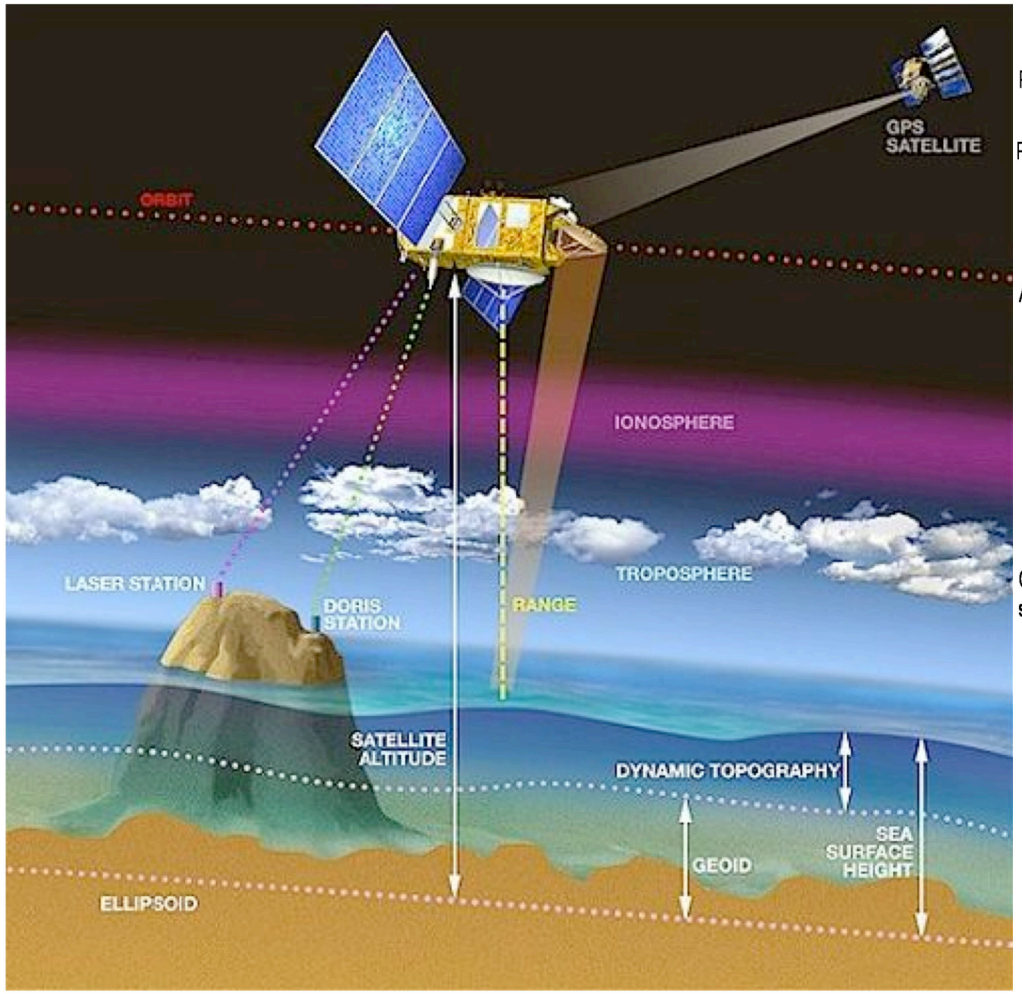

Phase delay of individual measurement	Radar altimetry design by radar engineering
Phase delay of integrated measurement	Radar altimetry integration time by radar engineering
Ionosphere delay corrections	Ionosphere model and altimeter dual frequency by radar engineering and geophysics
Atmospheric humidity delay corrections	Atmosphere humidity model and on-board microwave radiometer by microwave engineering and meteorology
Dry atmosphere delay correction	Atmospheric pressure and temperature model by meteorology
Dry atmosphere sea level correction	Atmospheric pressure and temperature model by meteorology
Sea state bias level correction	Waves model and backscatter ocean behavior model by oceanographers and ocean radiation interaction
Correction for true position of the GNSS satellites and true position of the satellite	On-board navigation payload, GNSS satellite ephemeris and precise orbit determination by orbital mechanics engineering
Dynamic topography correction	Ocean geoid model by geodesy
Tides aliasing correction	Tides modelling by oceanography and geophysics
Multiple satellites correction	Multiple satellite constellation modeling by multidisciplinary teams
Final ocean currents recovery performance	Ocean circulation model by oceanography

calibration and validation are paramount for meaningful long-time series

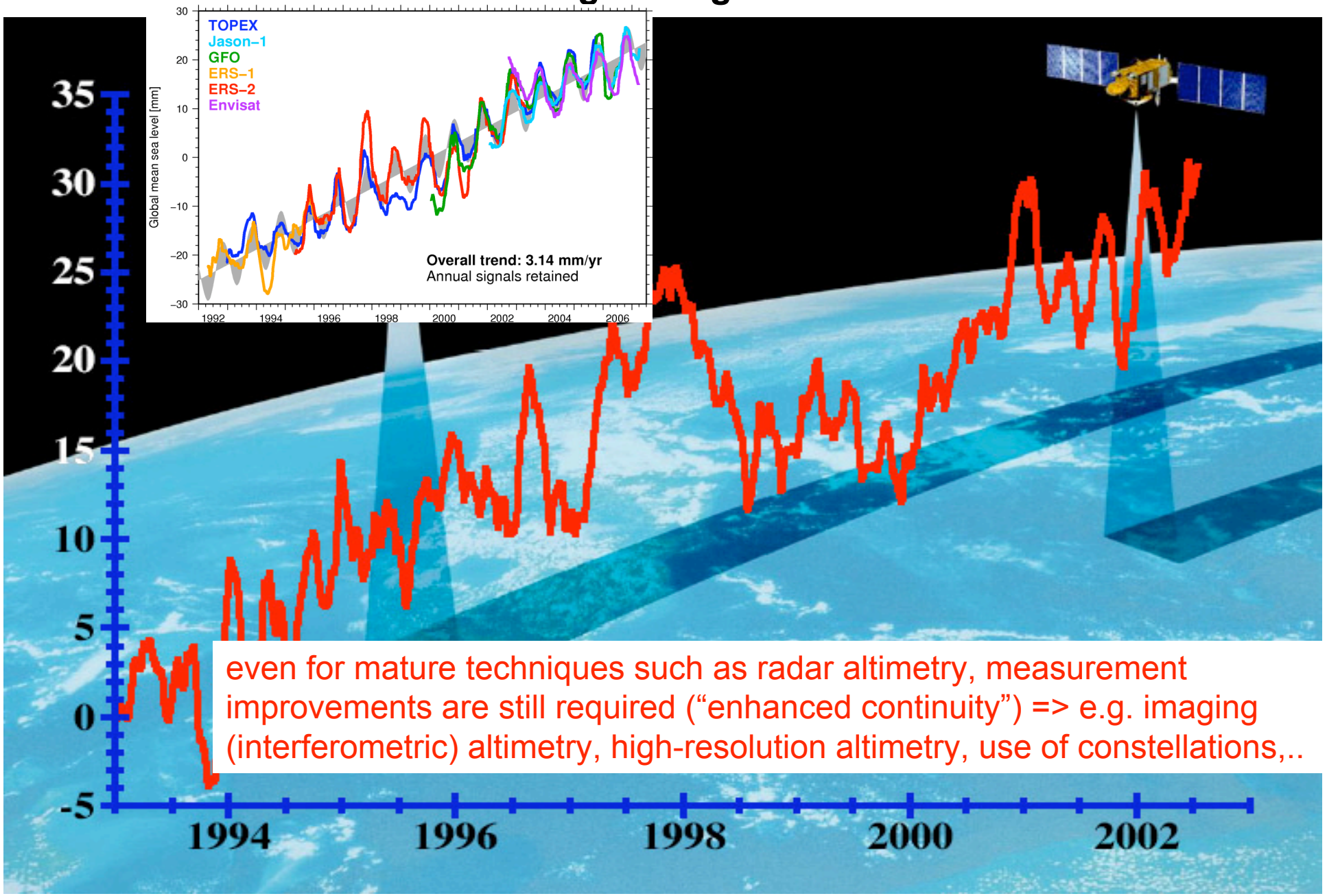

even for mature techniques such as radar altimetry, measurement improvements are still required (“enhanced continuity”) => e.g. imaging (interferometric) altimetry, high-resolution altimetry, use of constellations,..

a detour.. ocean altimetry over a swath

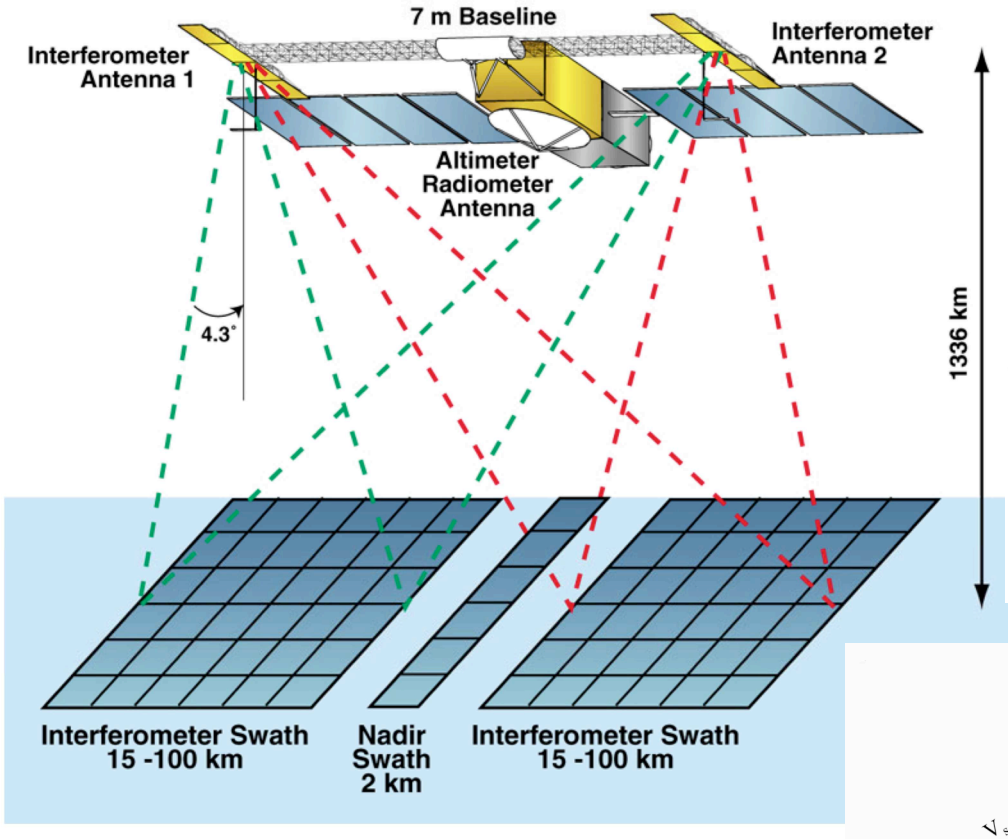

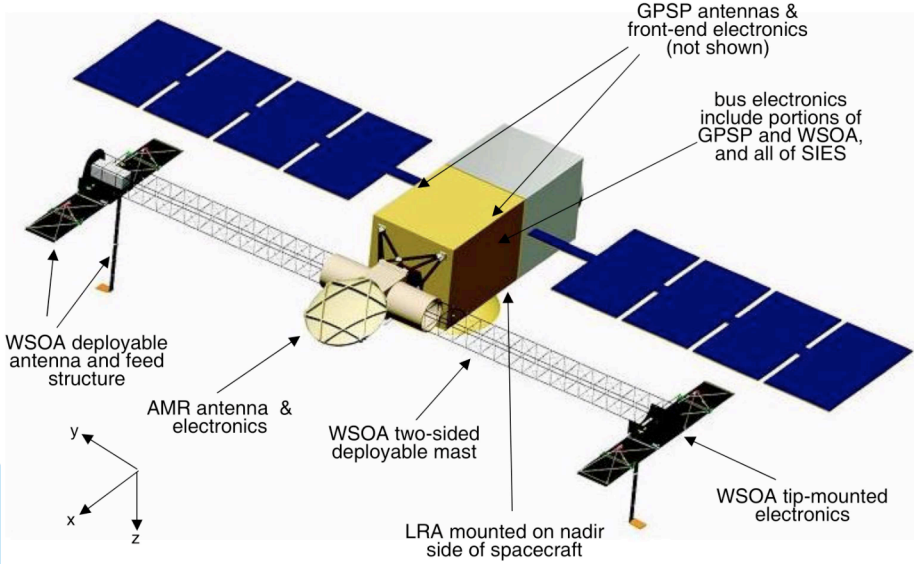

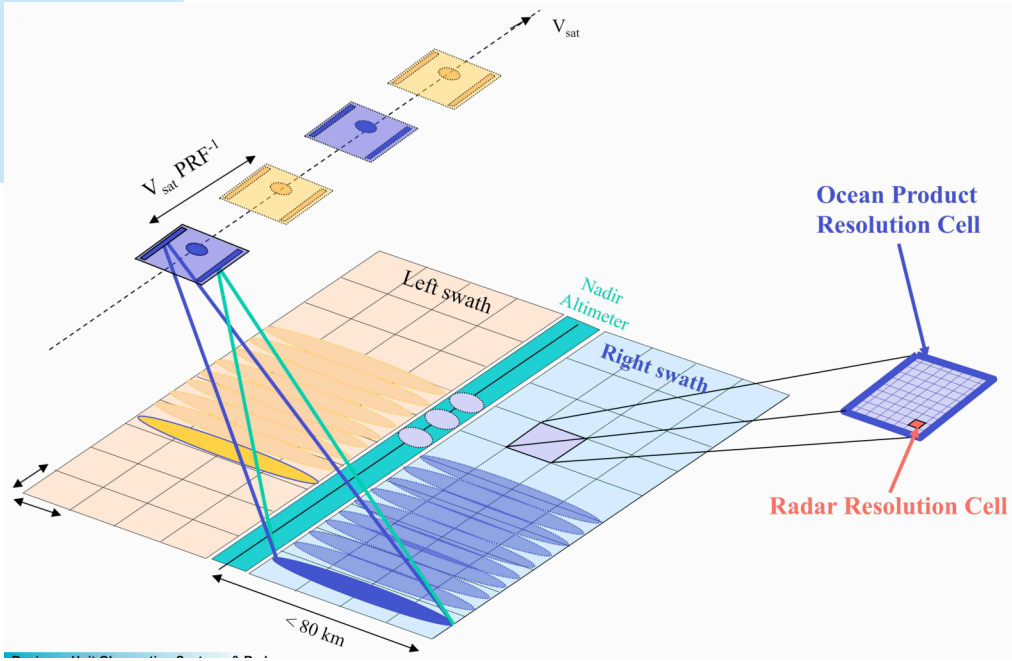

geometry of the measurement

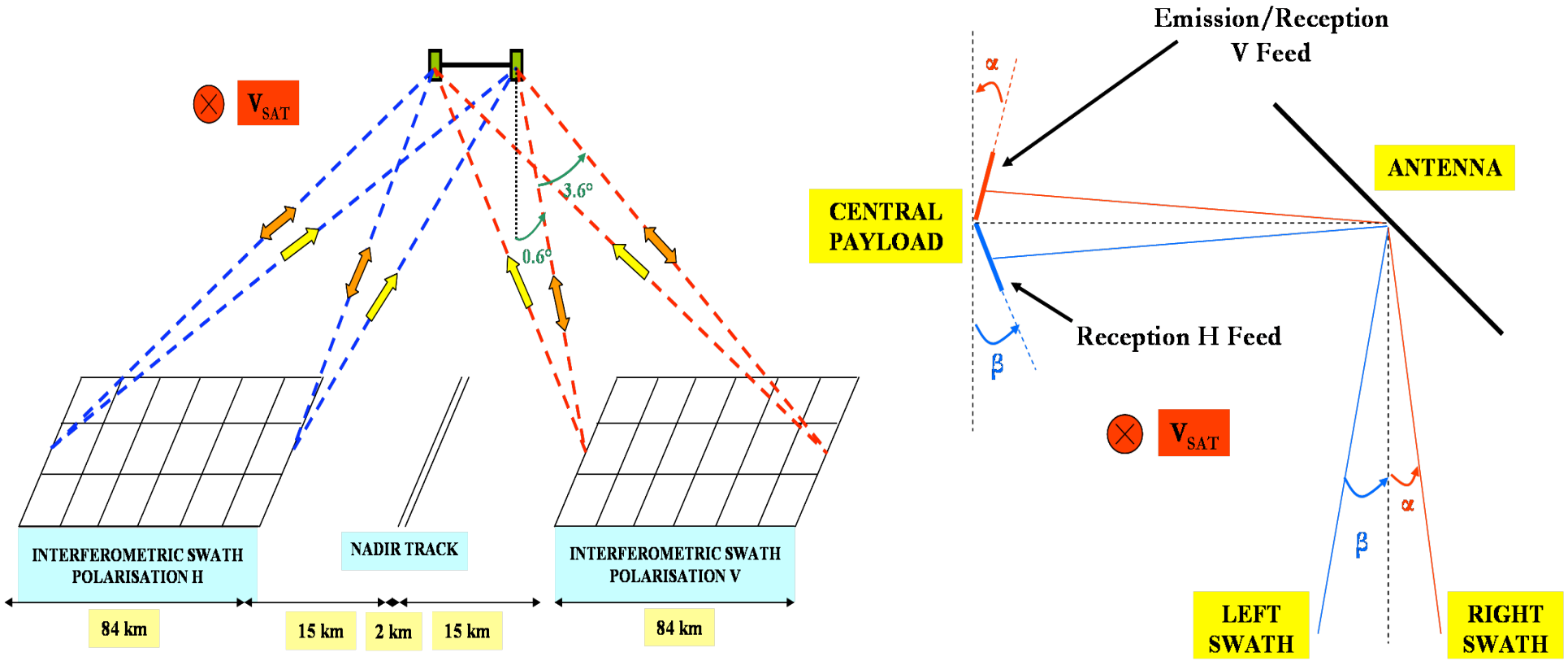

- later (?) design: off-nadir dual-polarisation observation by two passive antennas
- low look angles: compromise between a wide swath and good signal power return
- both swath accesses done with the feed positions

swath altimetry: basic error analysis

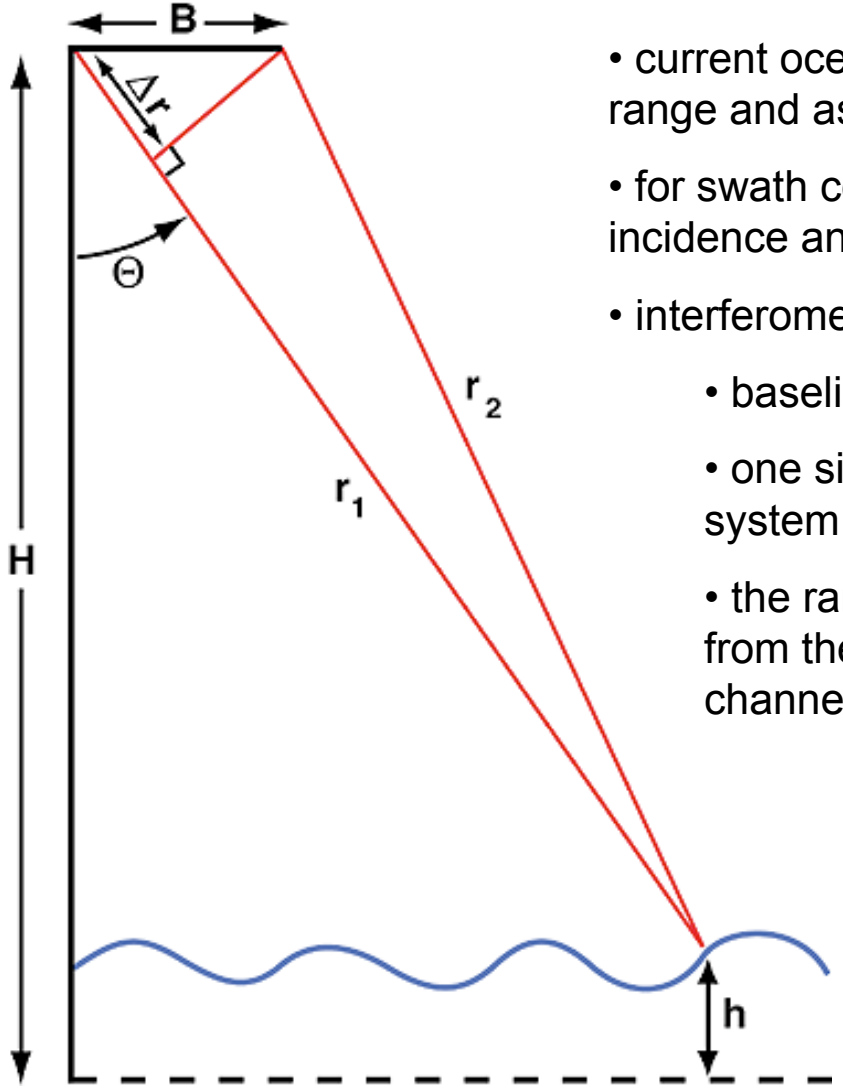

- current ocean altimetry (excl. Cryosat) measures a single range and assumes the return is from the nadir point
- for swath coverage, additional information about the incidence angle is required to geo-locate the return signal
- interferometric altimetry uses basically triangulation
  - baseline B forms base (must be ultra-stable)
  - one side, the range accuracy is ensured by the system timing accuracy
  - the range difference between two sides is obtained from the phase difference between the two radar channels:

$$\Phi = 2\pi \Delta r/\lambda = 2\pi B \sin\theta/\lambda$$

$$h = H - r\cos\theta$$

$$\delta h = r \sin\theta\, \delta\theta = y\, \delta\theta$$

observed electromagnetic (EM) quantities

- absolute intensities in specific wavelength intervals
- intensities relative to the intensity of a reference source at same wavelength
- ratios of intensities at different wavelengths
- variations of intensities
- degree of polarisation
- field amplitude and phase
- phase and group delays
- variations of these delays
- Doppler shift
- spectra
- ..

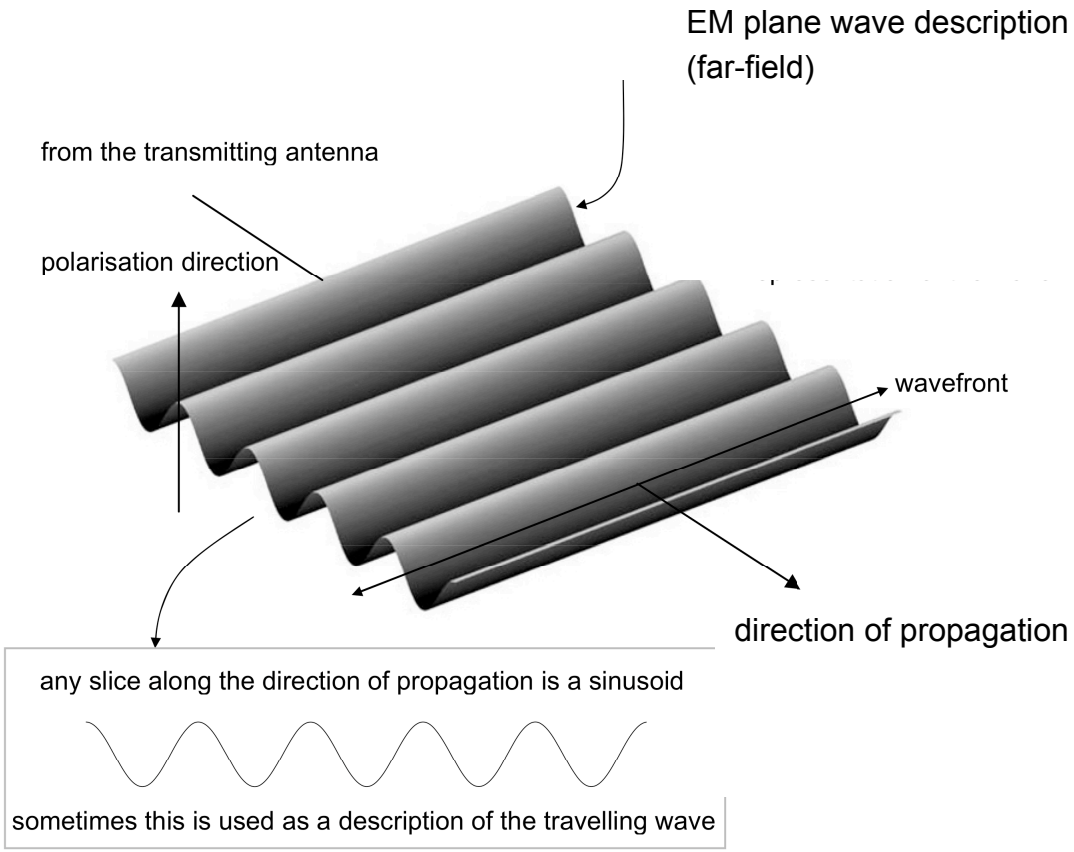

the RS information triangle

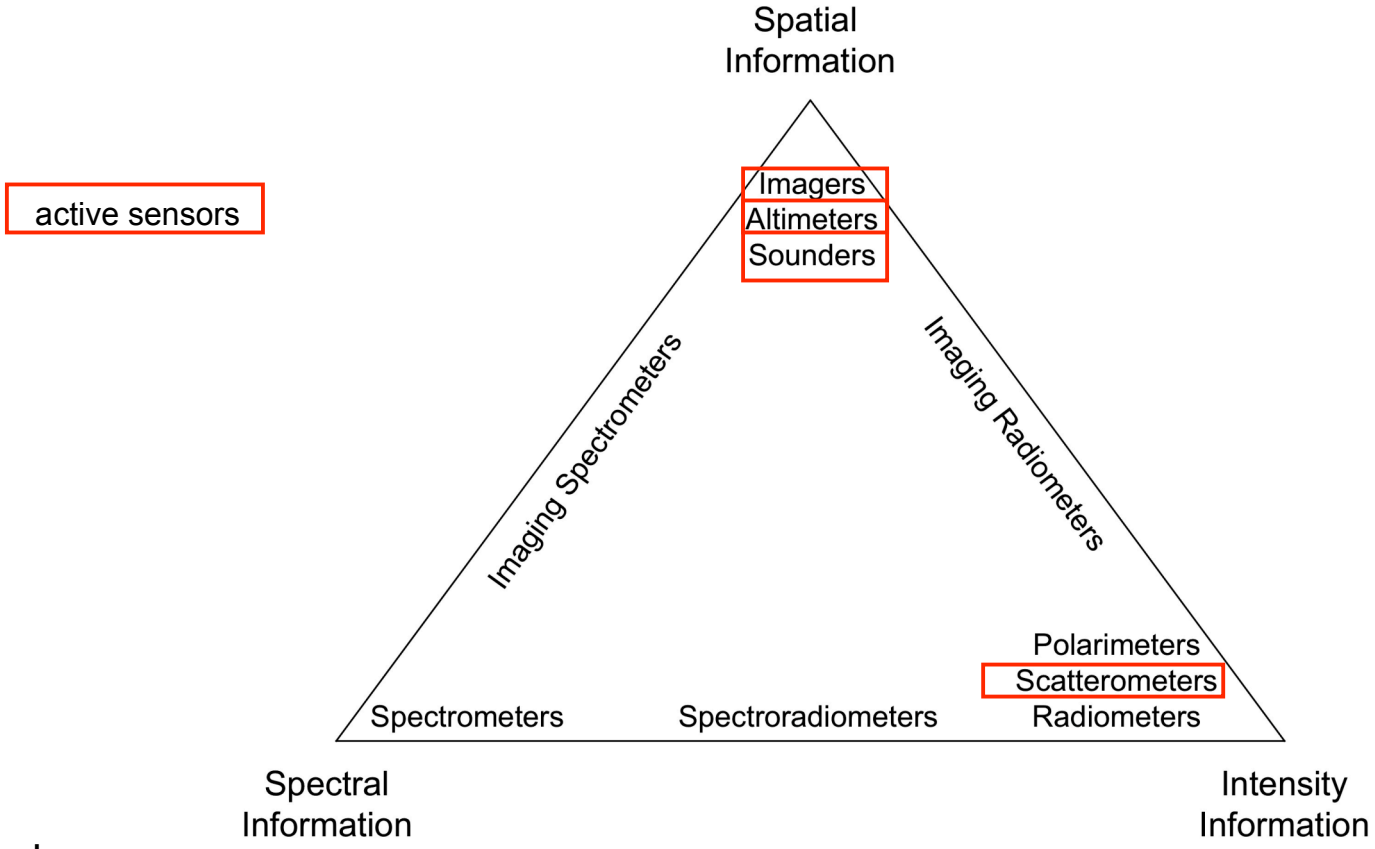

include:
- specialised radars for sounding clouds, precipitation,,..
- lidars for doppler wind, cloud and atmospheric composition sounding
- atmospheric sounding by occultation

- information value increases quickly when more information ‘types’ are combined

- future sensor types based on emerging technologies may require modifying this diagram

remote sensing information vs. sensor type

Type of information needed	Type of sensor
High spatial resolution and wide coverage	Imaging sensors (active and passive), cameras
High spectral resolution over limited areas or along track lines	Spectrometers, spectro-radiometers
Limited spectral resolution with high spatial resolution	Multispectral imagers/mappers
High spectral and spatial resolution	Imaging spectrometers
High-accuracy intensity measurement along line tracks or wide swath	Radiometers, scatterometers
High-accuracy intensity measurement with moderate imaging resolution and wide coverage	Imaging radiometers
High-accuracy measurement of location and profile	Altimeters, sounders
Three-dimensional topographic mapping	Scanning altimeters, radar interferometers, stereoscopic cameras

generic sensing concept

- monostatic vs bistatic (active) sensing

- use of constellations and formations of orbiting sensors

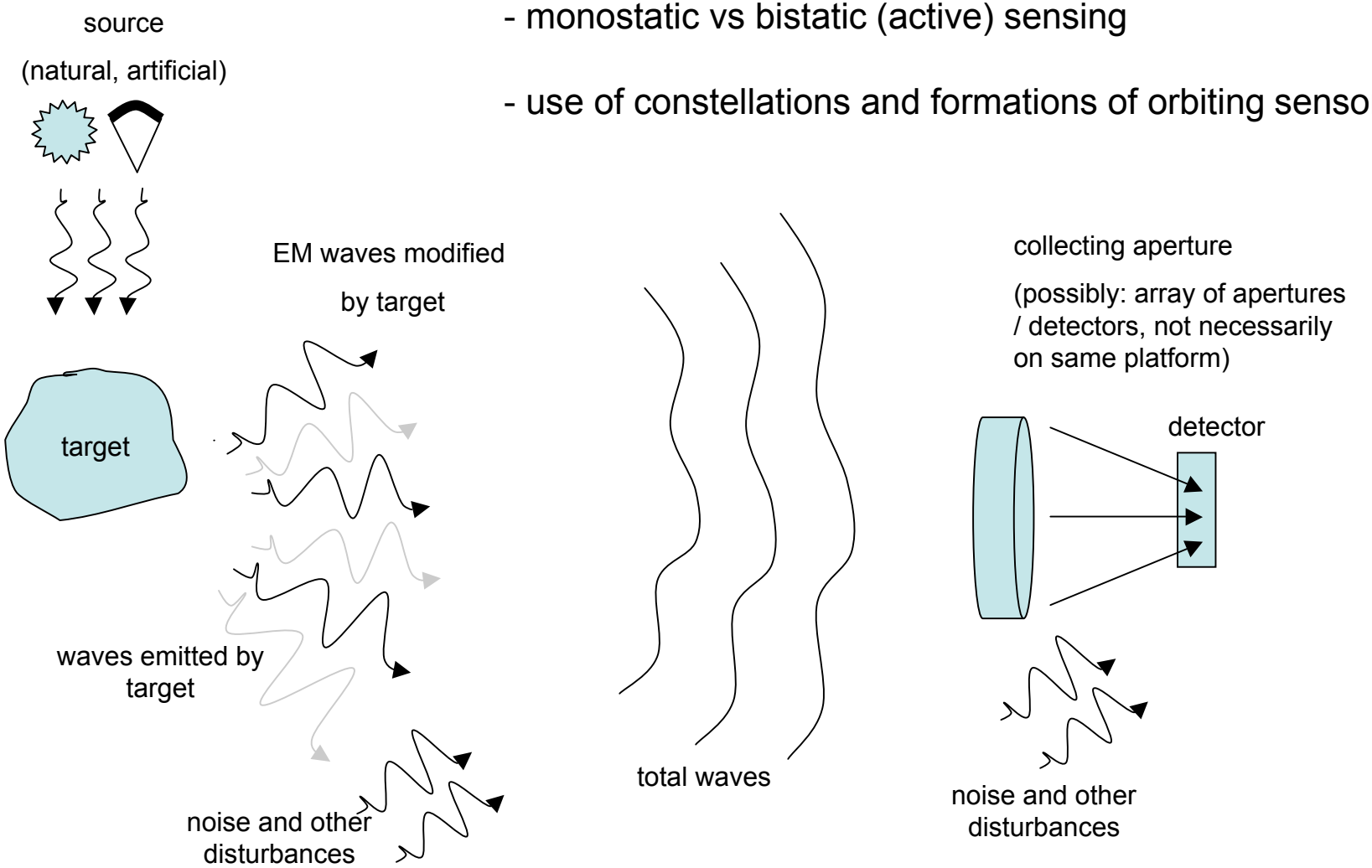

formations and ‘convoys’ for EO

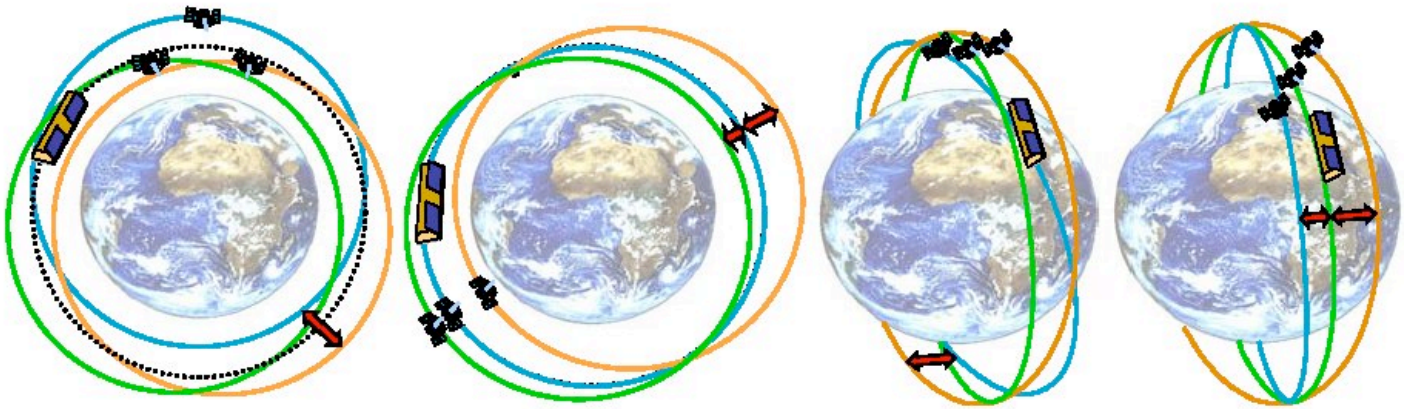

examples of formation configurations: cartwheel, two-scale cartwheel, cross-track pendulum and bi-nodal pendulum (cf. also TerraSAR-X/Tandem-X in DLR web site)

as long-term in-orbit ‘infrastructure’ to build upon

Sentinel 1 – SAR imaging
All weather, day/night applications, interferometry

2012 A / 2015 B

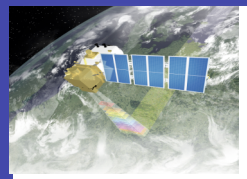

Sentinel 2 – Multi-spectral imaging
Land applications: urban, forest, agriculture,..
Continuity of Landsat, SPOT

2013 A/ 2016 B

Sentinel 3 – Ocean and global land monitoring
Wide-swath ocean color, vegetation, sea/land surface temperature, altimetry

2013 A/ 2017 B

Sentinel 4 – Geostationary atmospheric
Atmospheric composition monitoring, trans-boundary pollution

2018+

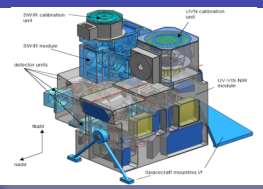

Sentinel 5 – Low-orbit atmospheric
Atmospheric composition monitoring
(S5 Precursor launch in 2014)

2019+

observation geometries

- (near) nadir: whiskbroom (single / multi-element), pushbroom, scanning (across-track, conical,..),..

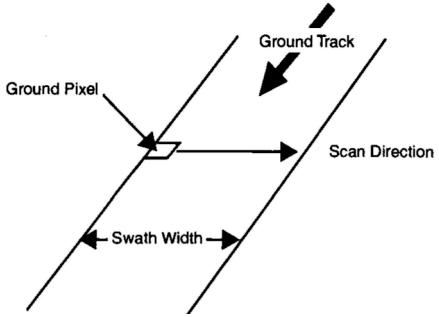

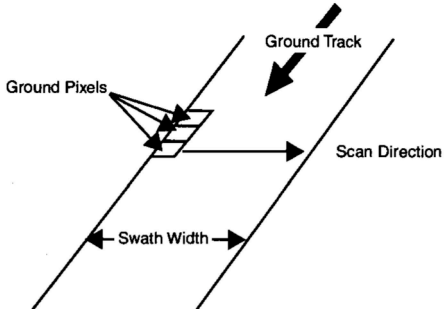

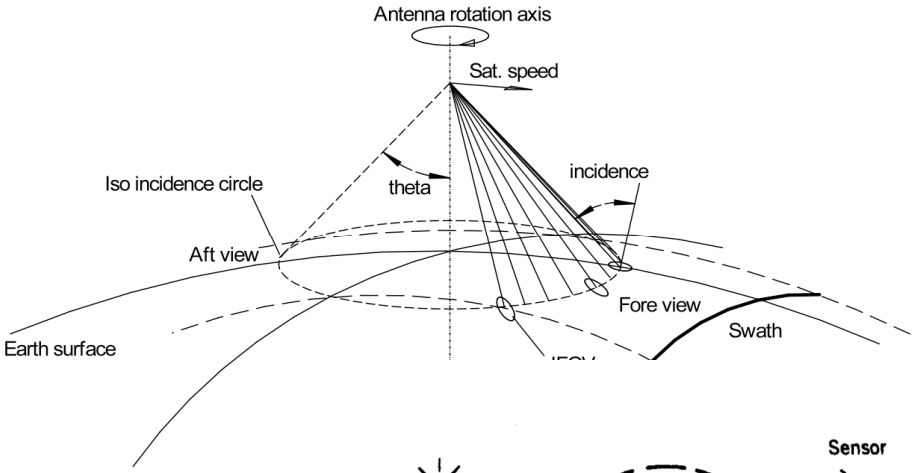

- limb
- other side-looking (with agility, for e.g. BRDF)
- off-nadir access through interferometric processing

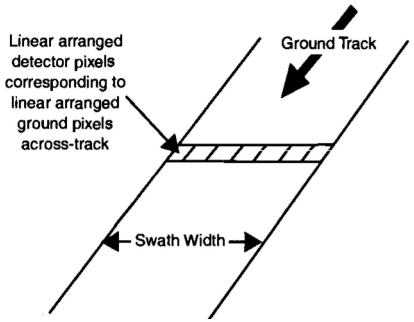

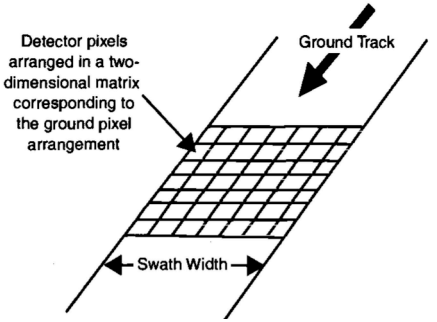

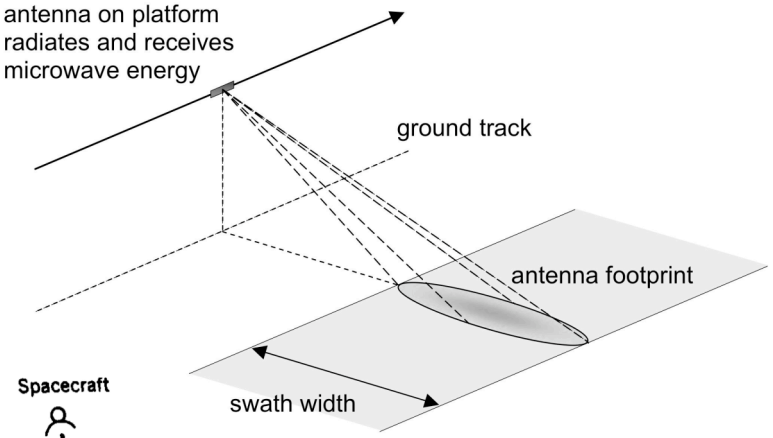

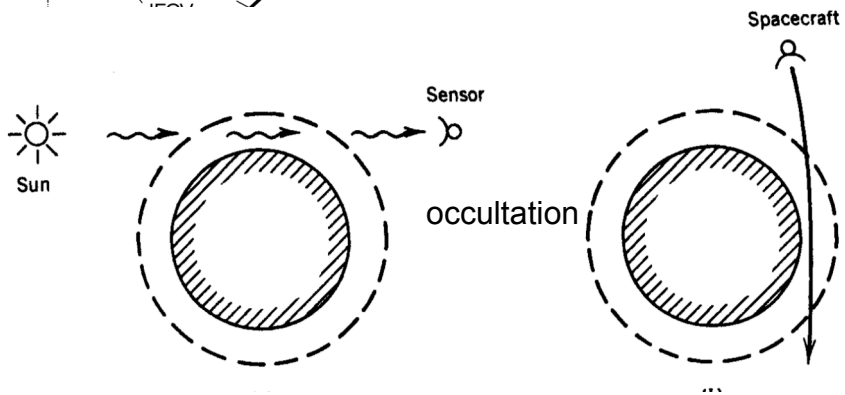

example of limb observations and 'formation': PREMIER

(PRocess Exploration through Measurements of Infrared and millimetre-wave Emitted Radiation)

- Target trace gases:

  infrared: CH_4; organic compounds; nitrogen oxides

  mm-wave: CO; HCN & CH_3CN (biomass burning indicators); halogens

- Sensitivity to cirrus particle size

  IR: R_e < 100μm

  mm-wave: R_e >100μm

→ different penetration depths into troposphere for H_2O, O_3 & other trace gases measured in both spectral regions

nadir-sounding

- near-surface layer seen between clouds *but*
- little or no vertical resolution

limb-emission sounding

- High res. vertical profiling
- Tenuous trace gases detectable
- Cold space background
- Dense coverage cf solar occultatio

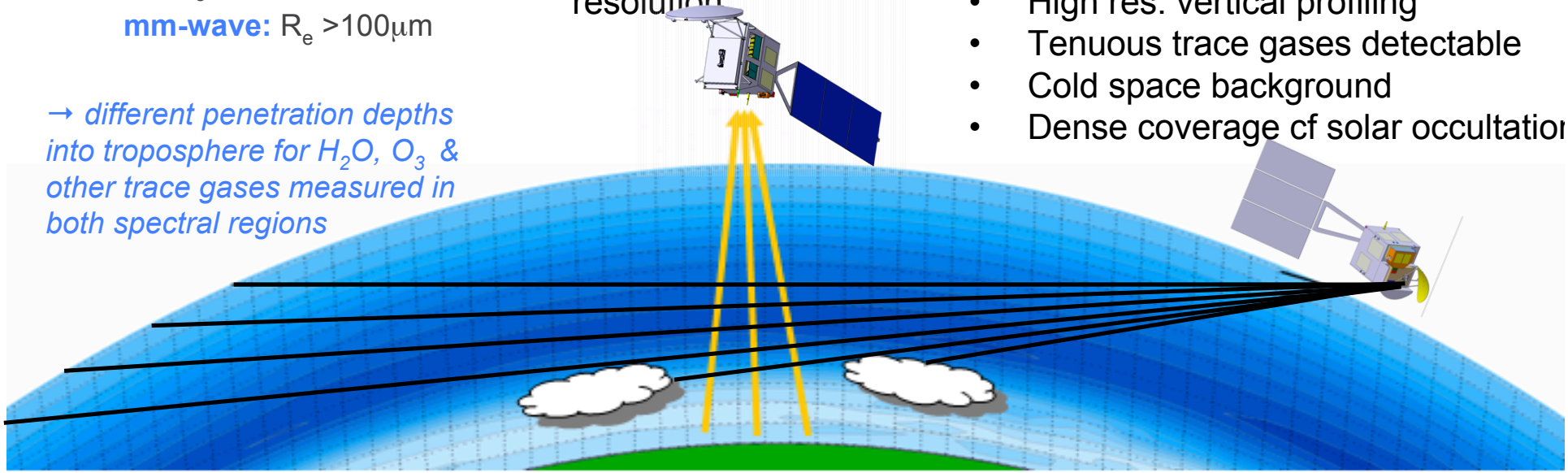

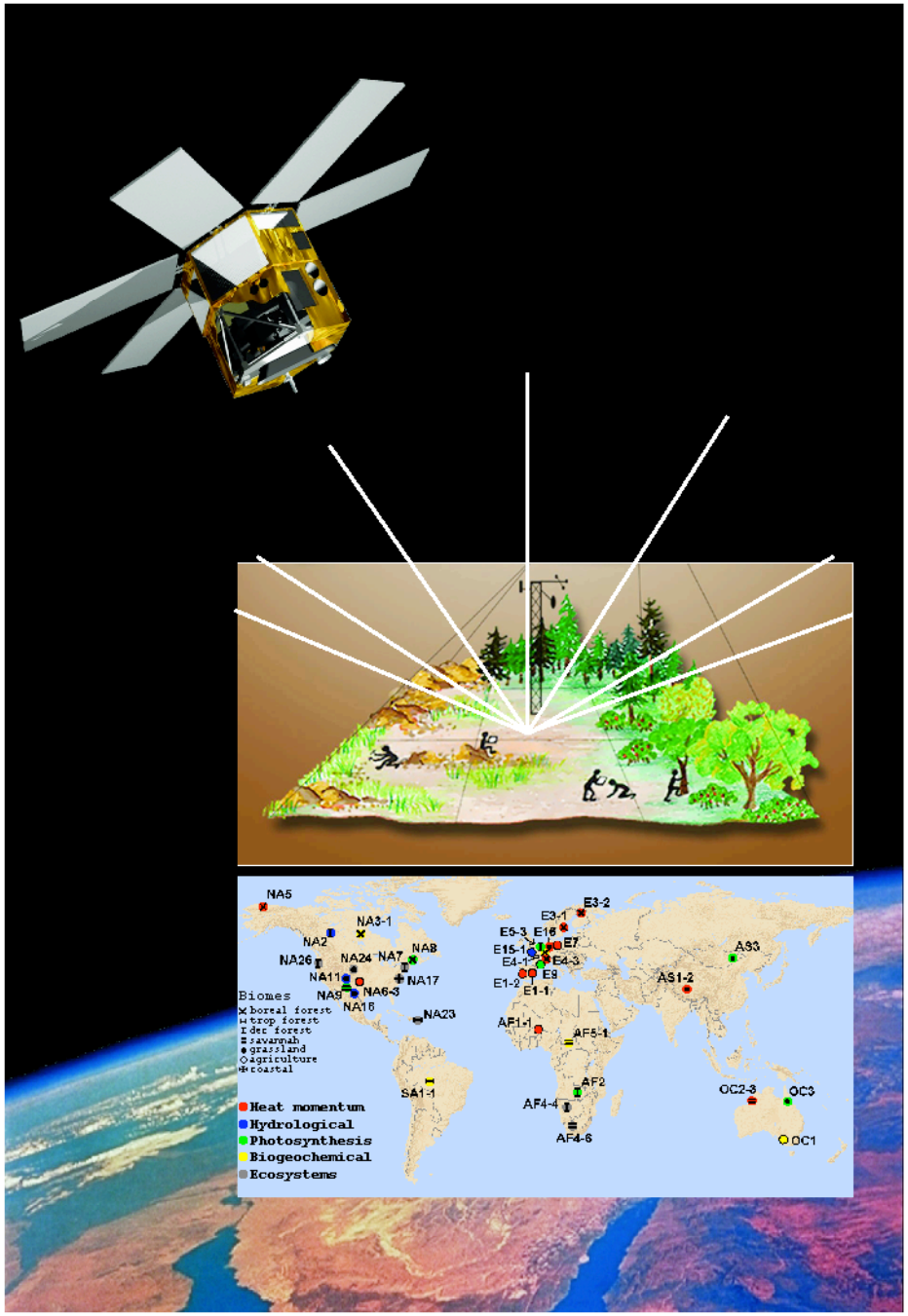

example of access with 'agility': land bi-directional reflectance distribution function (BRDF) hyper-spectral observations

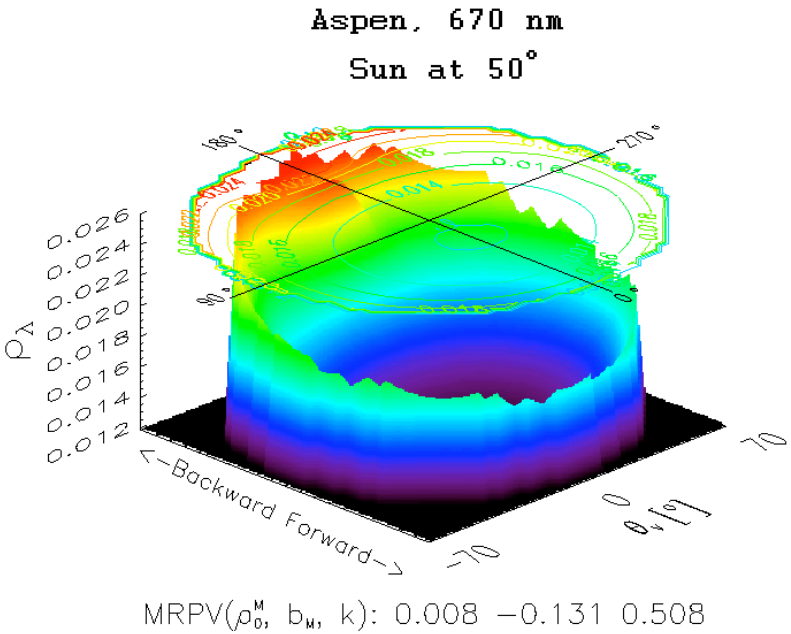

The ElectroMagnetic Spectrum

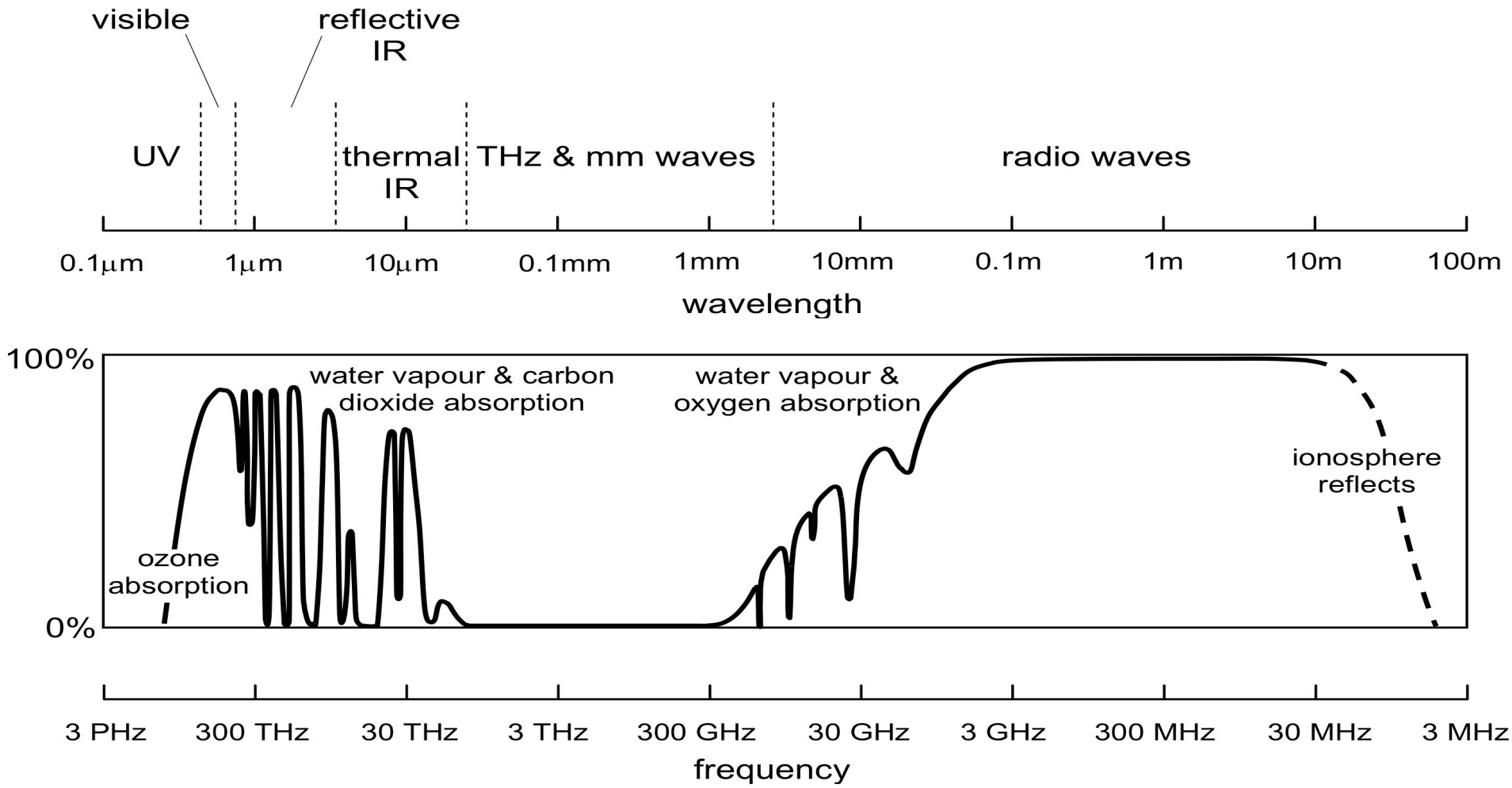

interactions vs. spectral regions

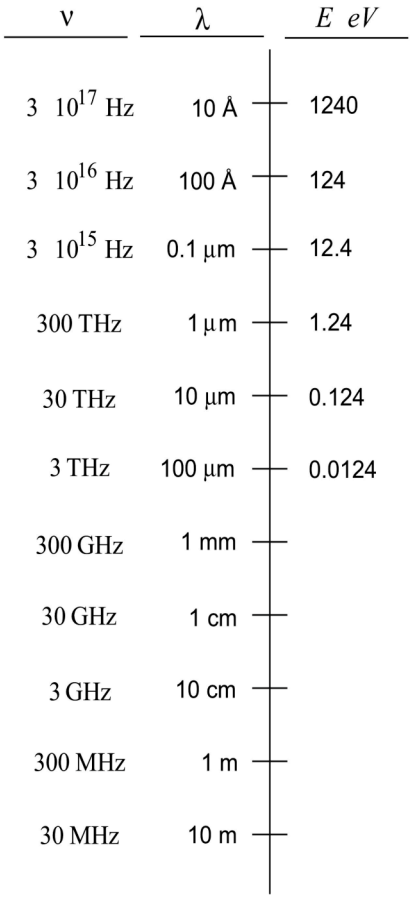

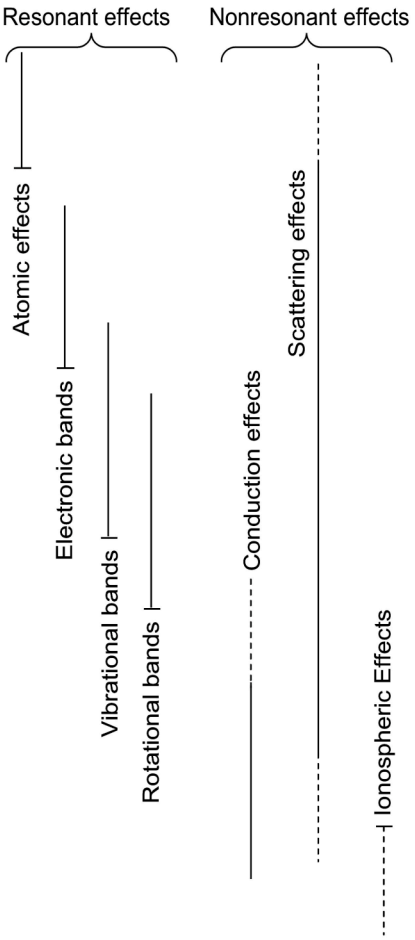

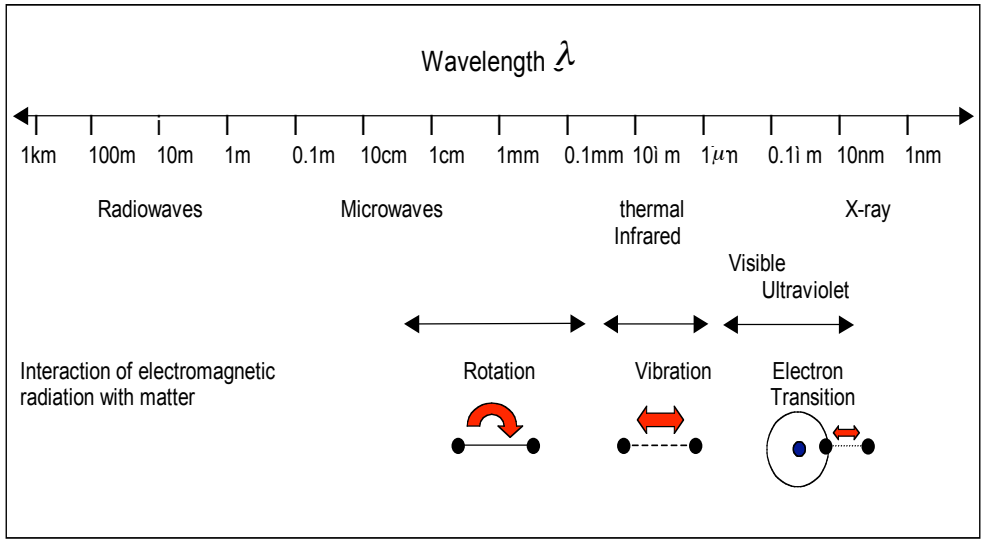

radiation interacts with atmosphere by

- – absorption (heating, shielding)
- – excitation (energy input, chemical reactions)
- – re-emission (energy balance)

interactions vs. spectral regions: water vapour

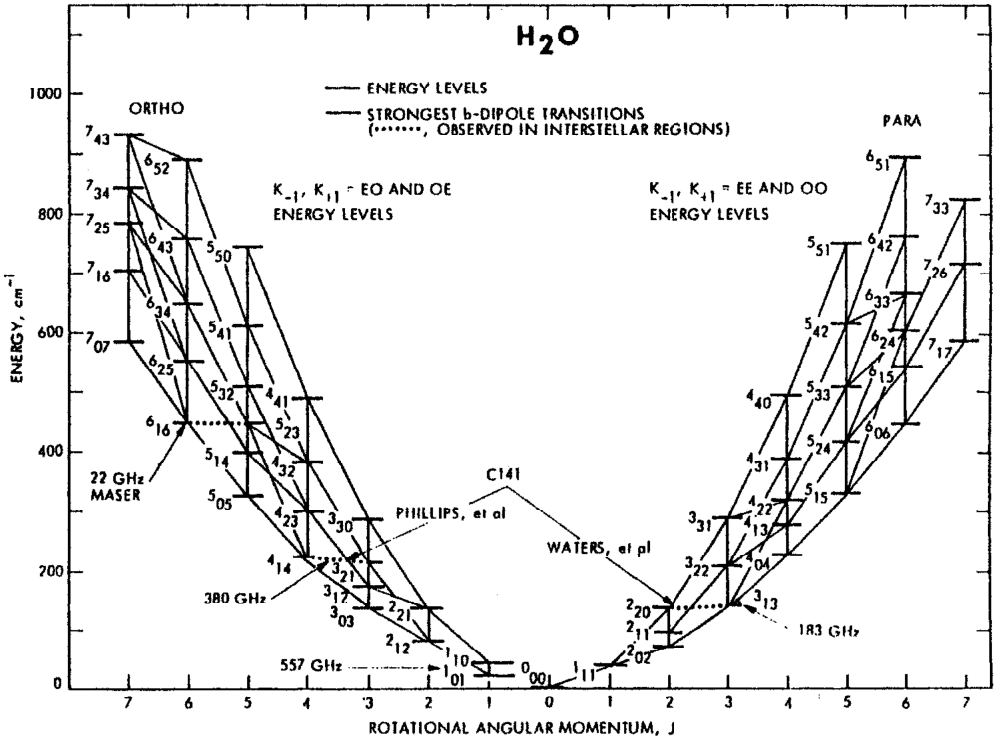

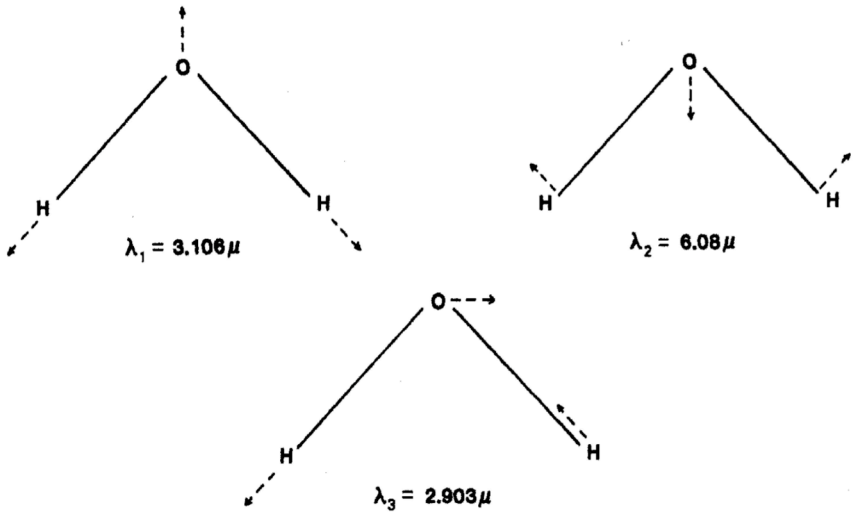

microwave vs. optical sensing

- wavelengths in the two regions differ by around 5 orders of magnitude (10^5): features observed are very different and usually highly complementary (order-of-magnitude spans also in each spectral region)
- very different spatial resolutions: only tens of km for microwave
- microwave sensing is little affected by atmosphere/clouds and can easily penetrate vegetation, dry soil, snow,..
- with microwaves, surfaces appear smoother than in the optical region hence larger occurrence of mirror-like reflections
- active sensing, especially with microwaves, offers larger control on incident energy, enabling new sensing capabilities
- passive optical sensing of the surface is constrained to the atmospheric windows (during daylight only for the 'solar spectrum'): in visible and near-infrared (approx.: 0.3 to 1.3 um), middle-infrared (approx: 1.5 - 1.8, 2.0 - 2.6, 3.0 - 3.6, 4.2 - 5 um), thermal infrared (7.0-15 um); for microwave also a (large) window (10 MHz - 100 GHz roughly)
- technological and legal constraints: microwave spectrum allocation (interference !), lidar safety issues,..

EM Spectrum: the Microwave Region

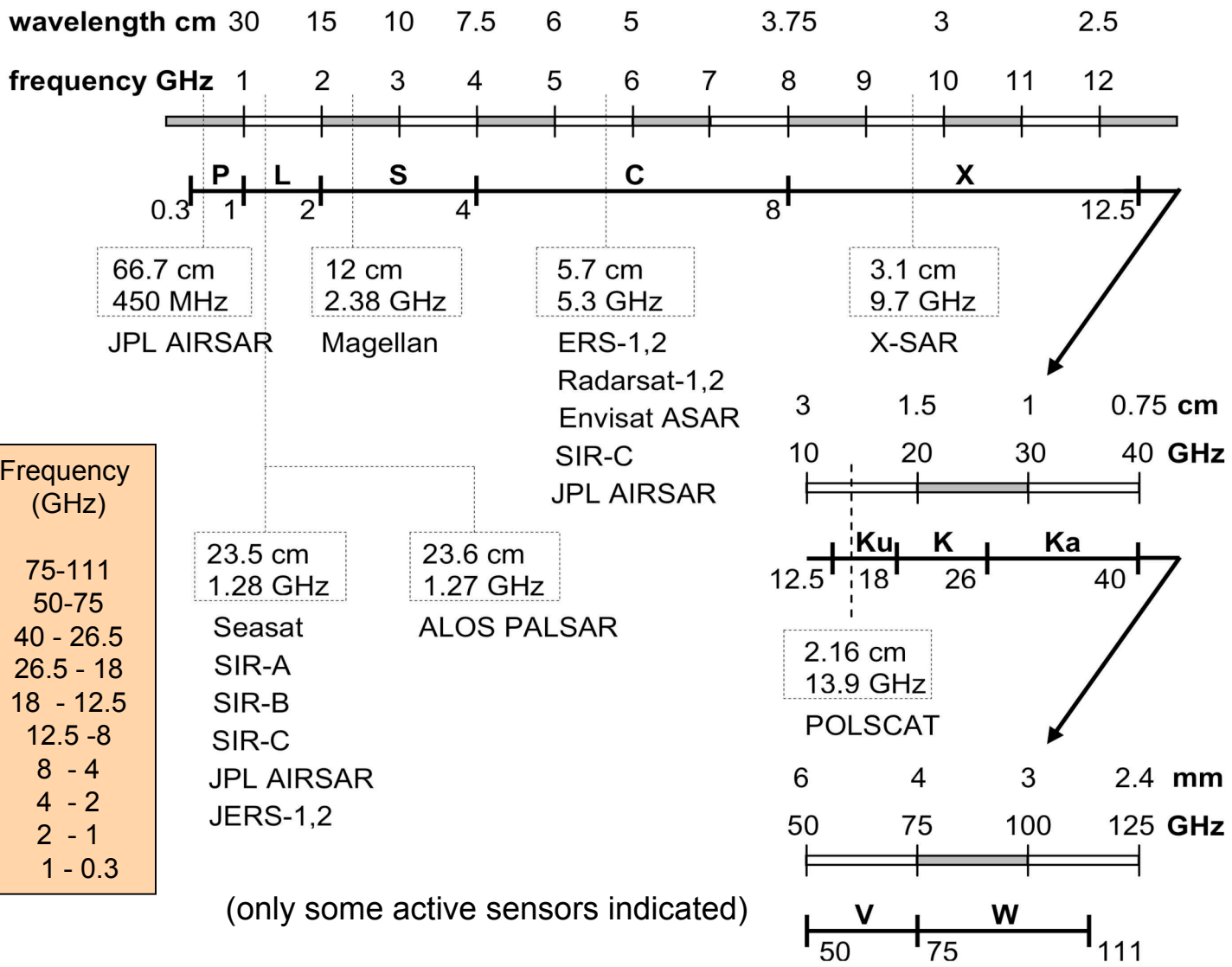

Frequency Band	Wavelength (cm)	Frequency (GHz)
W	0.24-0.3	75-111
V	0.4-0.6	50-75
Ka	0.8-1.1	40 - 26.5
K	1.1-1.7	26.5 - 18
Ku	1.7-2.4	18 - 12.5
X	2.4-3.8	12.5 -8
C	3.8-7.5	8 - 4
S	7.5-15	4 - 2
L	15 -30	2 - 1
P	30 -100	1 - 0.3

examples of RS systems

- Passive remote sensing:
  - Microwave radiometry incl. aperture synthesis
  - Infrared radiometry
- Active remote sensing:
  - Atmospheric sounding by occultation of GNSS signals
  - Synthetic aperture radar
- Other mission examples:
  - Optical observations for land and examples specific to biosphere

{radiometry = “science” describing the energy content and flow of incoherent EM radiation fields}

Microwave Radiometry

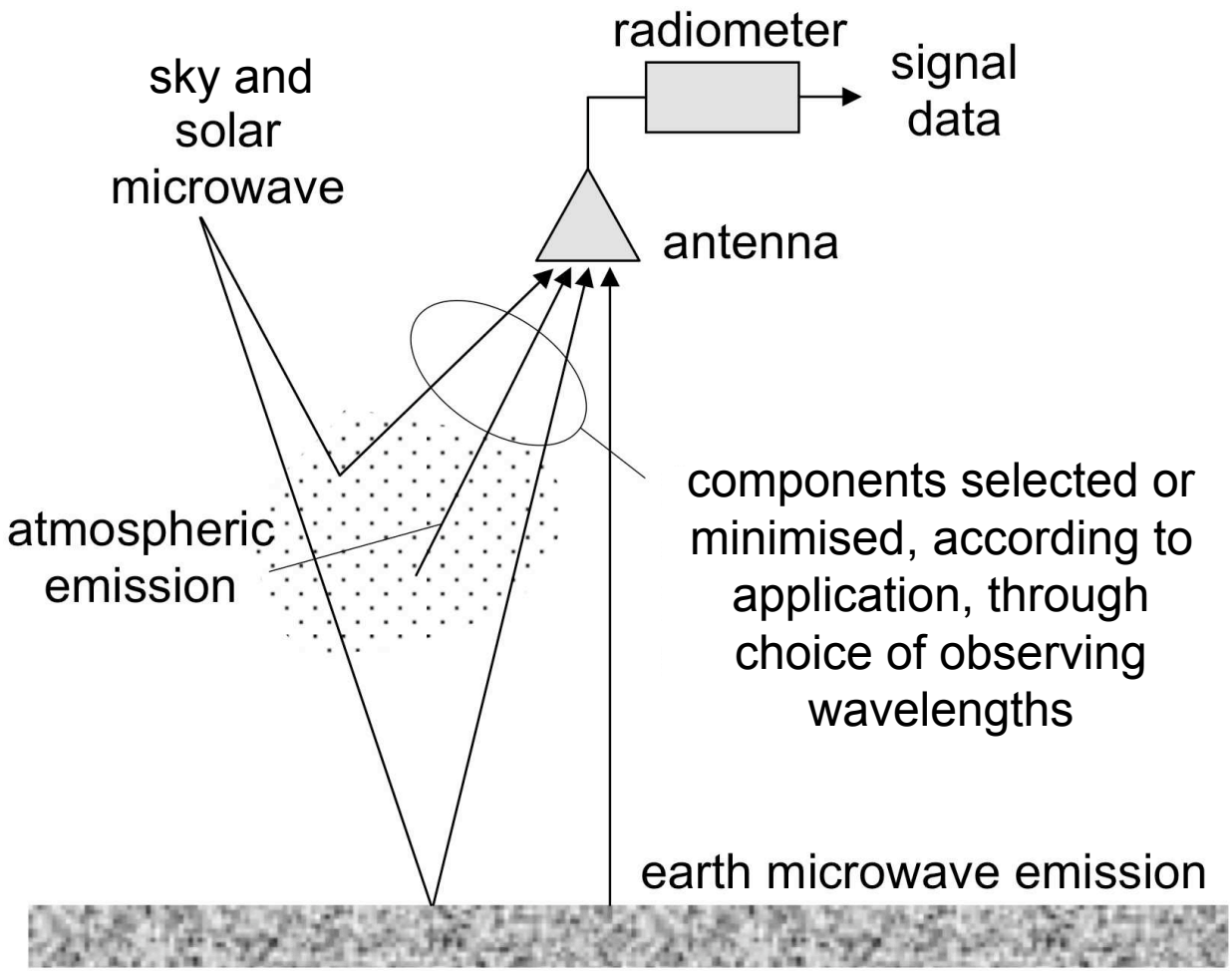

Microwave Radiometry: Nearly All Microwave Regions

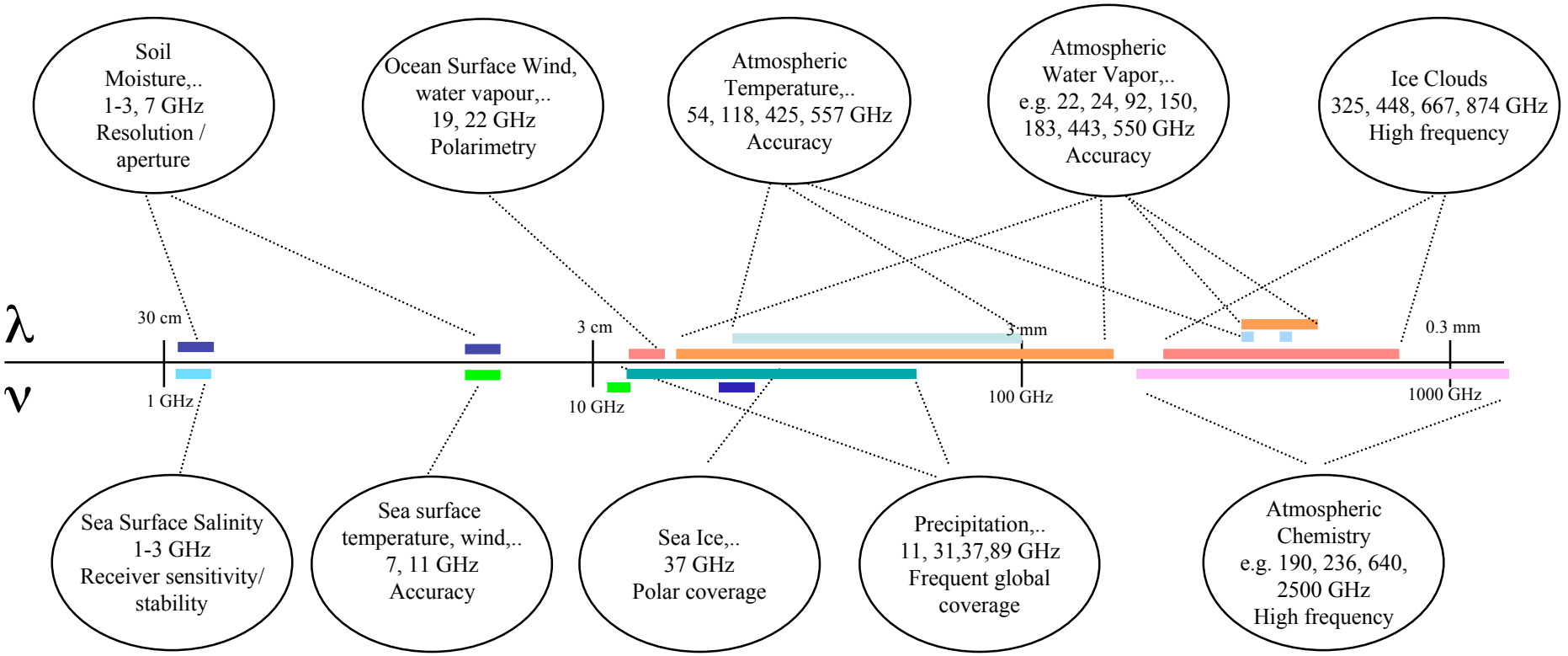

Radiometry: Principles (1)

- Planck law for blackbody spectral brightness [W/(m^2 Hz sr)]:

$$B_f(f,T) = \frac{2\pi h f^3}{c^2} \frac{1}{e^{\frac{hf}{kT}} - 1}$$

  where T is physical temperature [K], f is frequency [Hz]
- In microwave region, spectral brightness is directly proportional to temperature (Rayleigh-Jeans approx.):

$$hf << kT \Rightarrow B_f = \frac{2kT}{\lambda^2}$$

- Blackbody brightness in narrow bandwidth:

$$B_{bb} = \frac{2kT}{\lambda^2}\Delta f$$

- For a real body, brightness (around specific wavelength) is reduced and dependant on direction

$$B(\theta,\phi) = e(\theta,\phi)B_{bb} = \frac{2k}{\lambda^2}T_B\Delta f$$

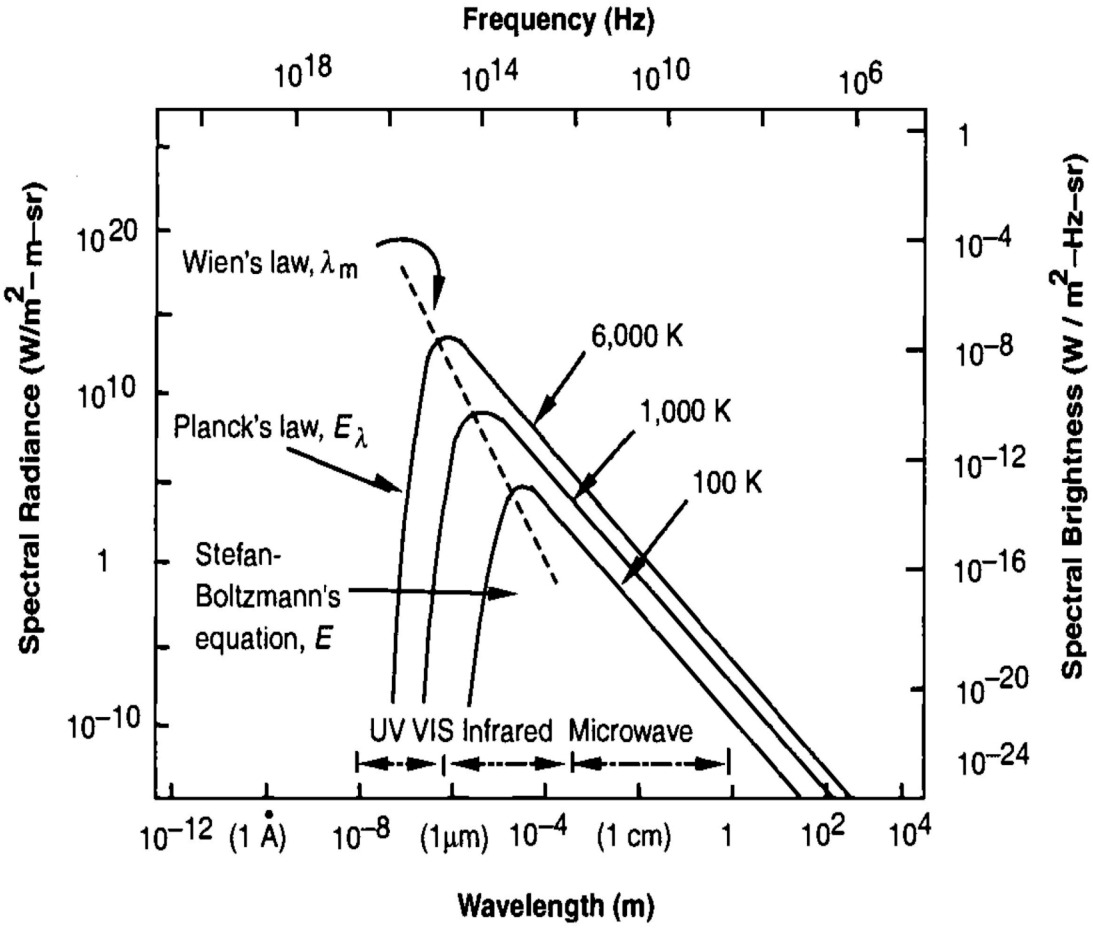

Microwave Radiometry: Principles (2)

- emissivity :

$$e(\theta,\phi) = \frac{B(\theta,\phi)}{B_{bb}} = \frac{T_B(\theta,\phi)}{T}$$

  depends on electrical properties of the body, frequency, direction of observation, polarisation,..
- T_B : brightness temperature (<= T)
- emission models predict the dependance of T_B on geophysical parameters :
  - ocean salinity, soil moisture, ice layer, vegetation water content,.. through complex permittivity of the land or water and multilayer models
  - surface winds through roughness of the sea surface
  - atmospheric parameters through radiative transfer models in absorbing media
- radiometers estimate T_B at different frequencies (=> spectro-radiometers) and polarisations

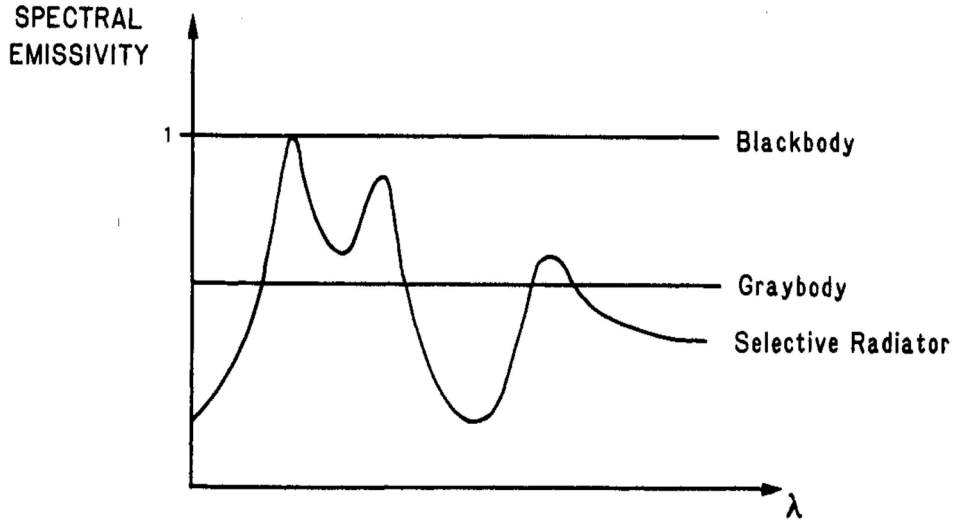

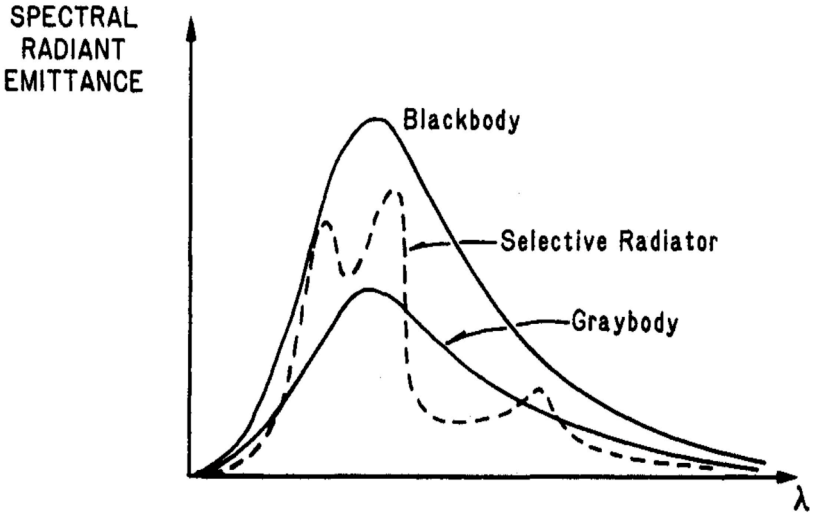

Microwave Radiometry: Principles (2)

- emissivity :

$$e(\theta,\phi) = \frac{B(\theta,\phi)}{B_{bb}} = \frac{T_B(\theta,\phi)}{T}$$

depends on electrical properties of the body, frequency, direction of observation polarisation,..

- T_B : brightness temperature (<= T)

- emission models predict the dependance of T_B on geophysical parameters :
  - ocean salinity, soil moisture, ice layer, vegetation water content,.. through complex permittivity of the land or water and multilayer models
  - surface winds through roughness of the sea surface
  - atmospheric parameters through radiative transfer models in absorbing media

- radiometers estimate T_B at different frequencies (=> spectro-radiometers) and polarisations

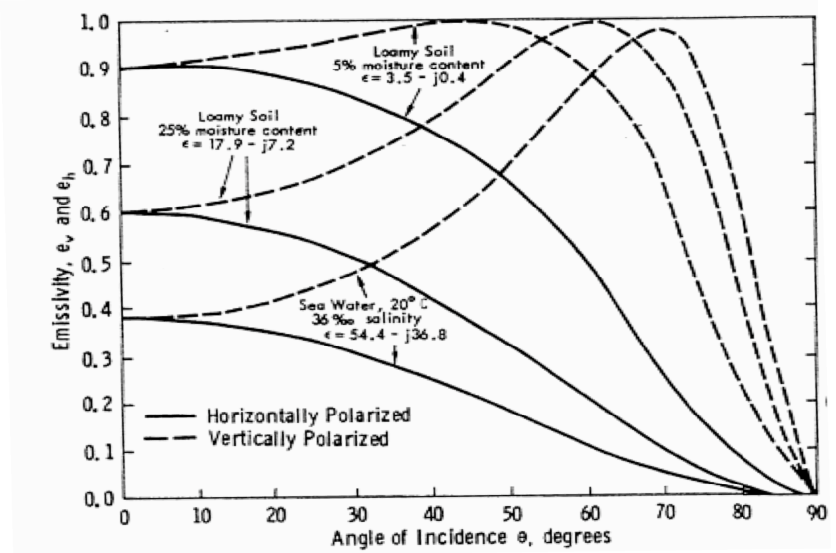

Modelled Brightness Temperature of salty water at nadir

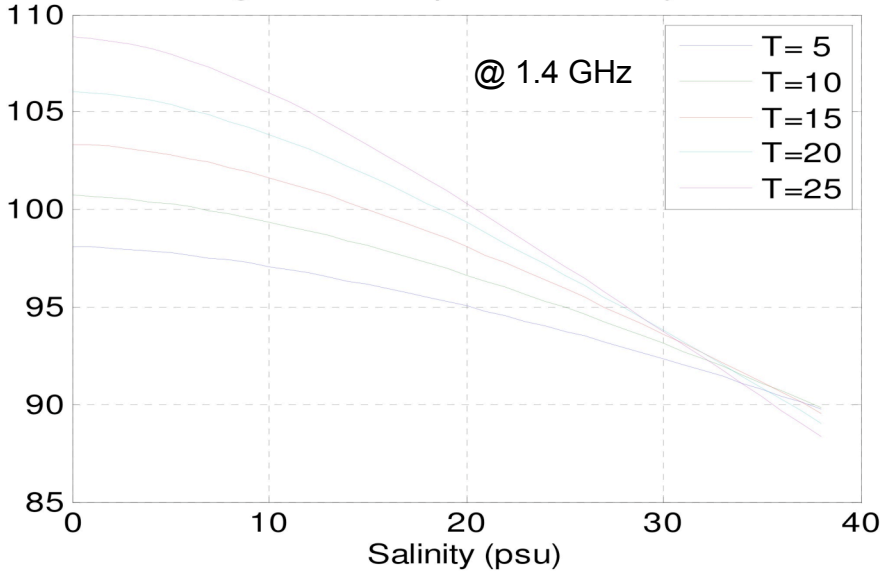

Blanch and Aguasca Model: IGARSS 2004

Microwave Radiometers

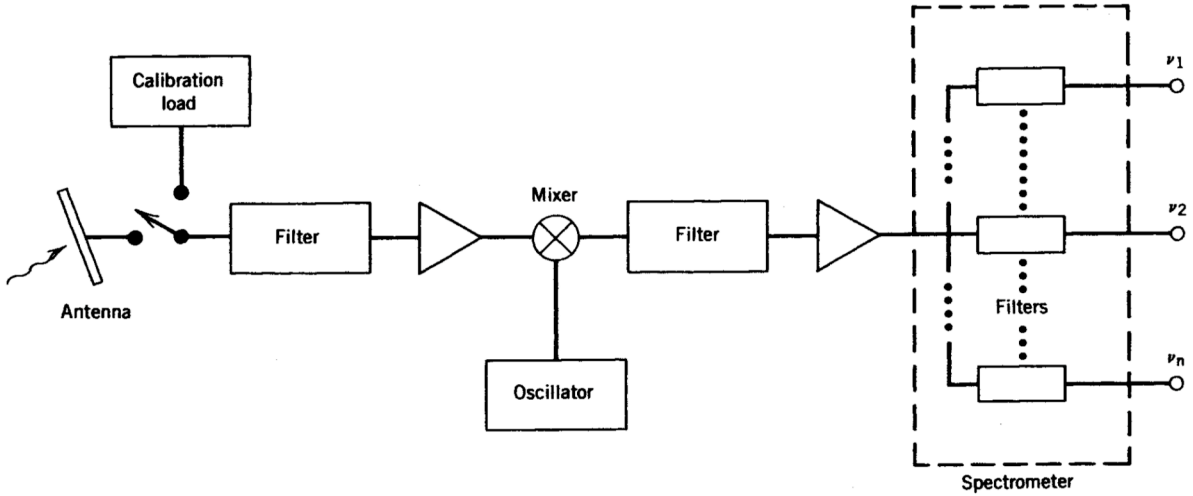

- Different practical radiometer schemes in use:
  - Total power radiometer - shown above, specifically a heterodyne multispectral radiometer - high sensitivity (varying with inverse of square root of bandwidth integration-time product) but poor stability
  - Dicke radiometer: uses rapid sequence of comparisons with reference source to compensate for drifts, at expense of sensitivity
  - Noise injection radiometer: extension of Dicke radiometer, which becomes part of a zero-balance loop, for better drift compensation
- Calibration is paramount for radiometers, in particular to compensate for drifts => measure reference targets (on-board and external)
- In practice radiometers are required to image over a swath, achievable in different ways (typ. scanning the antenna cross-track or conically, but also with push-broom configuration)
- Antenna pattern important and to be accounted for (as weight of emissivity)

example: microwave atmospheric sounder for MetOp Second-Generation (under study)

- primary observation objectives:
  - temperature profiles in clear and cloudy air
  - water-vapour profiles in clear and cloudy air
  - cloud liquid water columns (droplet size < 100 μm)
- up to 33 narrow channels (at single polarisation) covering frequency bands from 23 GHz up to 230 GHz
- T_B sensitivity from 0.1 to 2.3 K, accuracy 0.2 K to 1.0 K
- contiguous footprints at 15 km over large swath (for 90% coverage in 12 hr)
- cross-track scanning (heritage MetOp AMSU, MHS)
- 0.35 m antenna

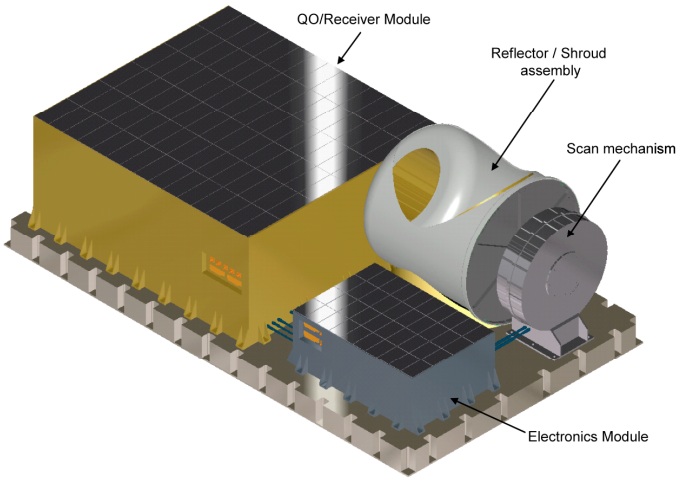

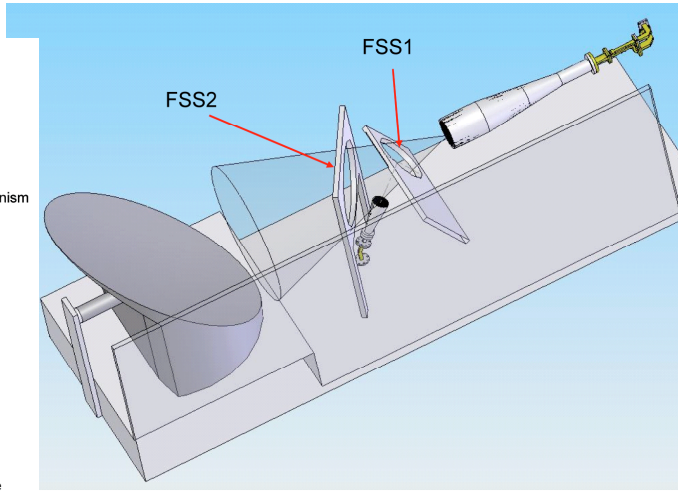

Channel	Frequency (MHz)	Bandwidth per passband (MHz)
MWS-1	**23.8**	**270**
MWS-2	**31.4**	**180**
MWS-3	**50.3**	**180**
MWS-4	**52.8**	**400**
MWS-5	*53.246±0.08*	*2x140*
MWS-6	**53.596±0.115**	**2x170**
MWS-7	*53.948±0.081*	*2x142*
MWS-8	**54.4**	**400**
MWS-9	**54.94**	**400**
MWS-10	**55.5**	**330**
MWS-11	**57.290344**	**330**
MWS-12	**57.290344±0.217**	**2x78**
MWS-13	**57.290344 ±0.3222±0.048**	**4x36**
MWS-14	**57.290344±0.3222±0.022**	**4x16**
MWS-15	**57.290344±0.3222±0.010**	**4x8**
MWS-16	**57.290344±0.3222±0.0045**	**4x3**
MWS-17	**89**	**4000**
MWS-18	*118.7503 ± 5.0000*	*2x2000*
MWS-19	*118.7503 ± 3.0000*	*2x1000*
MWS-20	*118.7503 ± 2.1000*	*2x800*
MWS-21	*118.7503 ± 1.5000*	*2x400*
MWS-22	*118.7503 ± 1.1000*	*2x400*
MWS-23	*118.7503 ± 0.7000*	*2x400*
MWS-24	*118.7503 ± 0.4000*	*2x200*
MWS-25	*118.7503 ± 0.2000*	*2x100*
MWS-26	*118.7503 ± 0.0800*	*2x20*
MWS-27	**164-167**	**3000**
MWS-28	**183.311±7.0**	**2x2000**
MWS-29	**183.311±4.5**	**2x2000**
MWS-30	**183.311±3.0**	**2x1000**
MWS-31	**183.311±1.8**	**2x1000**
MWS-32	**183.311±1.0**	**2x500**
MWS-33	*229*	*2000*

example: microwave imager for cloud and precipitation (for same mission)

observation objectives:

- cloud and precipitation products including bulk micro-physical parameters
- water vapour and temperature gross profiles
- all-weather surface imagery including:
  sea ice coverage (and type)
  snow coverage, depth and water equivalent
  soil moisture products
  sea surface winds (complementary to wind scatterometer)

- 10 channels (9 in dual polarization) from 18.7 to 183 GHz
- 1 m antenna

Channel	Frequency (GHz)	Bandwidth (MHz)	Polarisation
MWI-5	18.7	200	H&V
MWI-6	23.8	400	H&V
MWI-7	31.4	200	H&V
MWI-8	50.3	400	H&V
MWI-9	52.61 or 52.80	400	H&V
MWI-12	89	4000	H&V
MWI-18	166.9	1425	V
MWI-19	183.31±8.4	2x3000	H&V
MWI-20	183.31±6.1	2x1500	H&V
MWI-22	183.31±3.4	2x1500	H&V

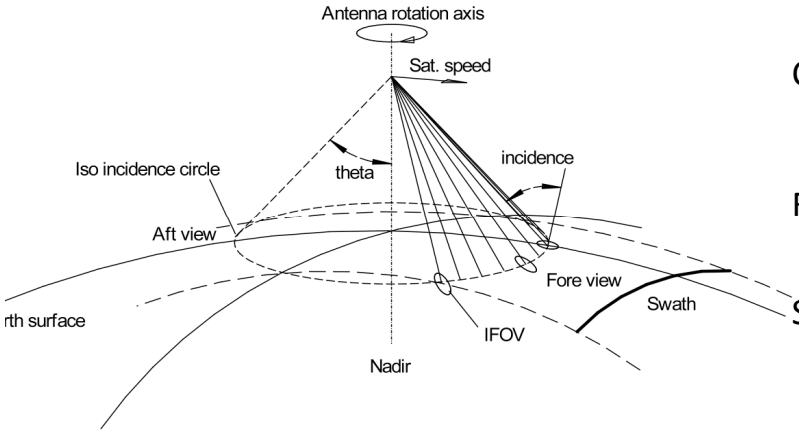

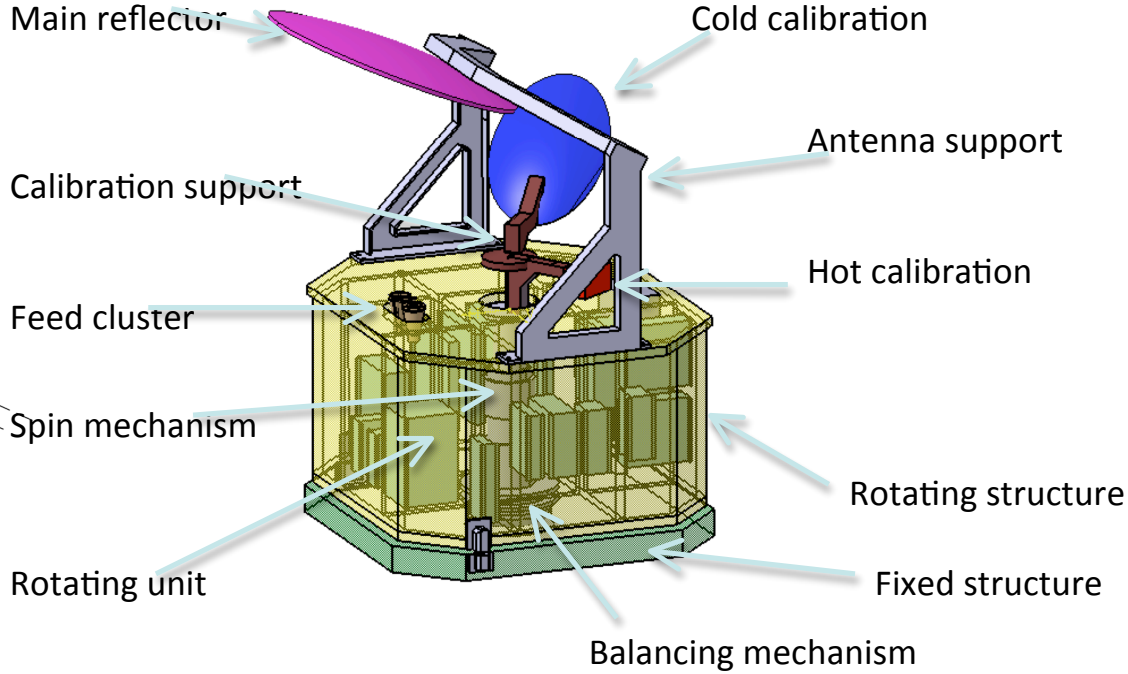

a different approach: interferometric radiometry by aperture synthesis

at very low frequencies, e.g. at 1.4 GHz (21 cm wavelength, L-band) which offers strong advantages for measuring soil moisture and ocean salinity, antennas become very large and difficult to scan

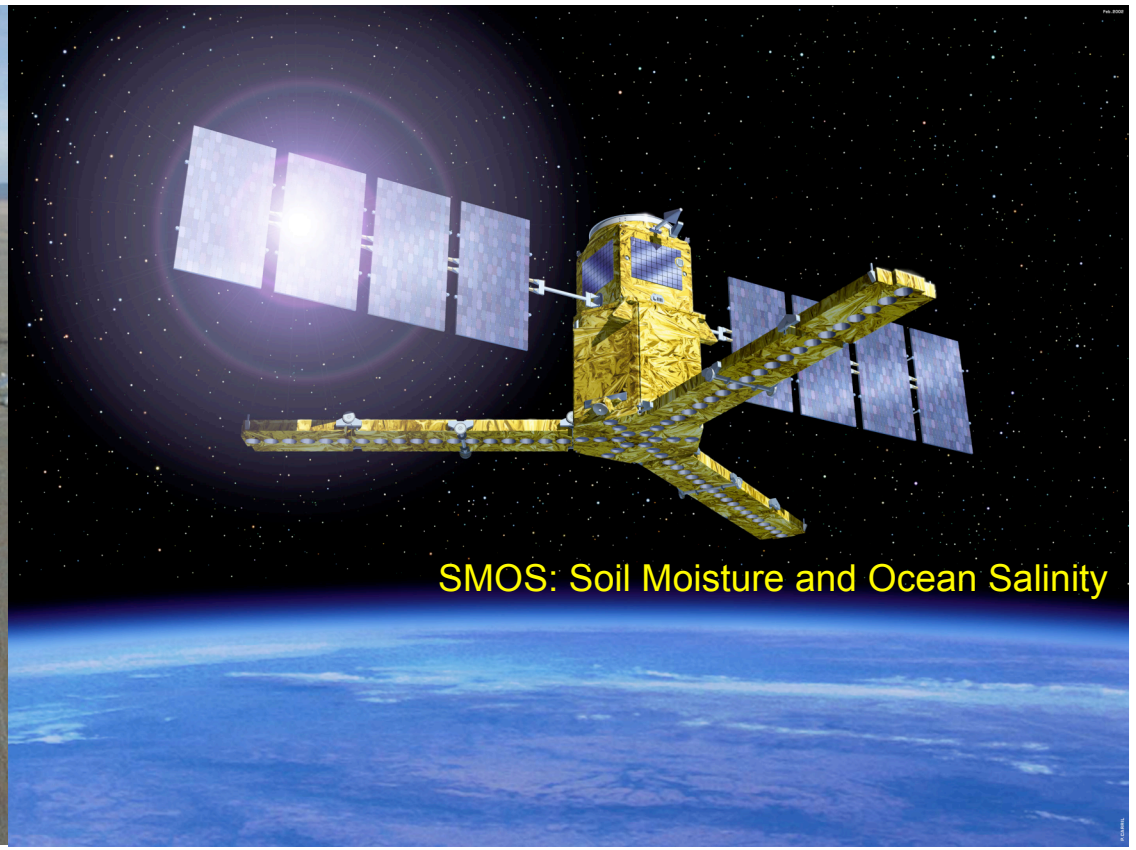

interferometric radiometry by aperture synthesis: the principle

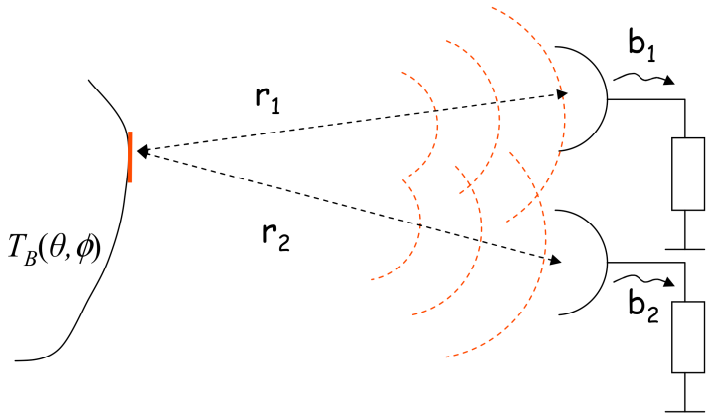

- Power spectral density:
  Antenna temperature

$$\overline{|b_1(f)|^2} = kT_{A1}$$

$$\overline{|b_2(f)|^2} = kT_{A2}$$

- Cross-Power spectral density:
  Visibility

$$\overline{b_1(f)b_2^*(f)} = kV_{12}$$

(units: Kelvin) (complex valued)

$$T_{A_{1,2}} = \frac{1}{\Omega_{1,2}} \iint_{4\pi} T_B(\theta,\phi)t(\theta,\phi)d\Omega$$

$$V_{12} = \frac{1}{\sqrt{\Omega_1\Omega_2}} \iint_{4\pi} T_B(\theta,\phi)F_{n1}(\theta,\phi)F_{n2}^*(\theta,\phi)e^{-jk(r_1-r_2)}d\Omega$$

Antenna field patterns — phase difference

For identical antennas:

Modified brightness temperature T'_B

$$V(u,v) = \iint_{\xi^2+\eta^2\le 1} \frac{T_B(\xi,\eta)t(\xi,\eta)}{\Omega_a\sqrt{1-\xi^2-\eta^2}} e^{-j2\pi(u\xi+v\eta)}d\xi d\eta$$

Obliquity factor

Antenna power pattern: $t(\xi,\eta) = |F_n(\xi,\eta)|^2$

Two-dimensional Fourier Transform: $V(u,v) = \mathcal{F}[T'_B(\xi,\eta)]$

interferometric radiometry by aperture synthesis: a recipe (1)

- the visibility function V(u,v) is measured by cross-correlating the signals from many pairs of antennas at different relative distances
- the (modified) brightness temperature is retrieved by inverse Fourier transform of the visibility function
- with an array of antennas no mechanical movement is needed! A ‘virtual antenna’ of large aperture is sampled spatially
- the brightness temperature is ‘modified’ because the source is extended (unlike in radio-astronomy)
- antenna couplings and variations among antennas/receivers must be minimal and in any case accounted for in the processing

interferometric radiometry by aperture synthesis: a recipe (2)

Fourier inversion $T'_B(\xi,\eta) = \int_{-\infty}^{\infty}\int_{-\infty}^{\infty} V(u,v)e^{j2\pi(u\xi+v\eta)}dudv$

Only limited values of (u,v) are available: The measured visibility function is necessarily windowed.

Retrieved brightness temperature $\hat{T}'_B(\xi,\eta) = \int_{-\infty}^{\infty}\int_{-\infty}^{\infty} W(u,v)V(u,v)e^{j2\pi(u\xi+v\eta)}dudv$

$$\hat{T}'_B(\xi,\eta) = \int_{-\infty}^{\infty}\int_{-\infty}^{\infty} T'_B(\xi',\eta')AF(\xi-\xi',\eta-\eta')d\xi'd\eta'$$

Convolution integral

- Array Factor: Inverse Fourier transform of the window
- It is the "synthetic beam". It sets the spatial resolution
- Its width depends on the maximum (u,v) values (antenna maximum spacing)

no window

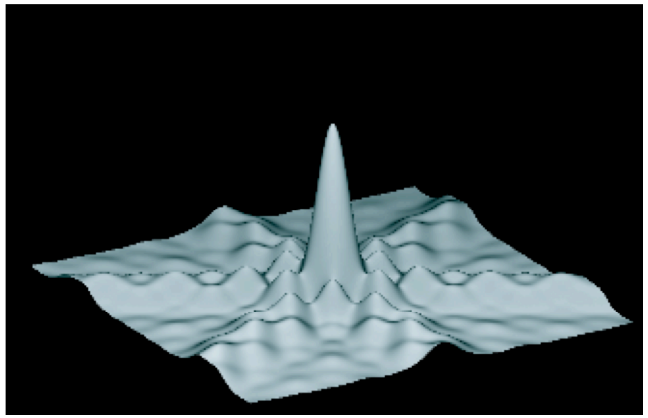

Rectangular window

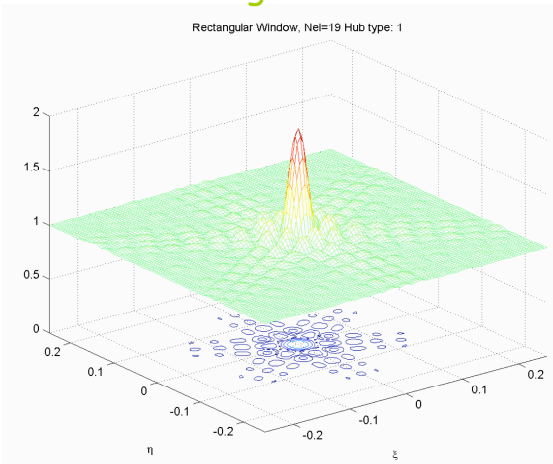

Δθ= 1.73 deg

Blackmann window

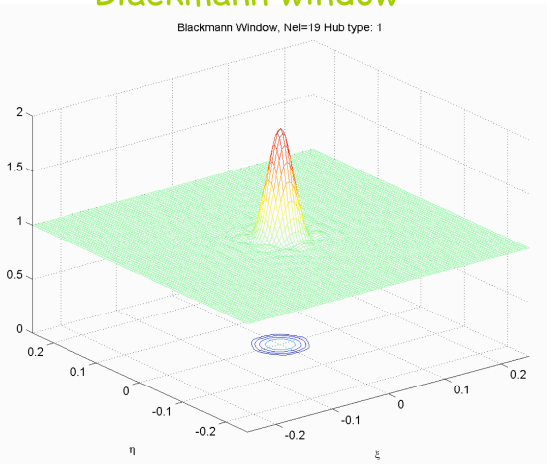

Δθ= 2.46 deg

interferometric radiometry by aperture synthesis

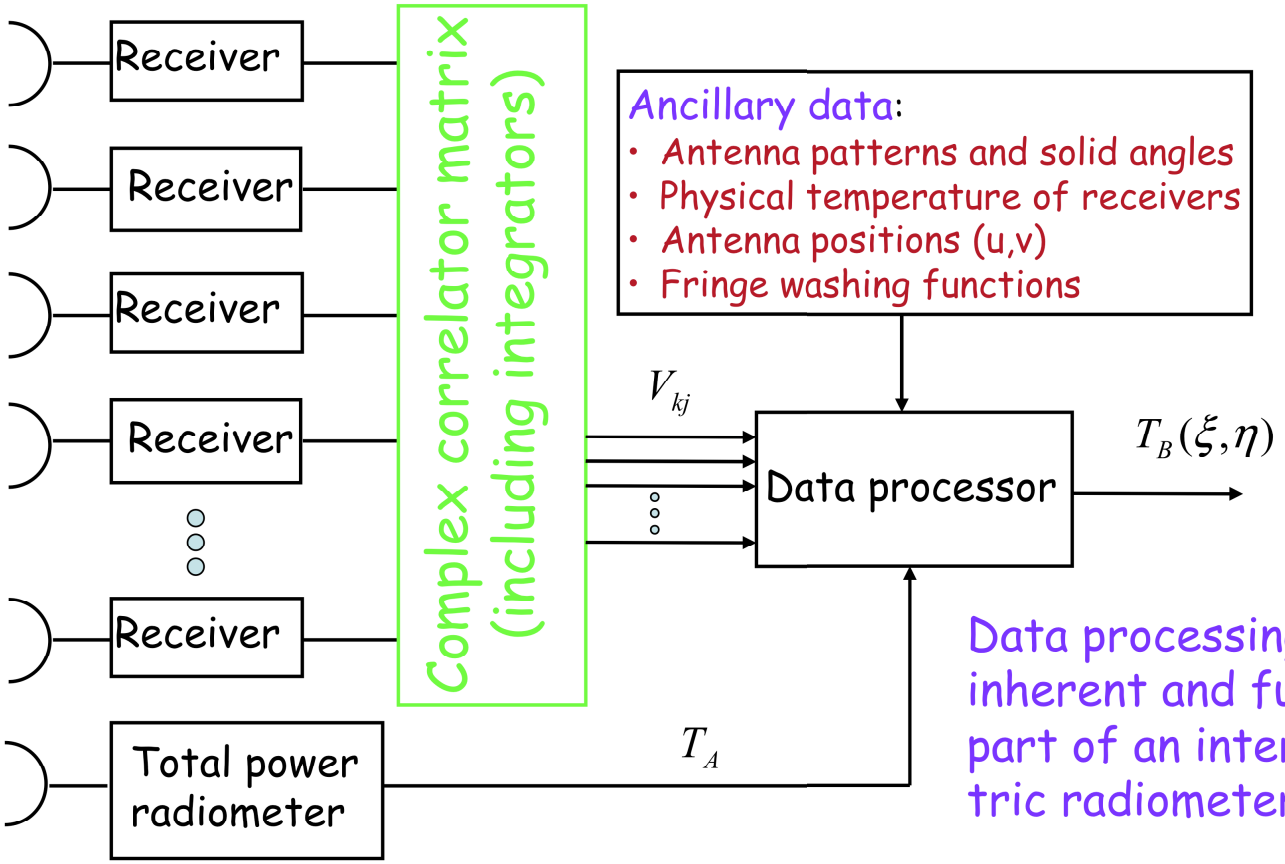

Data processing is an inherent and fundamental part of an interferometric radiometer.

aperture synthesis: improved spatial resolution and multi-angle observations over wide swath

(after complex ground processing)

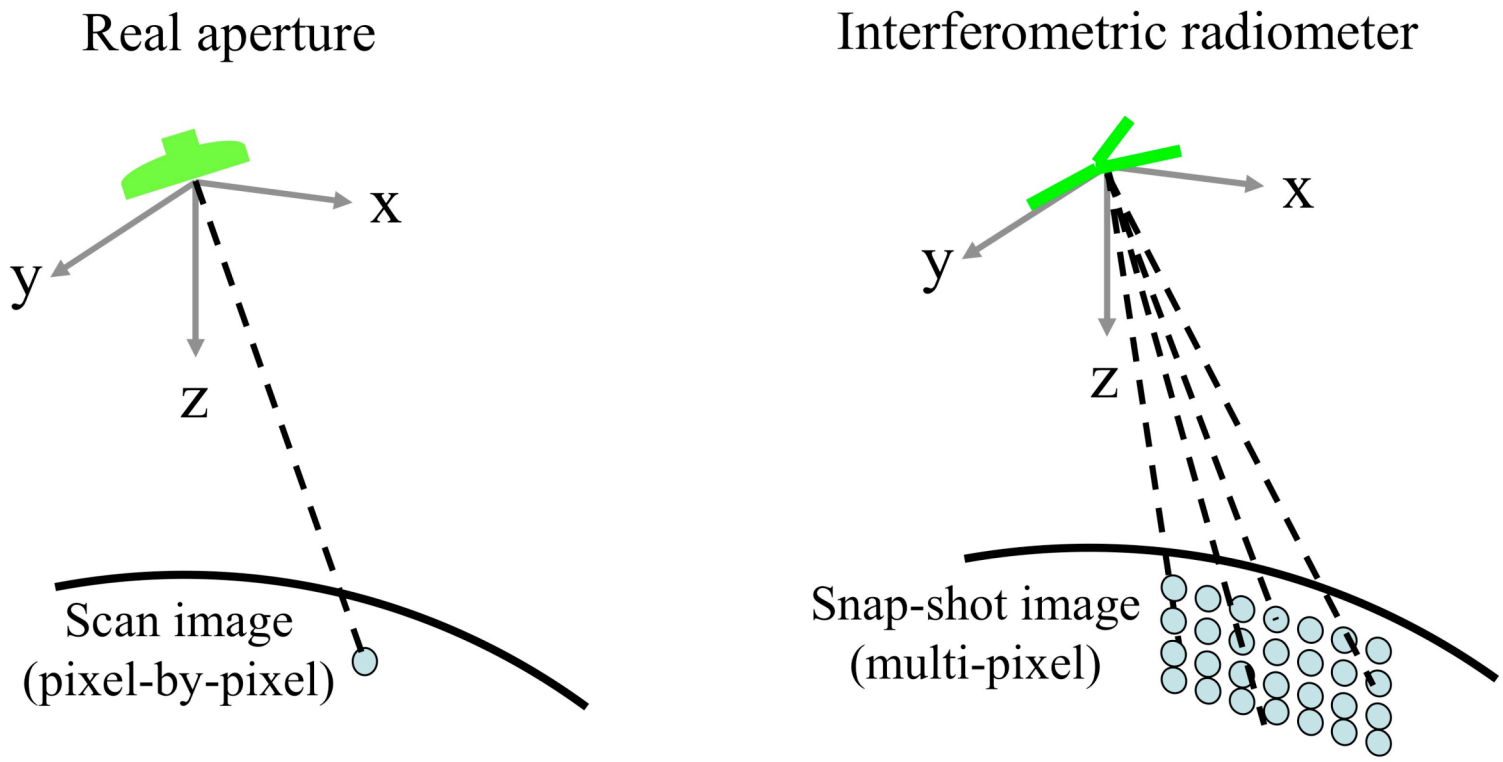

aperture synthesis principle can be applied to any wavelength (even optical, for e.g. metre-level resolution from geostationary orbit!), but offer larger advantages at long ones

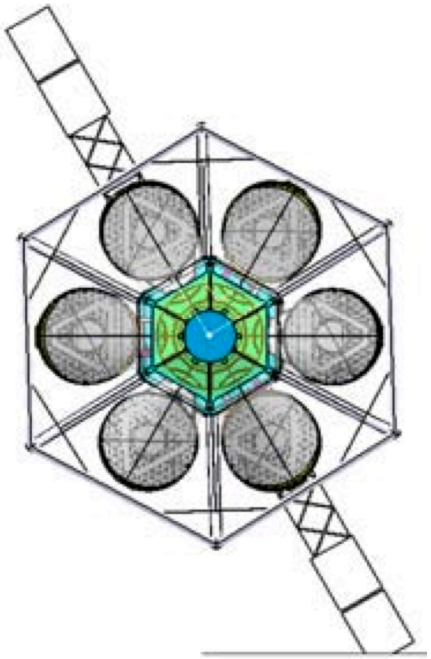

optical aperture synthesis: early concepts

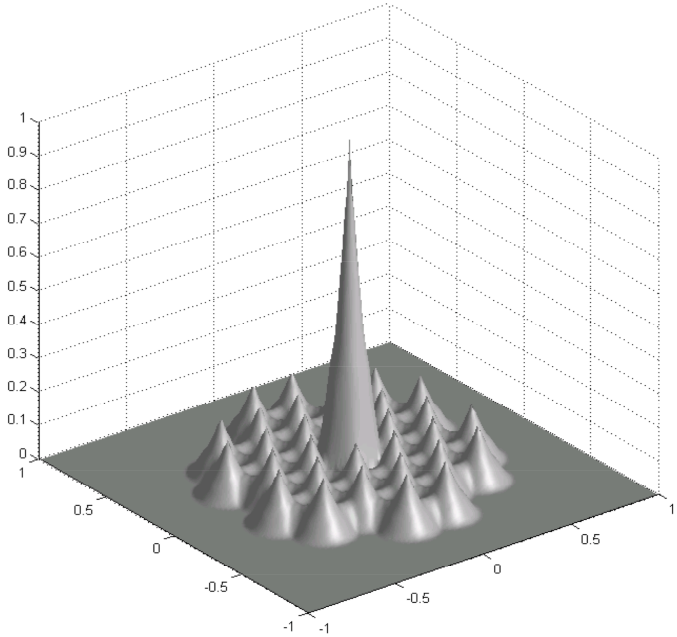

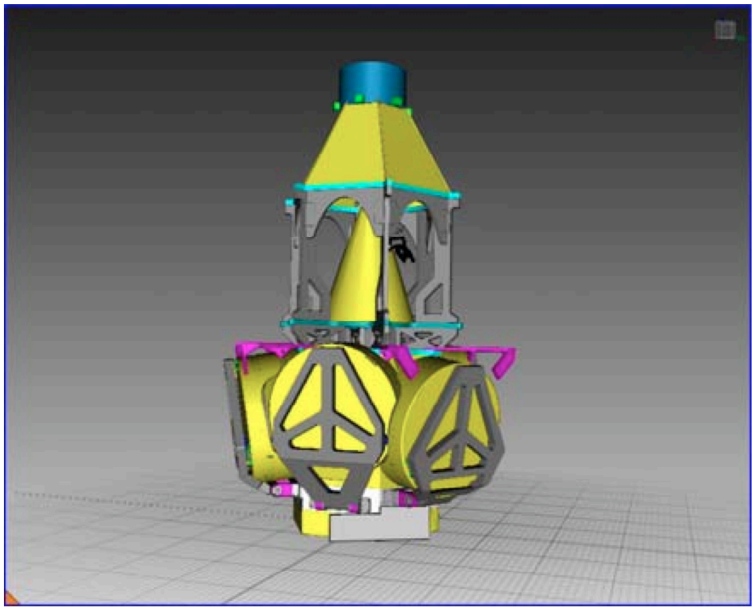

Folded position

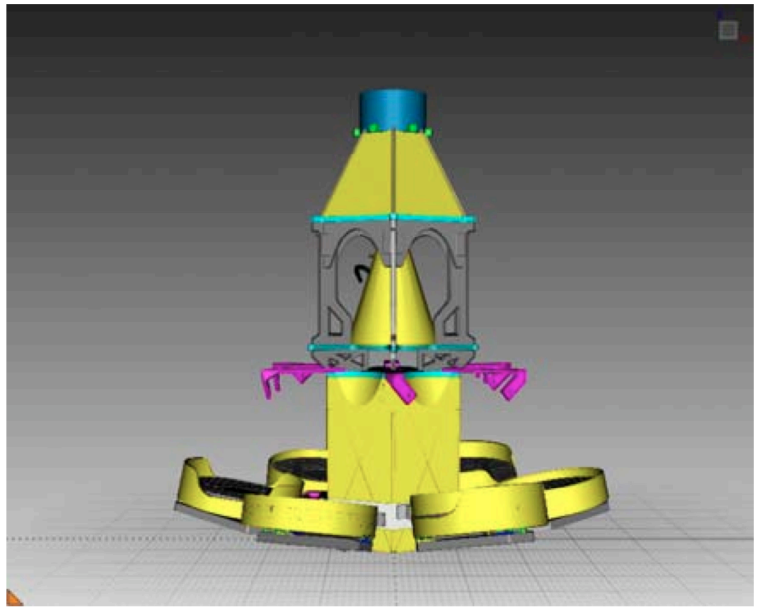

Unfolded position

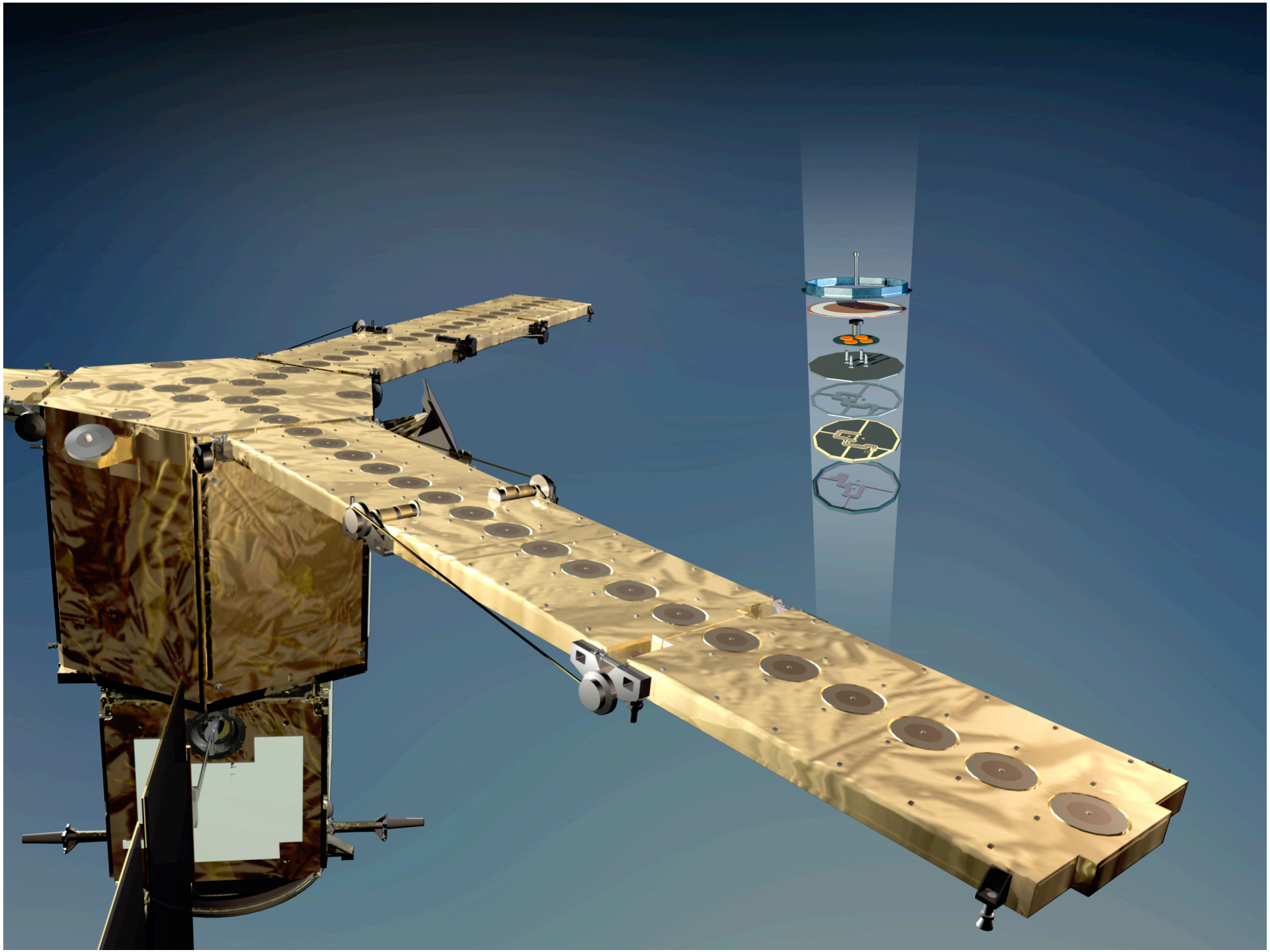

SMOS sensor under development

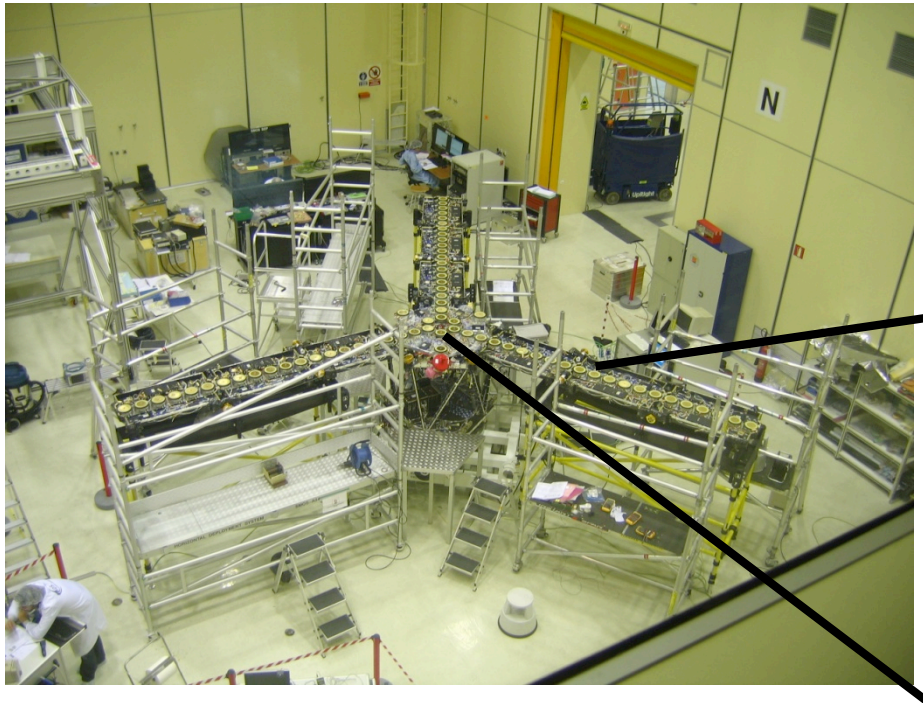

radiometer during assembly and integration: 3 arms and a hub, 72 receivers in total

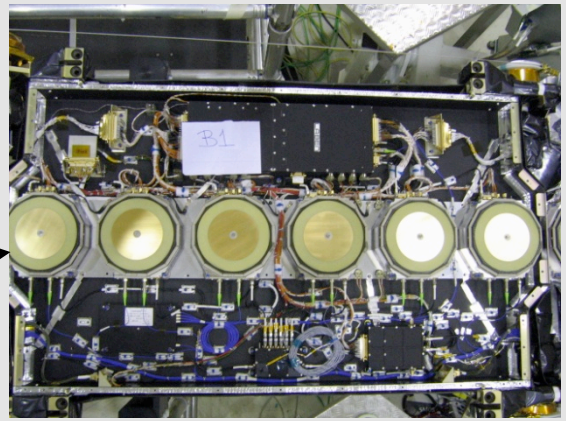

One arm segment carries:
- 3 segments with 6 receivers each
- On-board calibration system
- Control and Monitoring Node

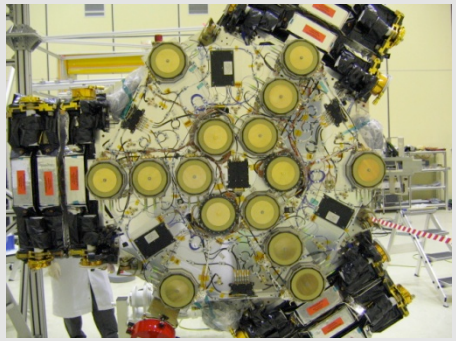

hub carries 15 receivers, on-board calibration system, control and monitoring electronics, correlator unit

quite complex post-processing..

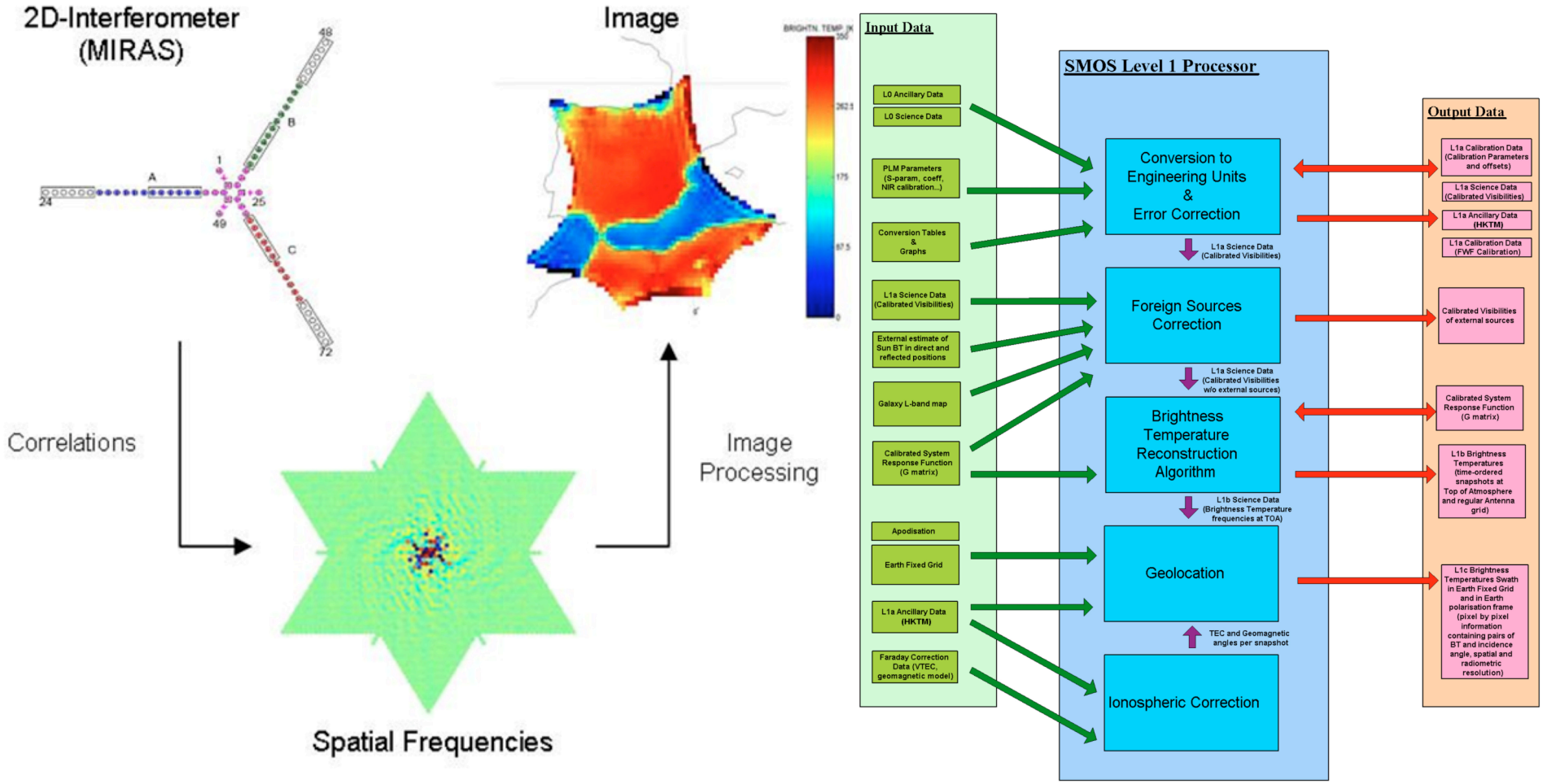

.. and complex calibrations (internal and external)..

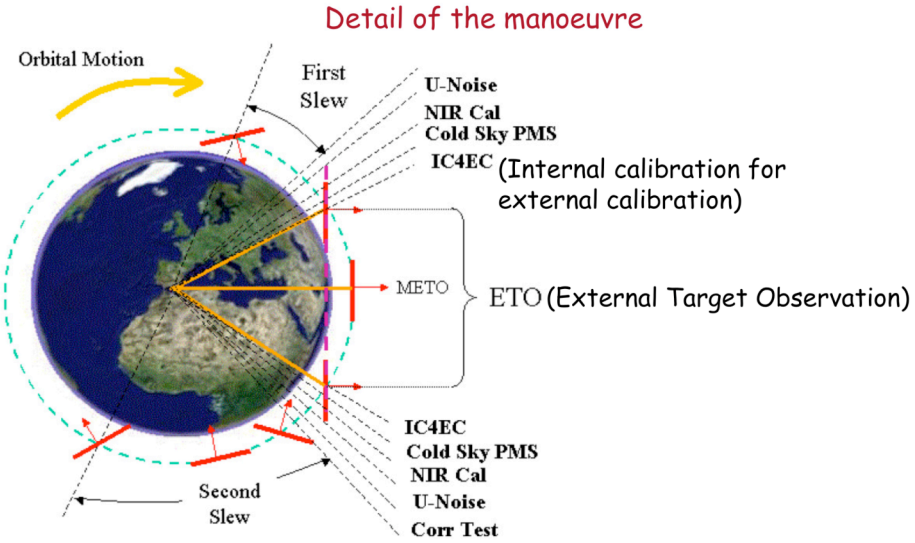

Atttitude	Mode	Epochs	Minutes
Nominal	Nominal Measurement	1	0.02
First Slew	Ext-Measurement	534	10.68
Inertial (ETO)	IC4EC	27	0.5
	Cold Sky PMS	31	0.6
	NIR Calibration	27	0.5
		26	0.5
		27	0.5
	LO cal	5	0.1
	Cold Sky PMS	31	0.6
	NIR Calibration	27	0.5
		26	0.5
		27	0.5
	LO cal	5	0.1
	Cold Sky PMS	31	0.6
	NIR Calibration	27	0.5
		26	0.5
		27	0.5
	Cold Sky PMS	31	0.6
	LO cal	5	0.1
	Cold Sky PMS	31	0.6
	NIR Calibration	27	0.5
		26	0.5
		27	0.5
	LO cal	5	0.1
	Cold Sky PMS	31	0.6
	NIR Calibration	27	0.5
		26	0.5
		27	0.5
	Cold Sky PMS	31	0.6
	IC4EC	27	0.5
Return Slew	Corr Test	30	0.6
	Ext-Measurement	1162	23.24

		Time	
Atttitude	Mode	Epochs	Minutes
Nominal	Nominal Measurement	1	0.02
First Slew	Ext-Measurement	534	10.7
Inertial (ETO)	U-Noise	50	1.0
	NIR Calibration	27	0.5
		26	0.5
		27	0.5
	Cold Sky PMS	31	0.6
	IC4EC	27	0.5
	Ext-Measurement (FTR / G-matrix)	740	14.8
	IC4EC	27	0.5
	Cold Sky PMS	31	0.6
	NIR Calibration	27	0.5
		26	0.5
		27	0.5
	U-Noise	50	1.0
Return Slew	Corr Test	30	0.6
	Ext-Measurement	1162	23.2

		Time	
Atttitude	Mode	Epochs	Minutes
Nominal	Nominal Measurement	1	0.02
First Slew	Ext-Measurement	534	10.68
Inertial (ETO)	IC4EC	27	0.5
	IC4EC	27	0.5
	Cold Sky PMS	31	0.6
	Cold Sky PMS	31	0.6
	LO sequence	5	0.1
	Ext-Measurement (FTR with LO every 106 epochs)	742	14.84
	LO sequence	5	0.1
	Cold Sky PMS	31	0.6
	Cold Sky PMS	31	0.6
	IC4EC	27	0.5
	IC4EC	27	0.5
Return Slew	Corr Test	30	0.6
	Ext-Measurement	1162	23.24

some results: over land

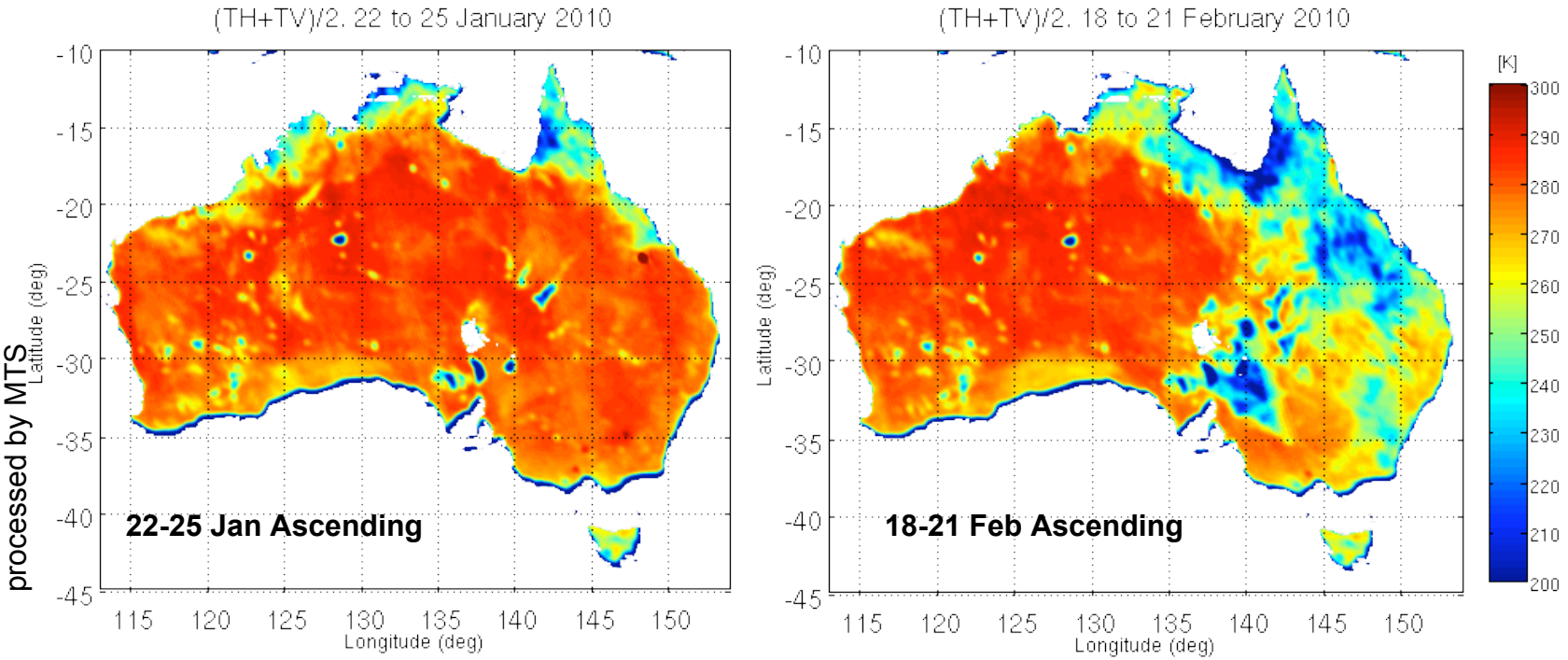

(after Corbella et al.)

Rainfall anomalies measured by TRMM over Australia from 17-Jan-2010 to 16-Feb-2010 ("Olga" Tropical storm)

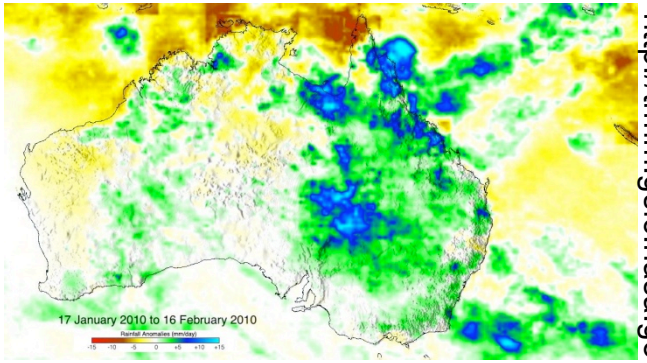

http://trmm.gsfc.nasa.gov/

soil moisture retrievals for 20 -23 June 2010

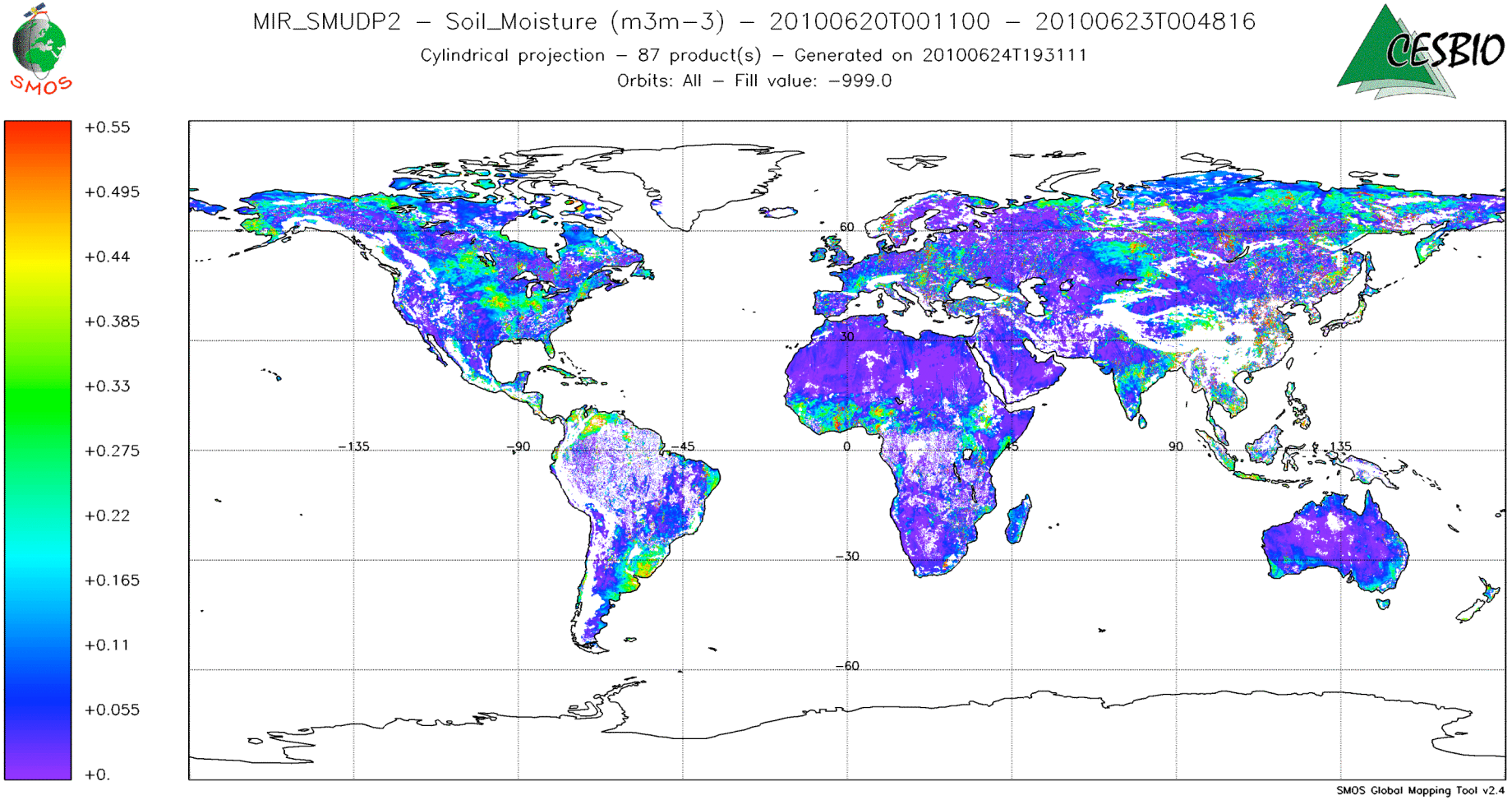

(after P. Richaume, 2010)

moving up in frequency..

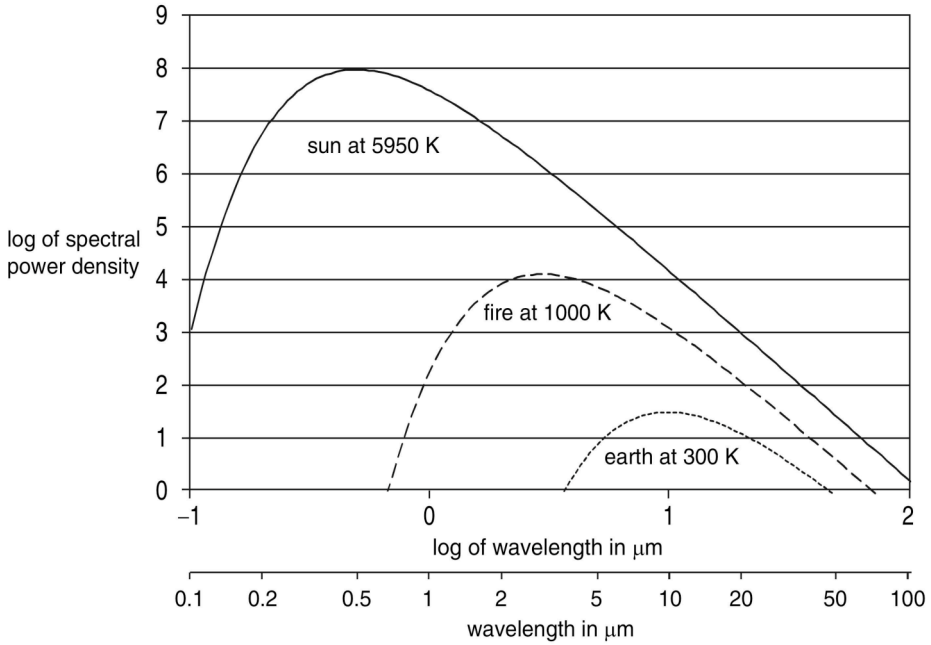

on the surface of the emitter

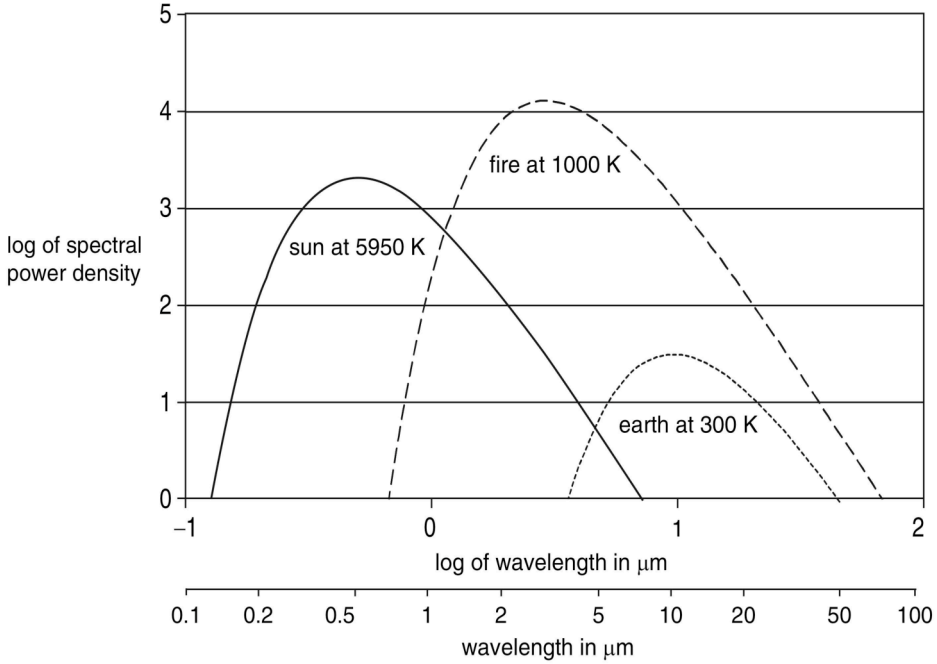

at the top of the Earth's atmosphere

sea-surface temperature to climate-benchmark quality: the (Advanced) Along-Track Sea-Surface Radiometer [(A)ATSR]

{in future: SLSTR: Sea and Land Surface Temperature Radiometer}

thermal infrared (12 micron) AATSR image of the Gulf of Oman: thermal structure in the ocean is observed

Why measure SST from space?

- SST controls ocean-atmosphere heat transfer
- More heat reaches the atmosphere from the Earth's surface than from direct solar heating
- Ocean-atmosphere heat transfer is a key "driver" of weather and climate
- SST is also a robust indicator of climate change
- SST is as an Essential Climate Variable (ECV)
- SST observations do need coverage, consistency of measurements and long-term continuity
- SST data can be used for process monitoring :
  - as tracer for major currents (e.g. Gulf Stream, Aghulas, KuroShio,)
  - for detection of major anomalies or periodic events (e.g el Nino)
  - for detection and monitoring of long-term changes

What measurement performance for SST ?

- Climate monitoring: trends expected at ~0.1 K per decade: aim for accuracy of 0.2 K with additional key requirement on stability of measurement: bias drift of less than 0.1 K/decade

- Ocean-atmosphere heat transfer: strong dependance on temperature in the tropics, a change by 0.3 K can affect rate by ~10%

- Process monitoring: for instance, el Nino is an anomaly of typically 2 to 4 K (should be observed to at least 10% accuracy)

⇒ exacting requirements on radiometer stability, on its calibration and on processing for e.g. atmospheric corrections

=> provide enhanced continuity to previous sensors, e.g. AVHRR

microwave vs. optical radiometer (for SST)

MICROWAVE

- Very little affected by clouds
- Low atmospheric effects
- Low spatial resolution: several tens of km
- Linear radiometric sensitivity
- Rain can be a problem
- Radio frequency interference can be a problem

OPTICAL

- Only usable in cloud-free areas
- Atmospheric correction mandatory, espec. for tropical observations
- Spatial resolution of ~1 km easily achieved
- Very high radiometric sensitivity
- Aerosols can be a problem

ENVISAT

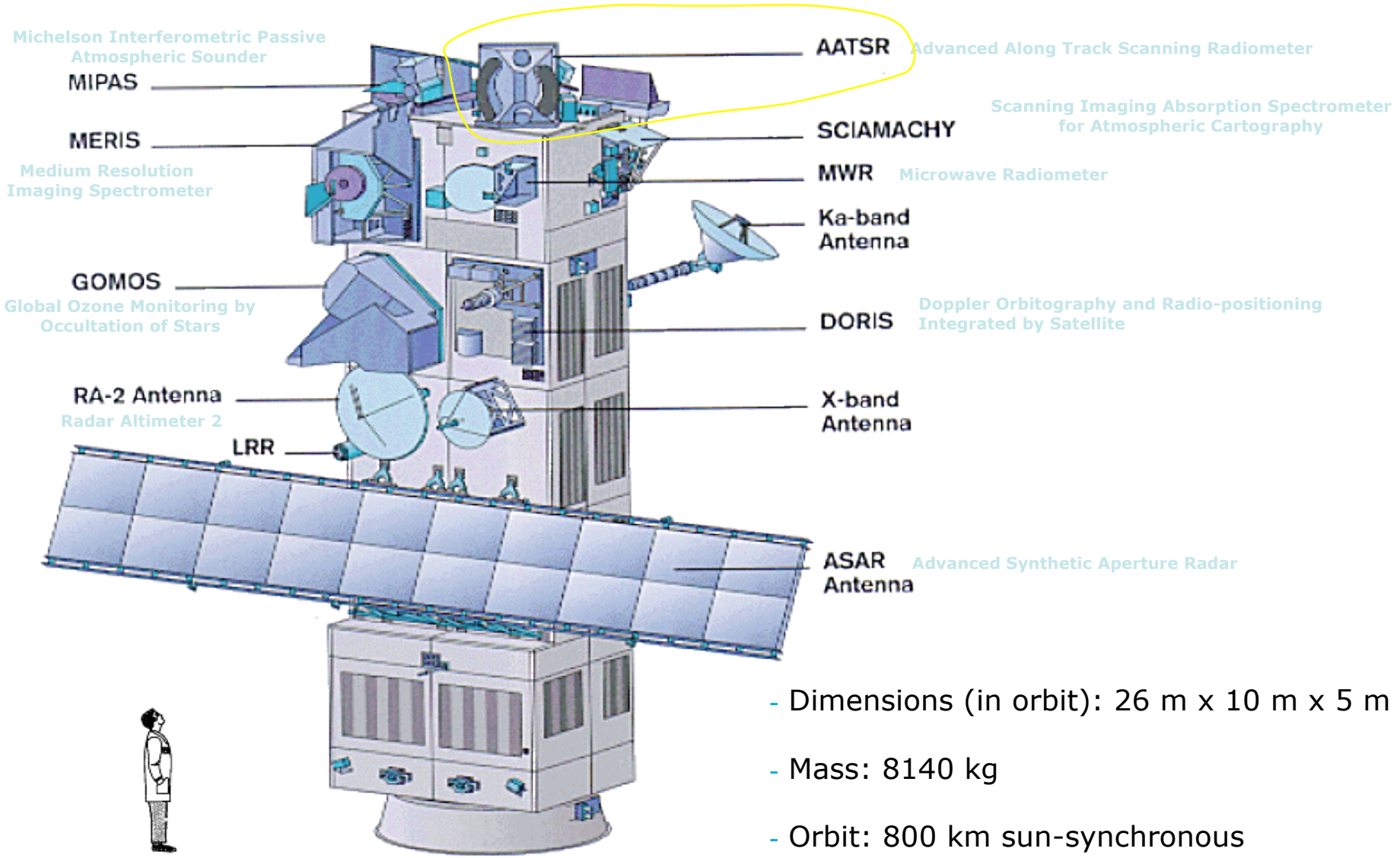

- Dimensions (in orbit): 26 m x 10 m x 5 m
- Mass: 8140 kg
- Orbit: 800 km sun-synchronous

(A)ATSR on ERS-1/-2/ENVISAT

- 7 spectral channels (as AVHRR, MODIS) with 3 thermal channels: 3.7, 11, 12 micron and 4 visible/near-infrared channels: 0.55, 0.67, 0.87 and 1.6 micron
- Spatial resolution of 1 km (as AVHRR)
- Dual-view: nadir and inclined 55 deg to nadir for direct measurement of atmospheric effects, eliminating in particular error due to aerosol contamination
- Low-noise detectors cooled to 80 K

SLSTR (GMES Sentinel-3)

- Additional SWIR channels: 1.38 and 2.25 micron
- 1-km resolution for TIR, better (0.5 km) for VNIR/SWIR
- Dual-view achieved over 750 km (faster revisit)
- Single view (nadir) over 1420 km swath
- Swaths overlapping with (inside) that of imaging spectrometer (OLCI) on Sentinel-3
- Additional land-related objectives:
  - Costal zones and vegetation monitoring
  - Fires detection and monitoring

principle of the atmospheric correction

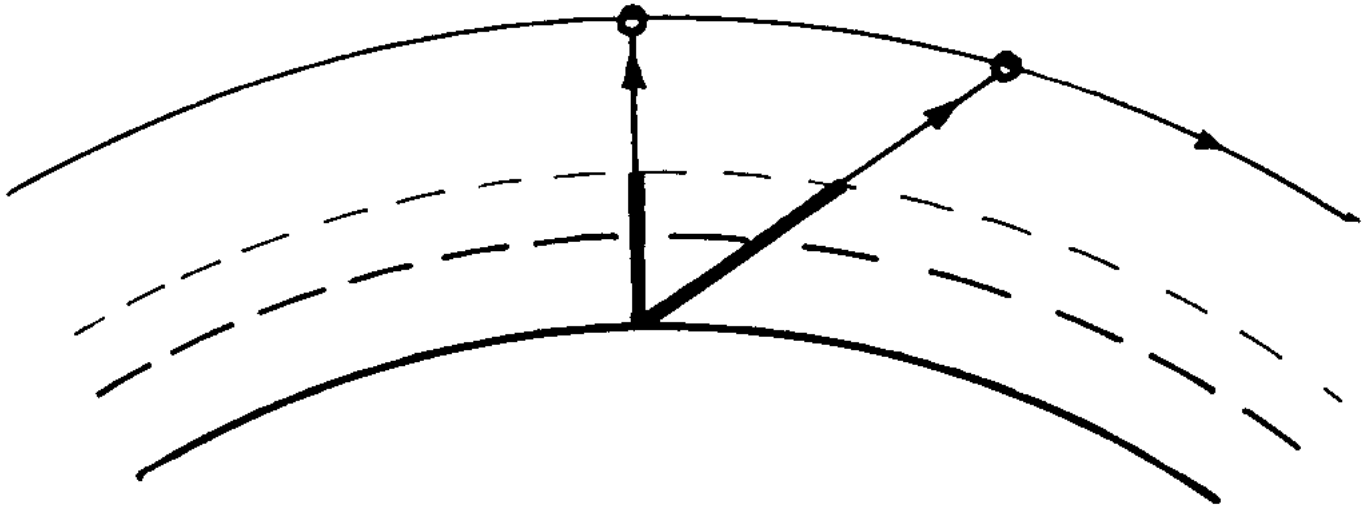

• the oblique view results in looking through longer path length of atmosphere than for nadir viewing

• by viewing the same area of sea twice, through different lengths of atmosphere, an objective estimate of atmospheric effect can be made

SLSTR observation geometry

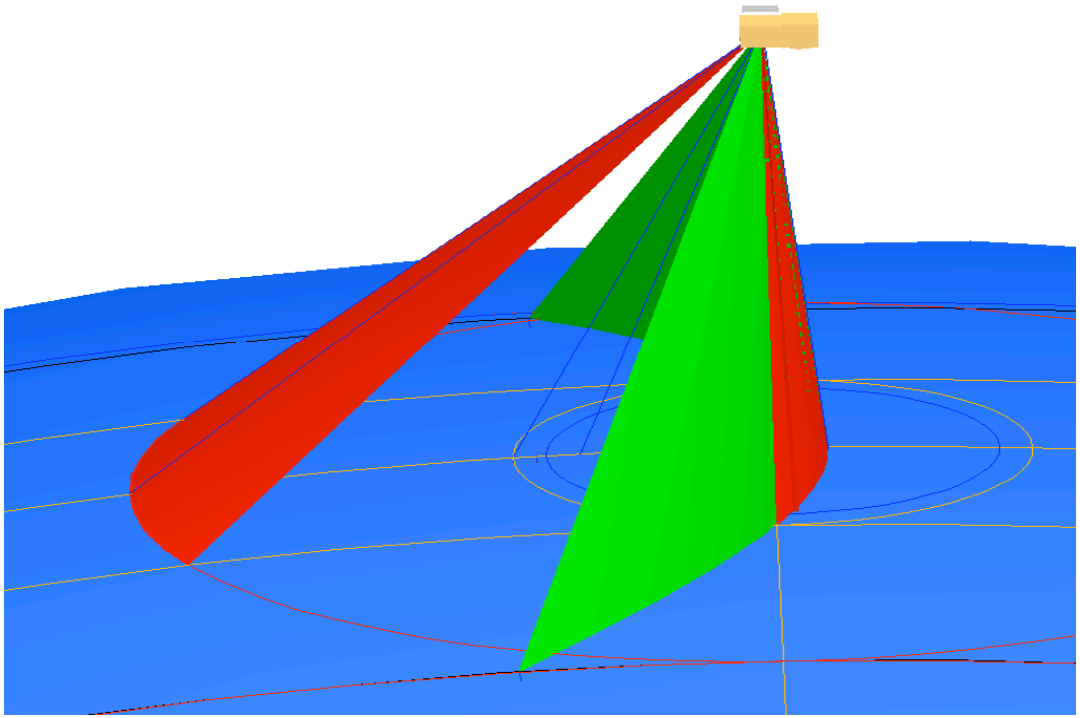

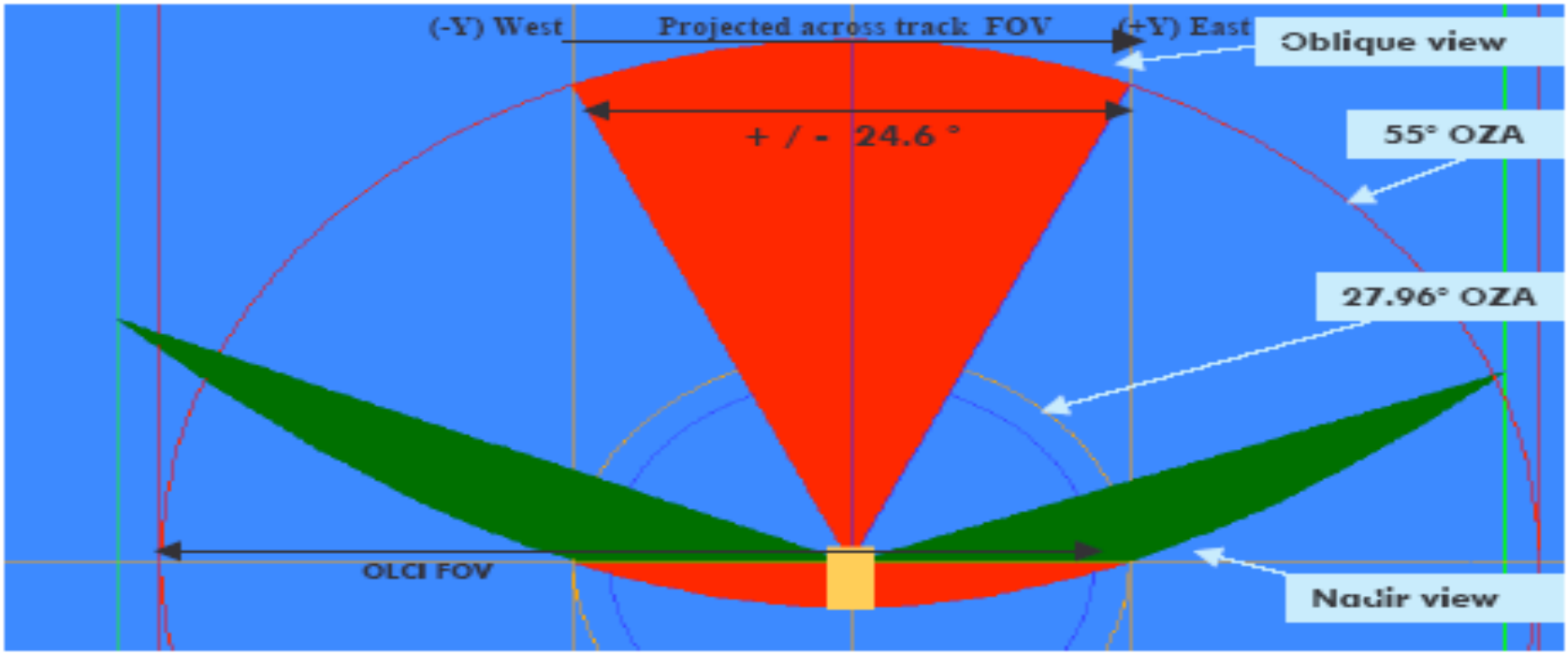

swaths of SLSTR and OLCI on Sentinel-3

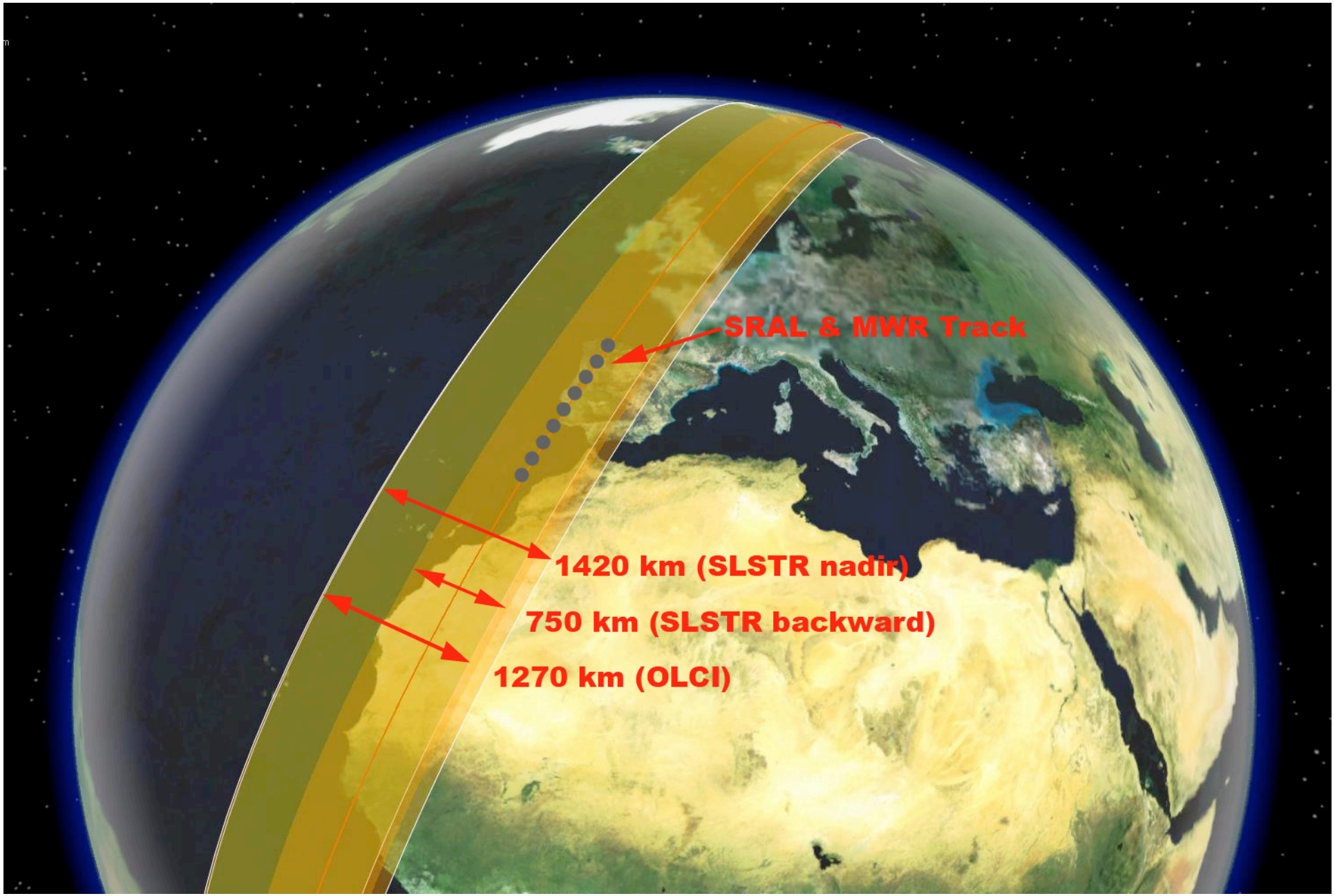

sensor design and role of on-board calibration

- design emphasizing straylight rejection and stable (low) temperatures

- on-board calibration, paramount to long-term accuracy:
  - stable blackbody targets for infrared calibration: two are provided, at different temperatures (AVHRR: single blackbody), with materials chosen for stability and uniformity, and temperatures accurately measured
  - visible channels (for image interpretation) also calibrated
  - detector response accurately measured on-ground (characterisation)

SLSTR overview

Radiometric performance:

- sensitivity, NEdT < 0.08K (TIR)
- SNR > 20 (solar @ Lmin) for vis/SWIR
- Absolute accuracy < 2-5%, 0.2 K
- Radiometric stability < 0.1%, 0.08 K
- Polarisation sensitivity < 0.07

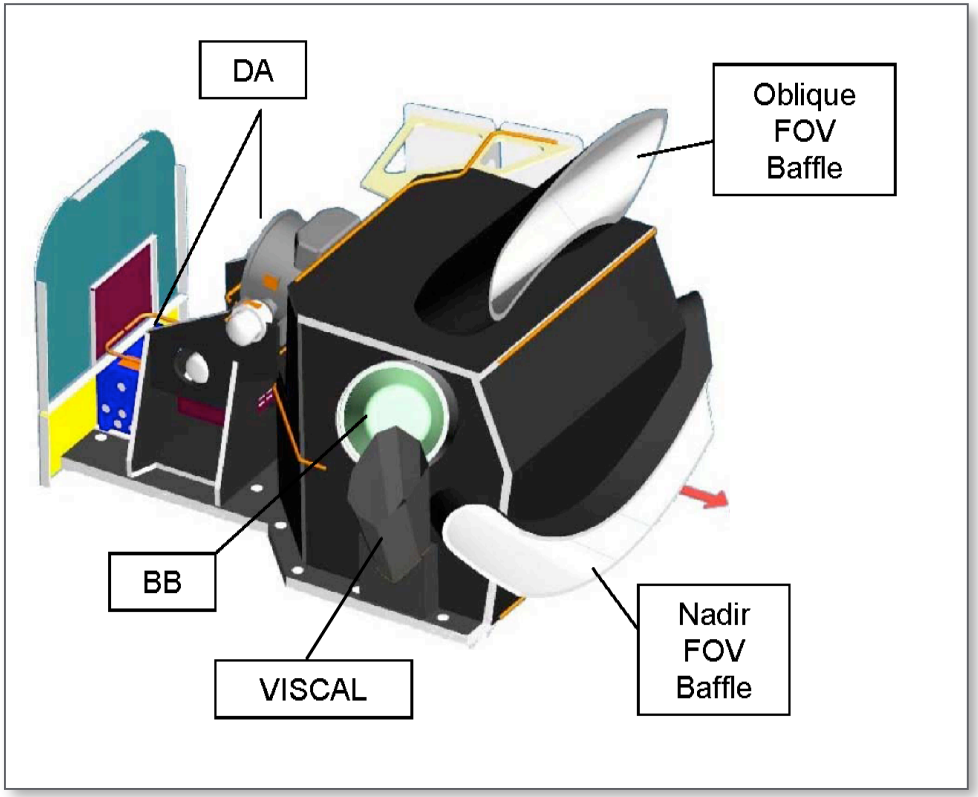

Some design features

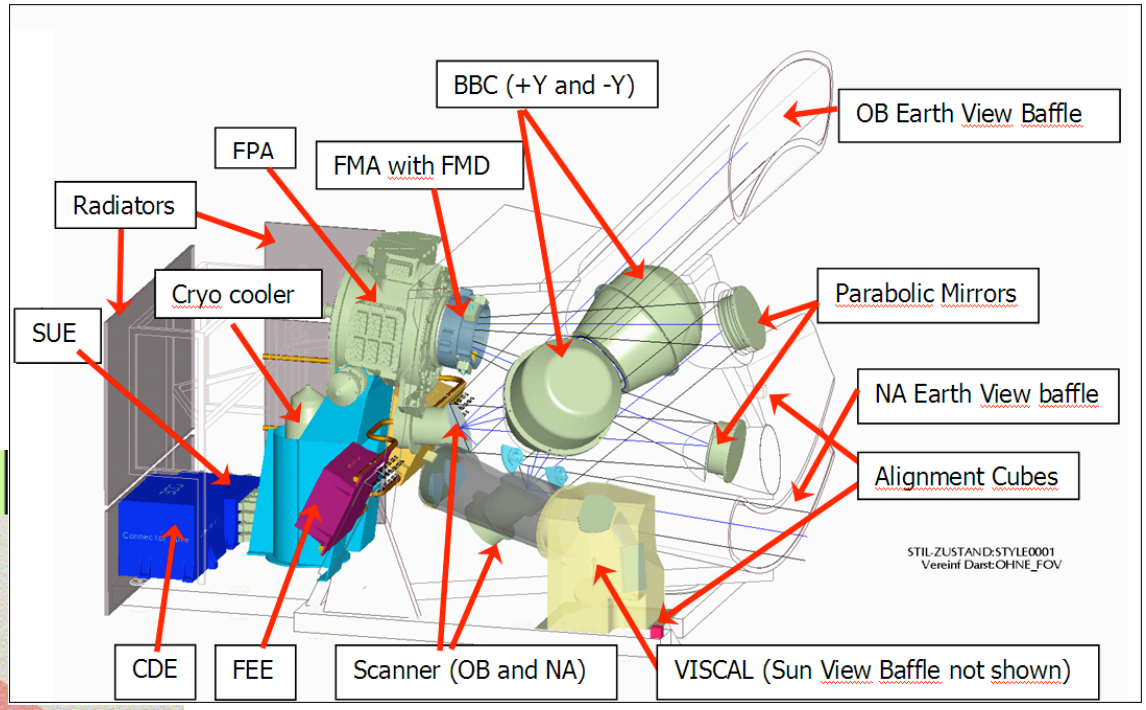

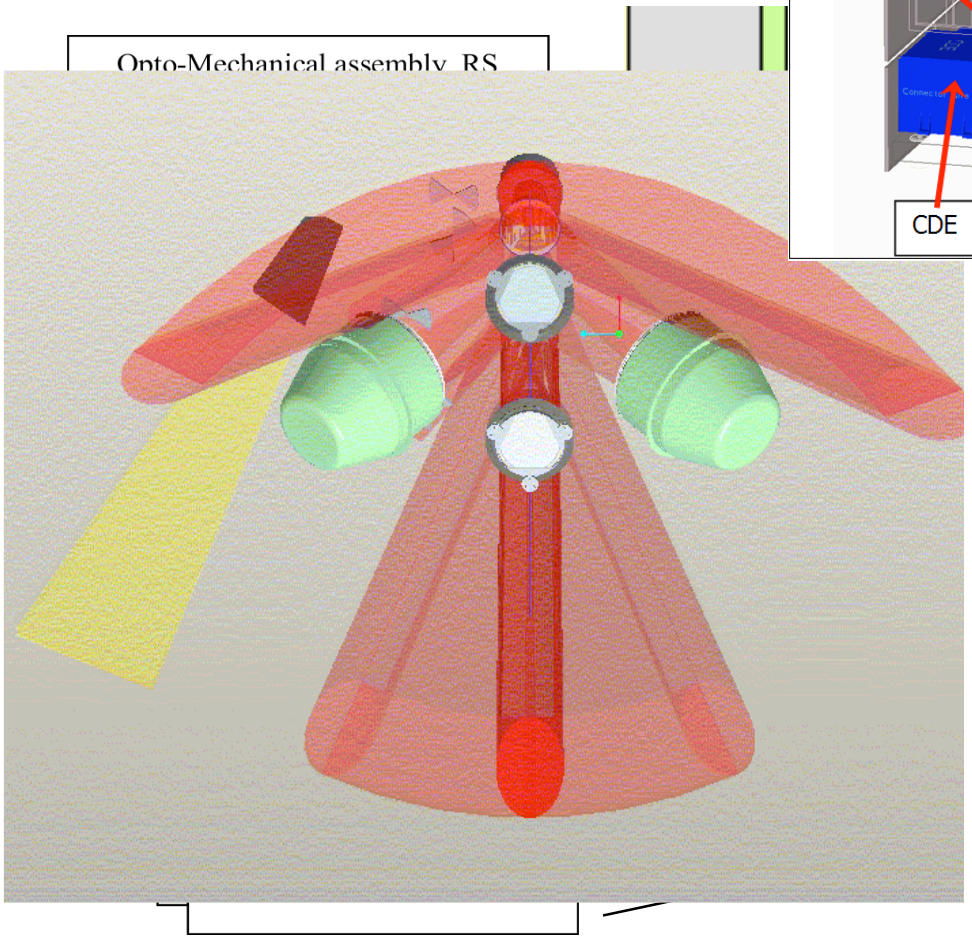

EARTH BACKWARD VIEW

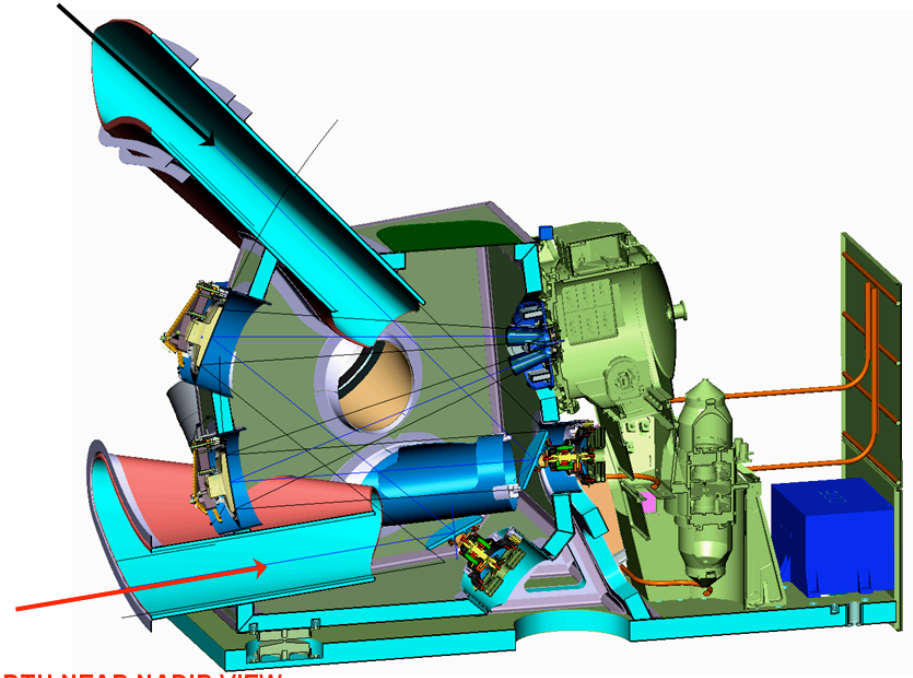

EARTH NEAR NADIR VIEW

SST from AATSR

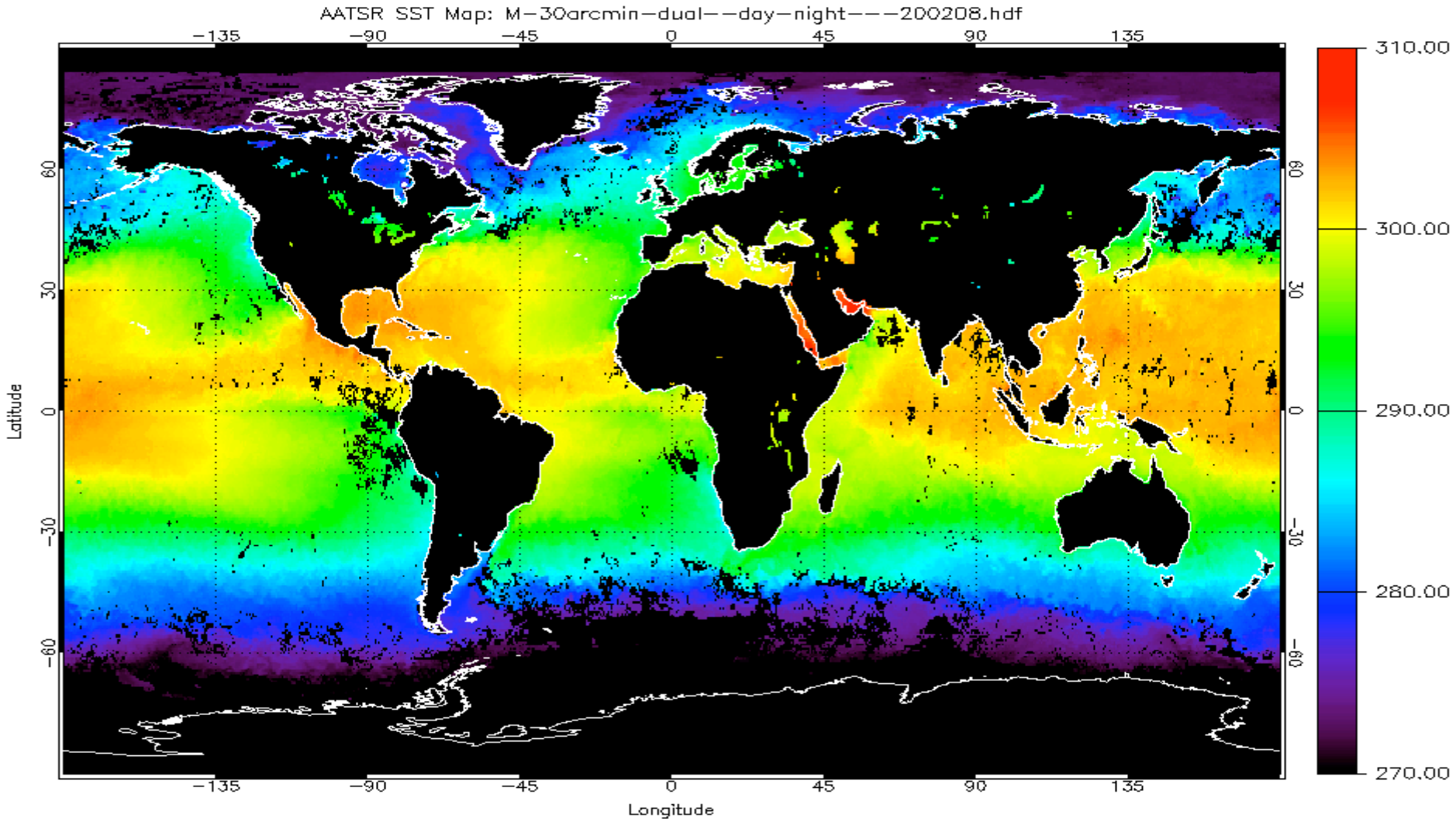

measurement of residual trends in global SST

ERS / Envisat
Trend: +0.13 K / decade

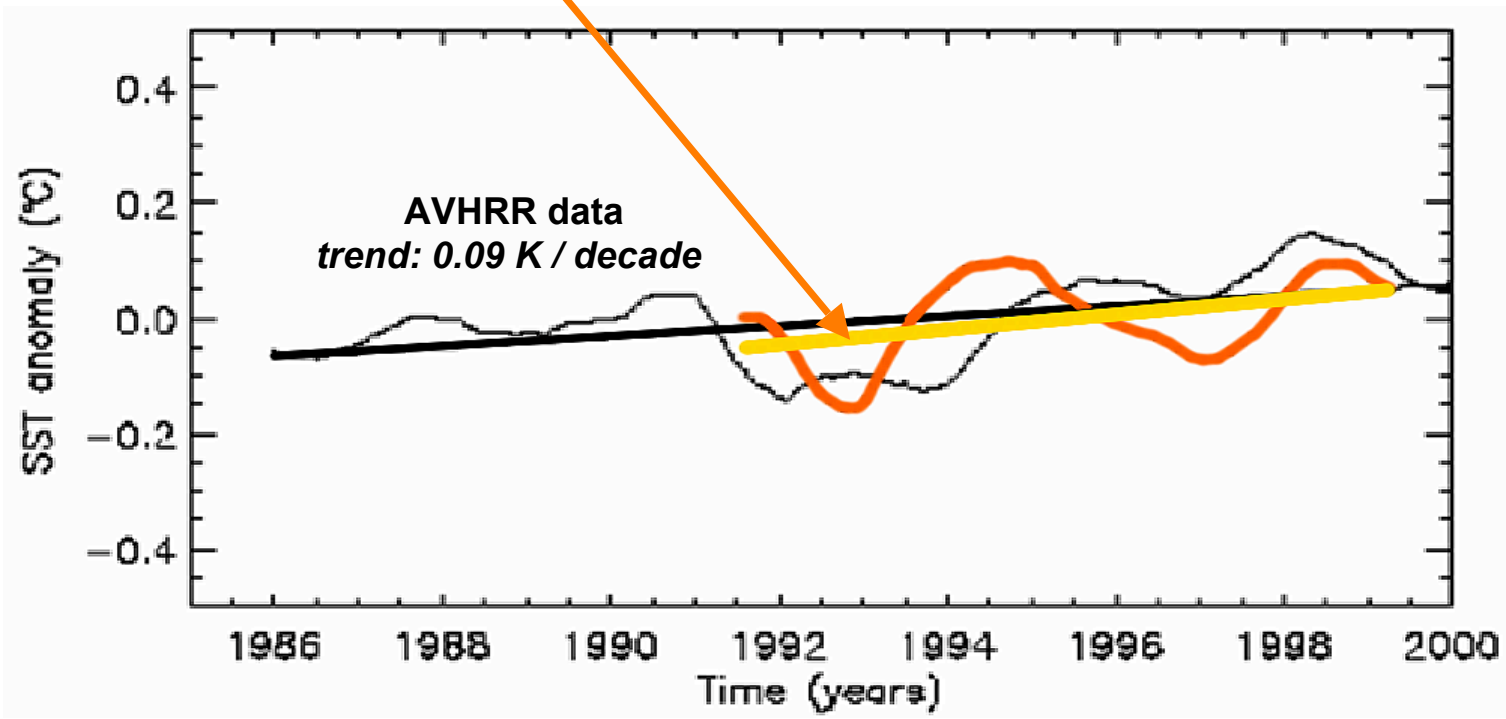

active microwave sensors: available bands
(and application examples)

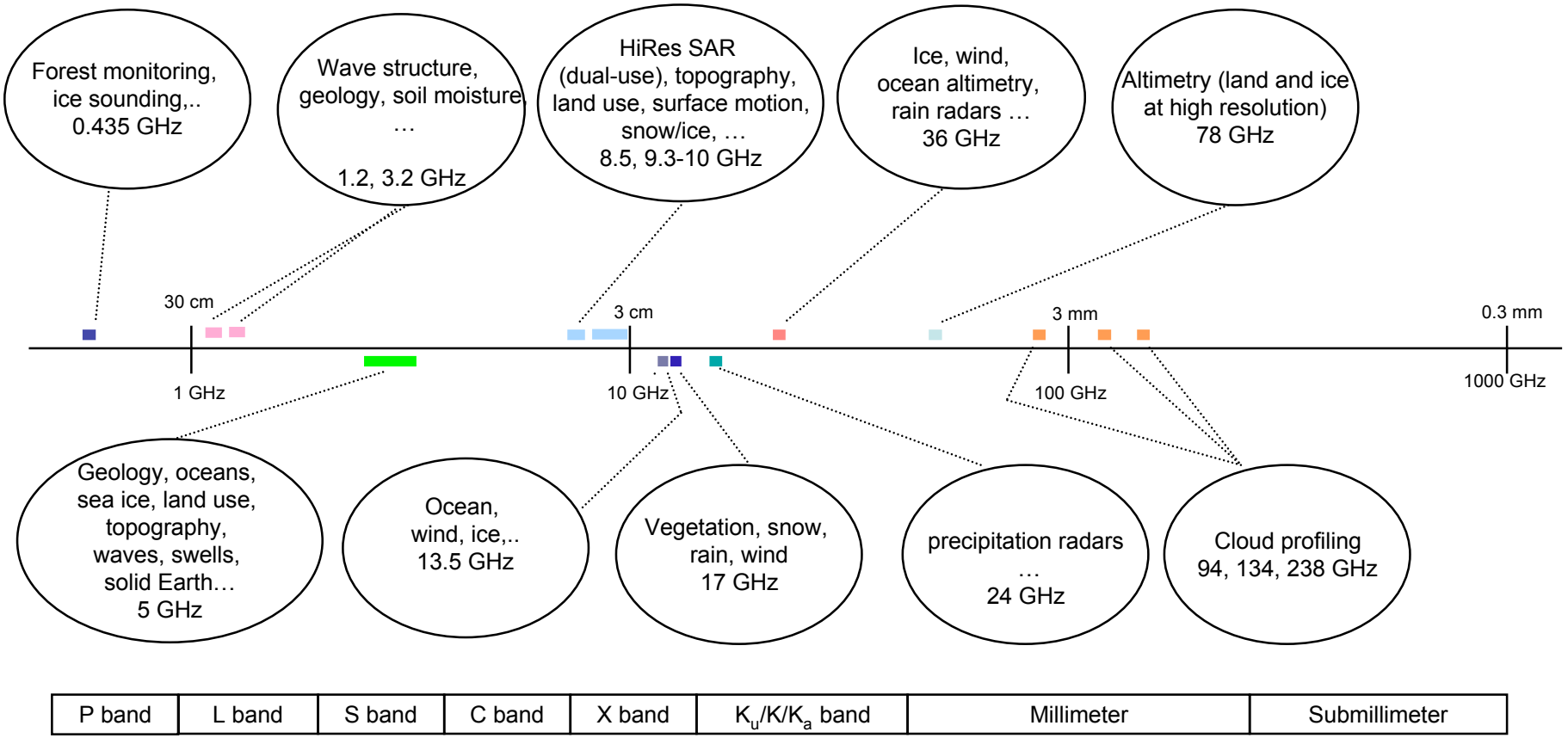

Radio Occultation (RO)

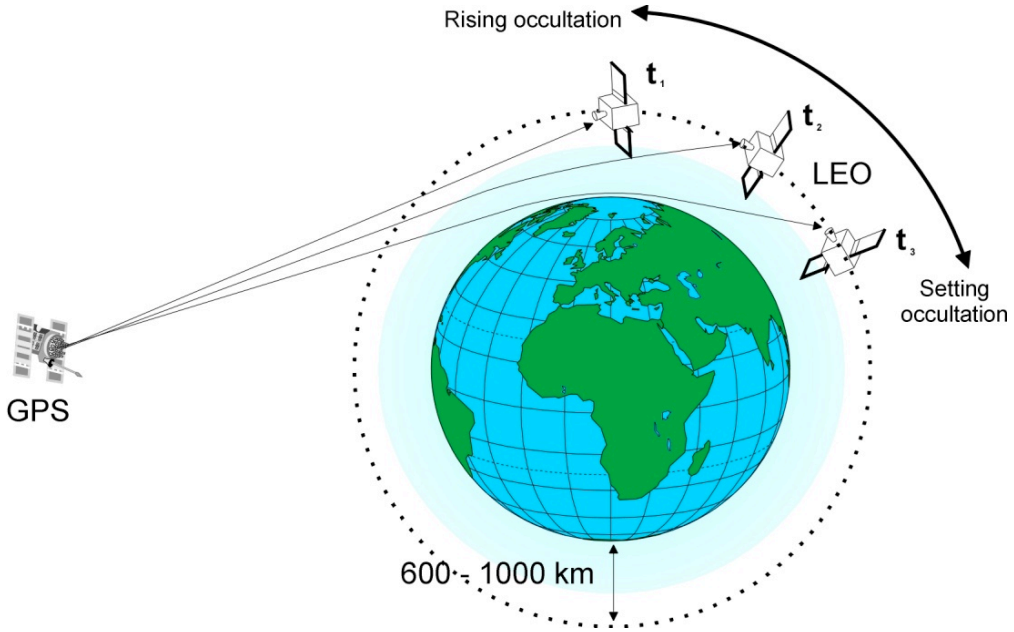

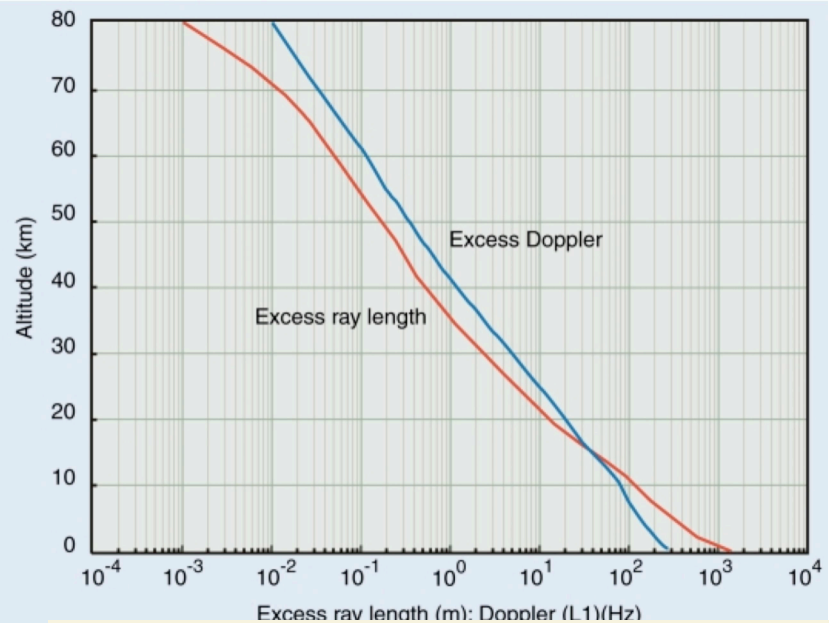

a “self-calibrating” technique - what more for benchmark?

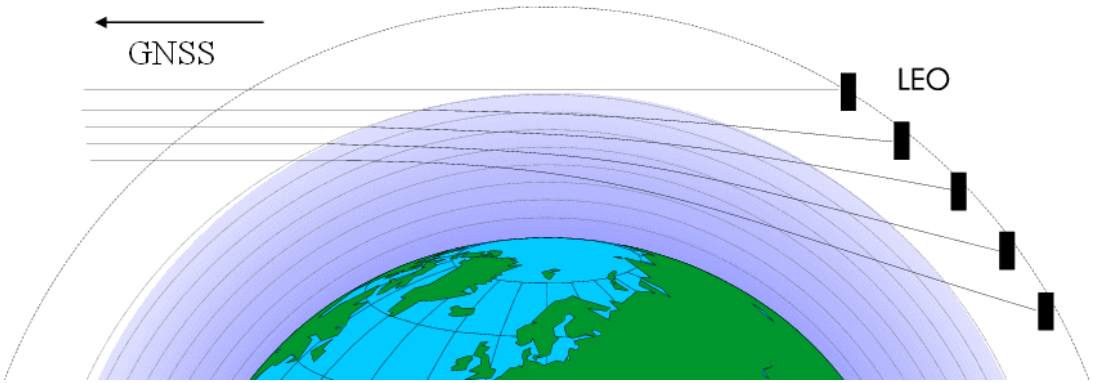

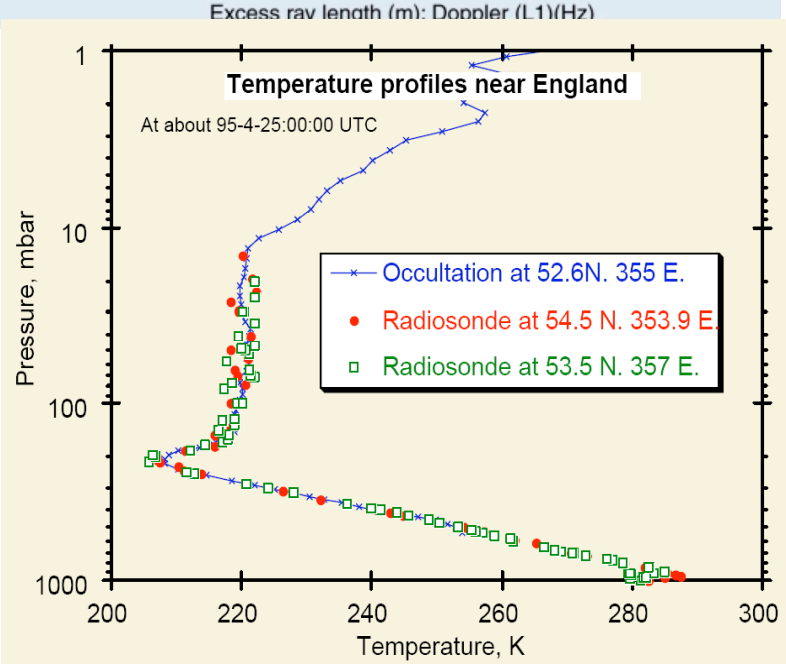

Radio Occultation Retrieval

Key relation for retrieval: $$N = (n-1)10^6 = 77.6\frac{P}{T} + 3.73\times 10^5\ \frac{e}{T^2} + 4.03\times 10^7\ \frac{n_e}{f^2} + 1.4W$$

N : refractivity; n : index of refraction; T : temperature (K); P : total pressure (millibar); e : partial pressure of water vapour; n_e : electron density (m^{-3}); W: liquid water content (g/m^3)

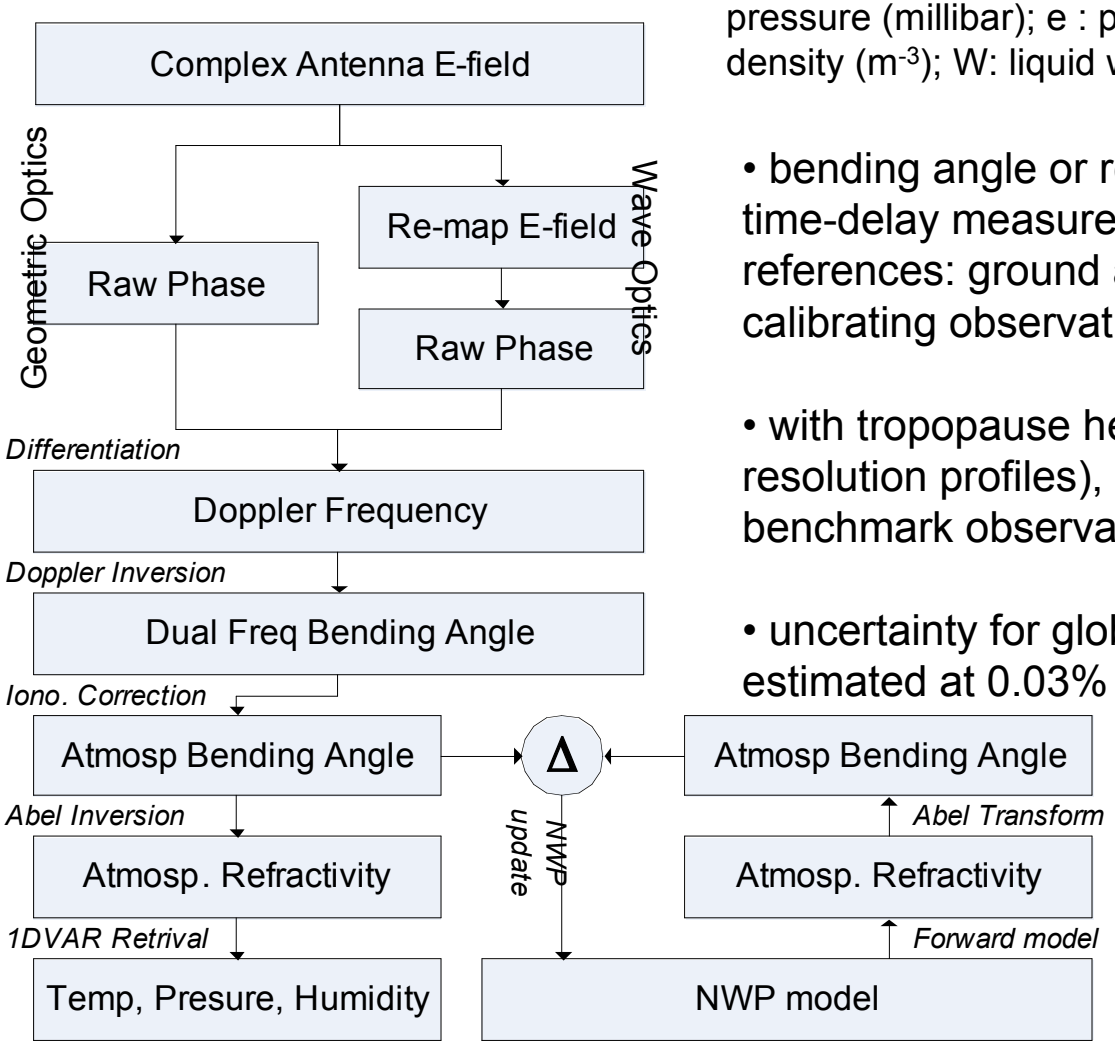

- bending angle or refractivity profiles are retrieved from time-delay measurements traceable to metrological references: ground atomic clocks => bias-free self-calibrating observations feasible

- with tropopause height (derived from the high-vertical-resolution profiles), the profiles can provide climate benchmark observations

- uncertainty for global refractivity trend monitoring was estimated at 0.03% over 5 year (Ho et al., JGR, vol 114, D23107)

RO products from MetOp and impact of different observing systems on ECMWF 24h forecasts

GRAS on MetOp observing GPS:
- 2 rising, 2 setting (atmosphere)
- 8 zenith (precise orbit determination)

providing as observations:
- about 650 profiles / day
- 0.2 km – 1 km vertical resolution

level 1b products (EUMETSAT):
- bending angle (within 2h 15 min)

level 2 products (GRAS SAF):
- refractivity (3h, pre-operational)
- temperature, water vapour (3h)

- proposals to extend occultation technique with ad-hoc transmitters / receivers on counter-orbiting satellites operating in K-band (water vapour profiling) and short-wave infrared (SWIR), to observe trace gases

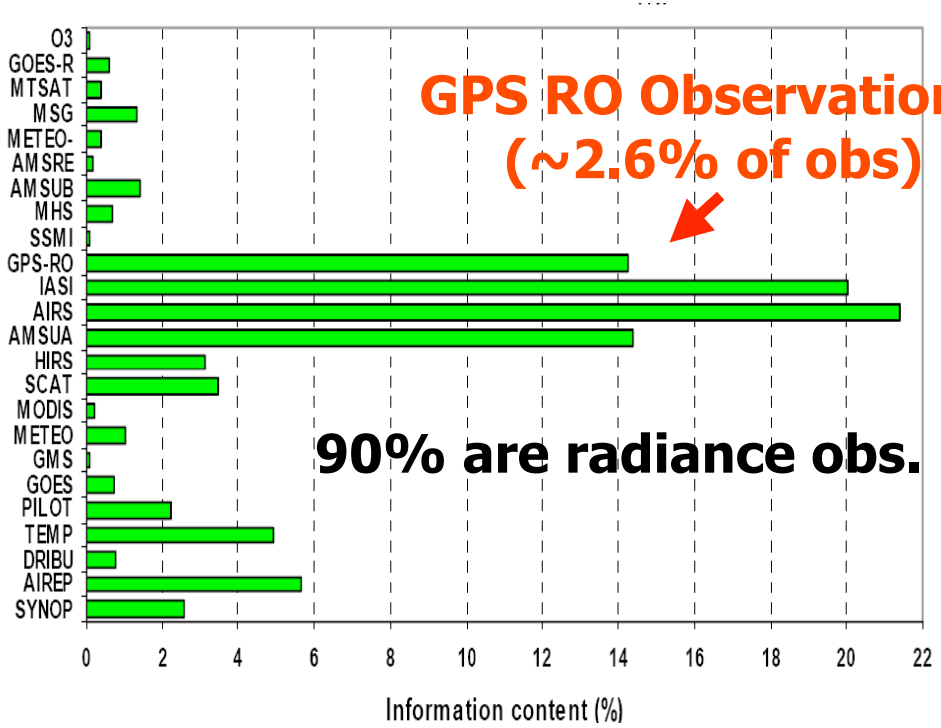

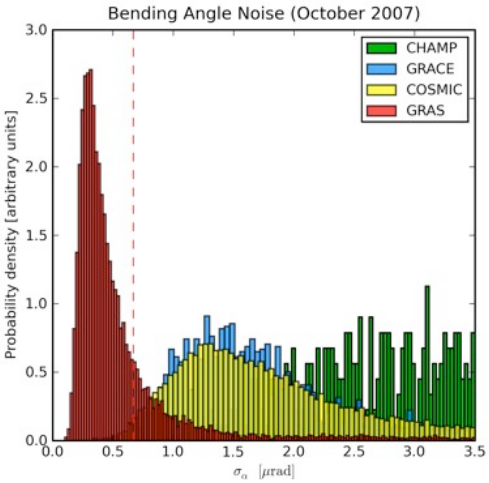

introduction to SAR

SAR basic product: 2D maps of radar reflectivity over a (wide) swath
Basic image is **complex**-valued (amplitude and phase) and 2-dimensional (range and azimuth)
SAR observes **strength** (detection) and **time delay** (ranging) of the return signals.

- advantages :
  - day and night operation
  - little effects of atmosphere (=> multi-temporal data analysis), except at highest *f*
  - sensitivity to dielectric properties (water content, biomass, ice,..)
  - sensitivity to surface roughness (ocean wind speed)
  - accurate measurements of distance (by interferometry)
  - sensitivity to artificial objects
  - sensitivity to target structure (use of polarimetry)
  - sub-surface penetration
  - …
- drawbacks:
  - complex interactions (understanding can be challenging, complex processing)
  - speckle effects (difficulty in visual interpretation)
  - topographic effects (side-looking, so sensitive to relief, even under vegetation cover)

RADAR SOIL PENETRATION

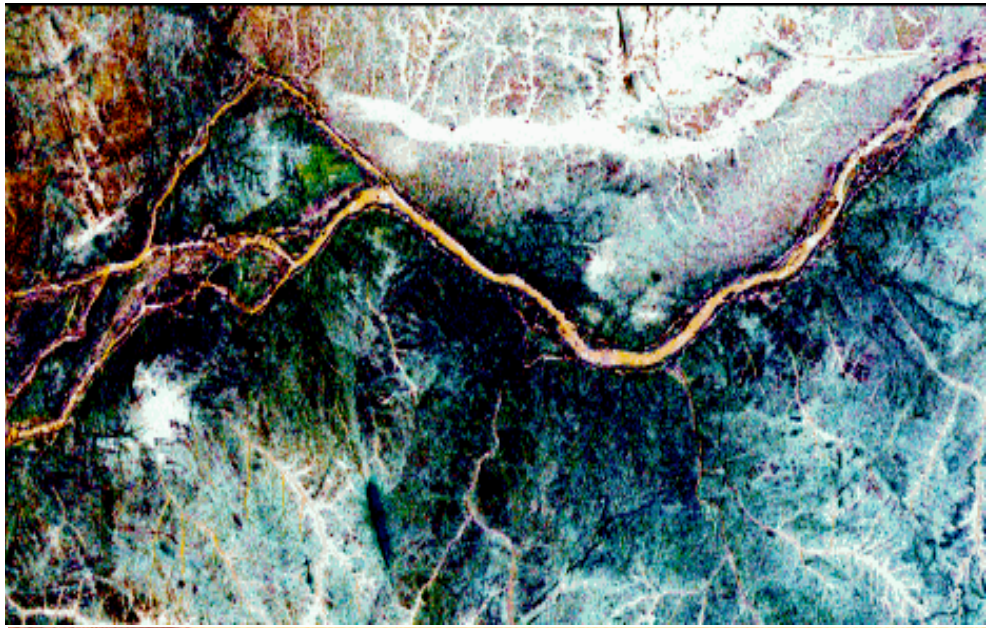

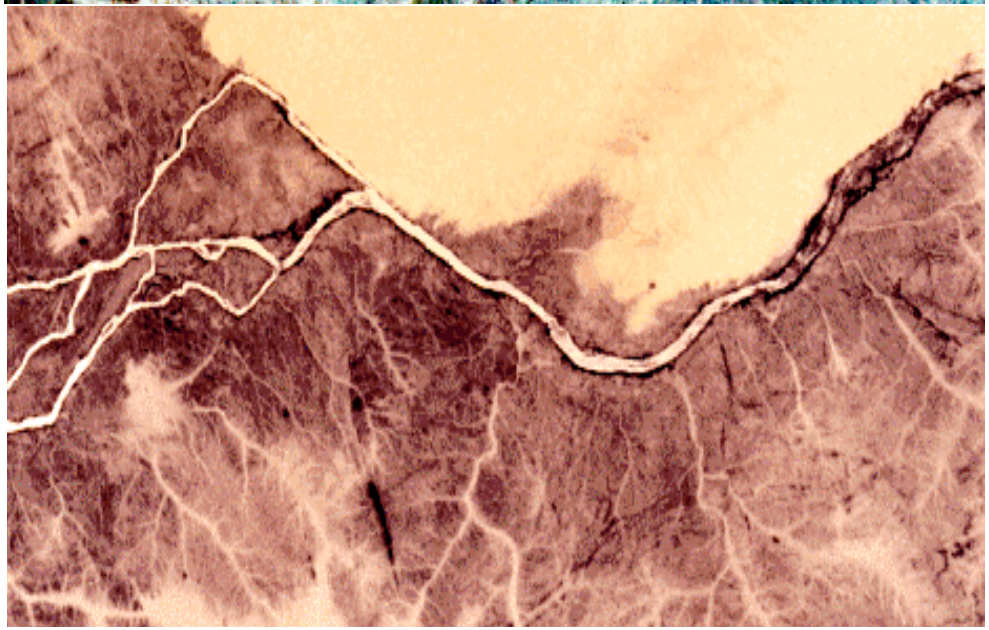

Left: SIR-C multi-frequency radar image (Nile)
(R : CHH, G : LHV, B: LHH).

Below: Wave penetration in bare soil for different SAR bands as a function of humidity

bande L ✖
bande C [
bande X u

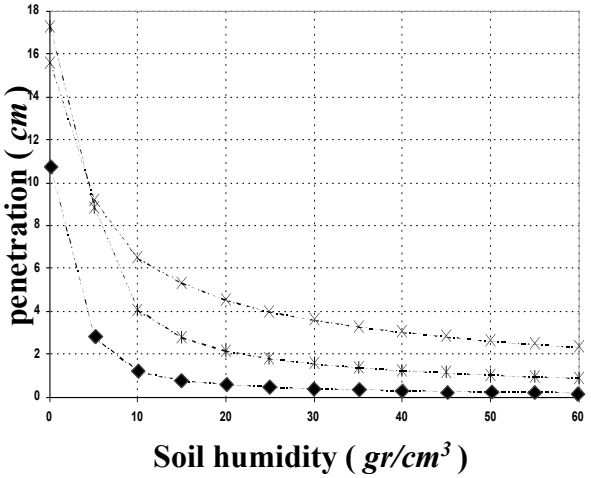

Left: IR optical image over the same region

From : www.jpl.nasa.gov/radar/sircxasr

Penetration in L band (23 cm)

In the LANDSAT-TM optical image (yellow-orange) a uniform sand cover is visible, masking the structures underneath.

The SIR-C image (gray shades) reveals the ancient river beds buried under the sand (source USGS)

oriental Oued Sahara (North-West Sudan)

source : http://www.observ.u-bordeaux.fr/~paillou/paillou.html

imaging radars

- use time-delay information (effective short pulse)
- two types: real-aperture radar and synthetic-aperture radar (SAR)
- real-aperture radar: resolution determined by antenna beamwidth in along-track direction (azimuth) and by pulse width in cross-track direction (range)
- SAR: **high-resolution image** of the surface over a wide swath to one side of ground track, using the satellite forward motion to synthesize a long antenna

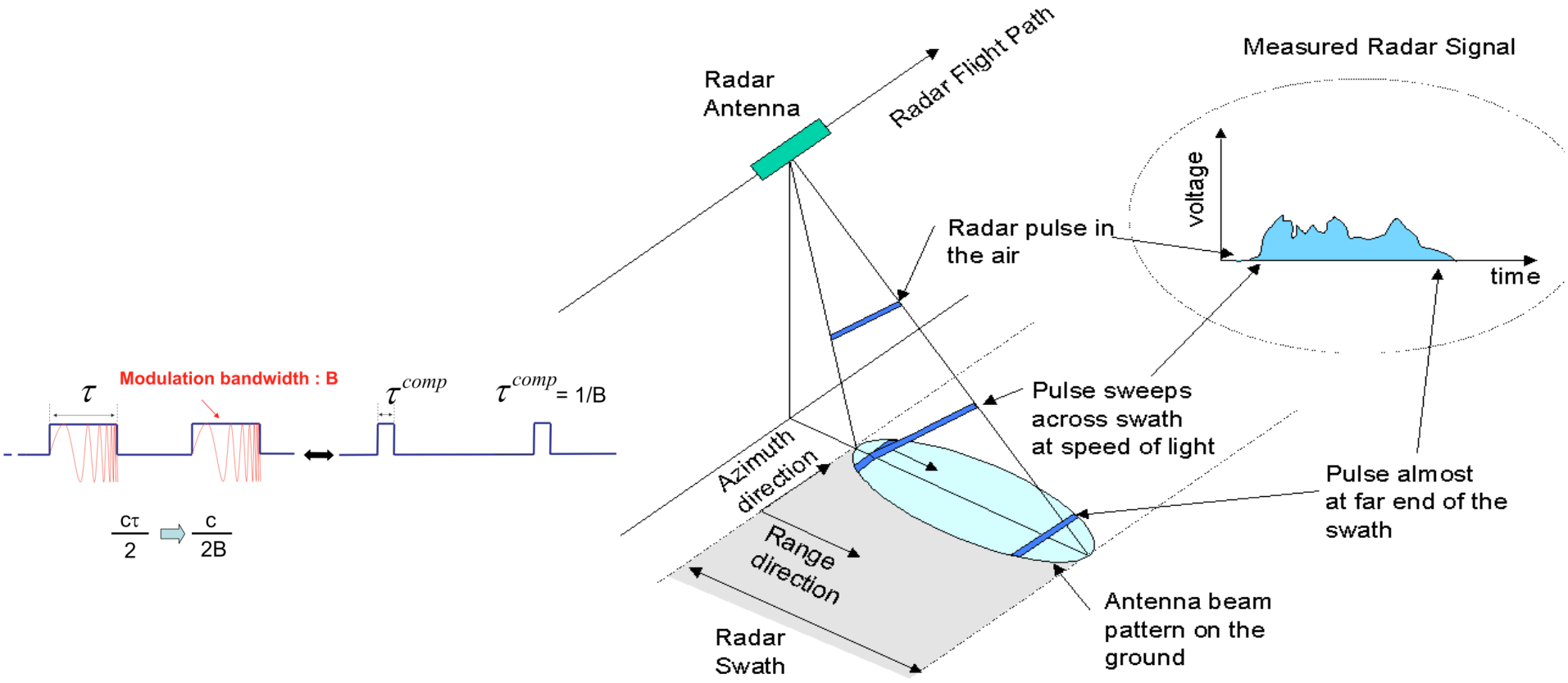

basic SAR principle

• the single antenna moving along the flight path is equivalent to an array of antennas if the received signals are coherently processed and the target can be assumed static

• the echoes at successive positions are recorded coherently, i.e. both amplitude and phase as function of time (“complex image”)

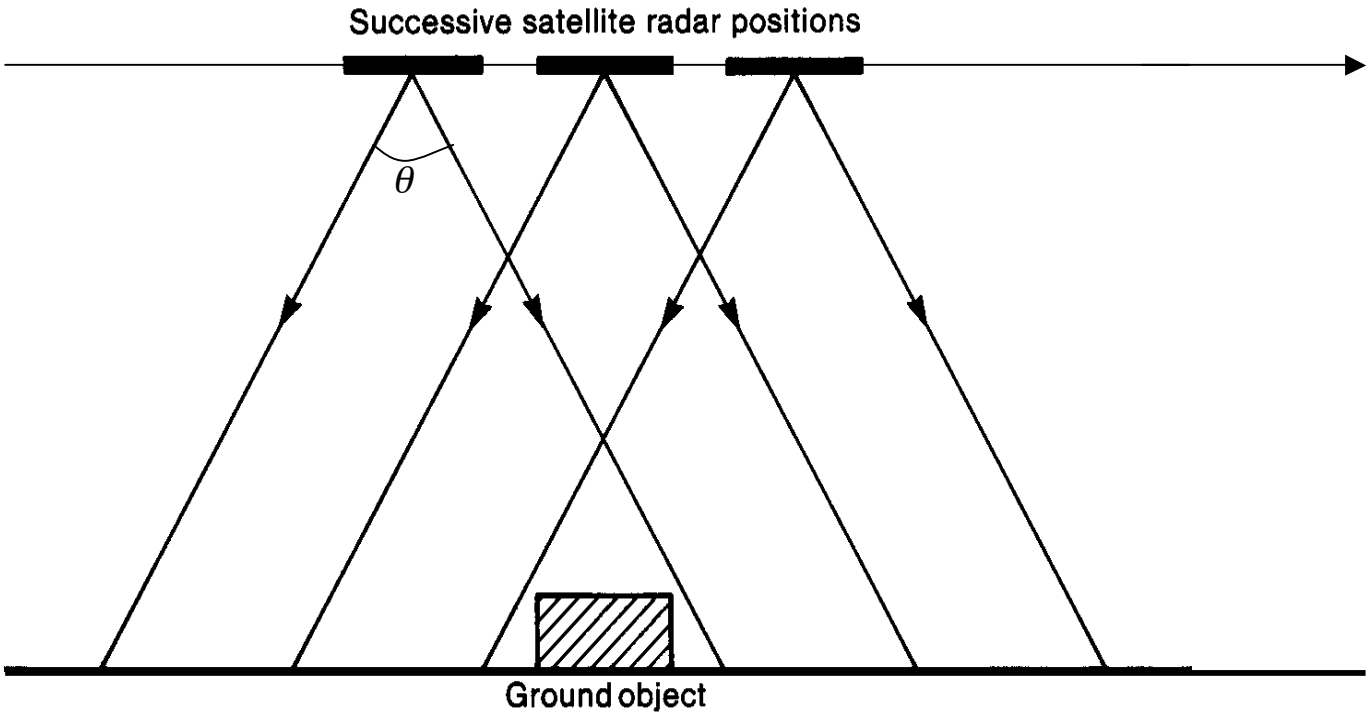

SAR azimuth resolution

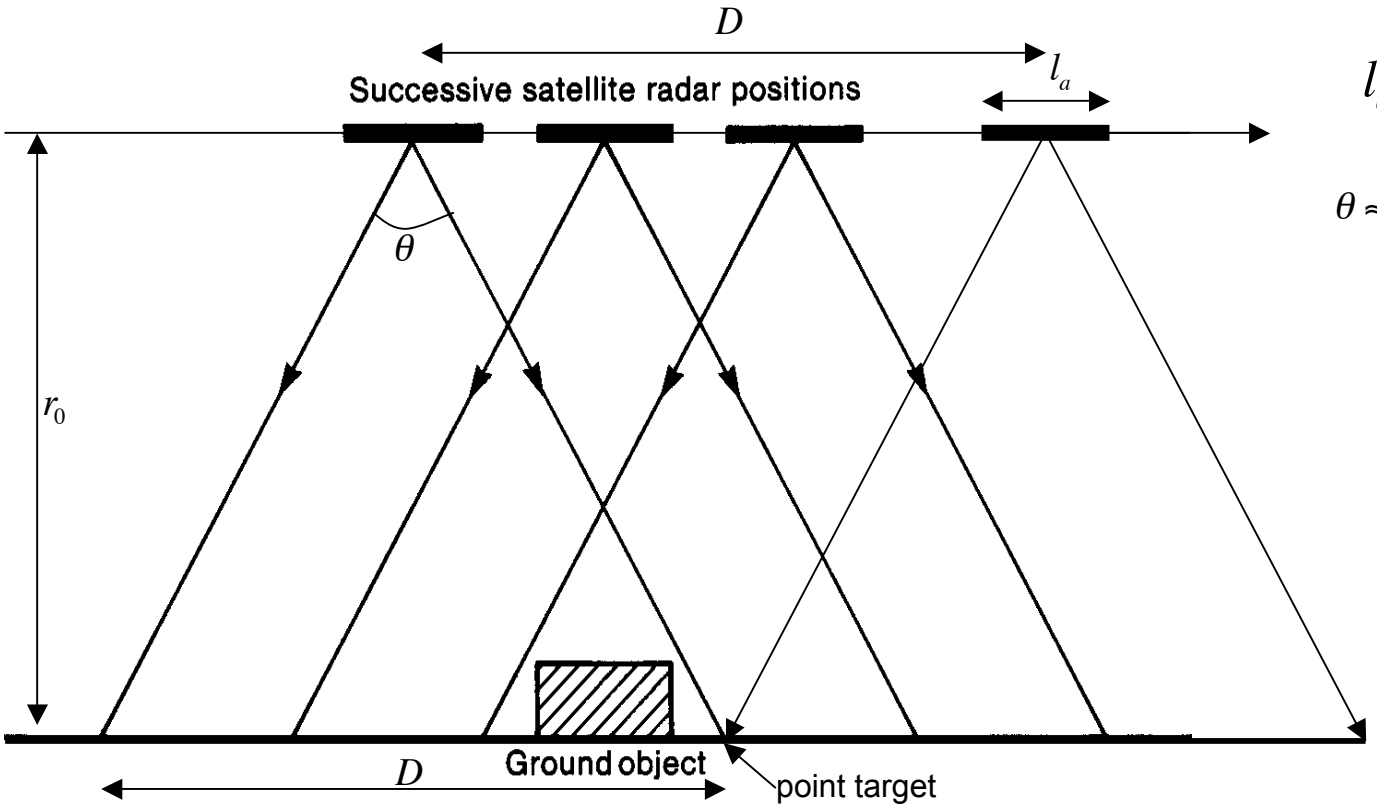

l_a : real azimuth aperture length

$\theta \approx \frac{\lambda}{l_a}$: real aperture beamwidth

$$D \approx r_0 \theta \approx \frac{r_0 \lambda}{l_a}$$

point target observed over the (integration) time:

$$T = \frac{D}{v} \approx \frac{r_0 \lambda}{v l_a}$$

SAR azimuth resolution

similar approach used in SAR (doppler) altimetry

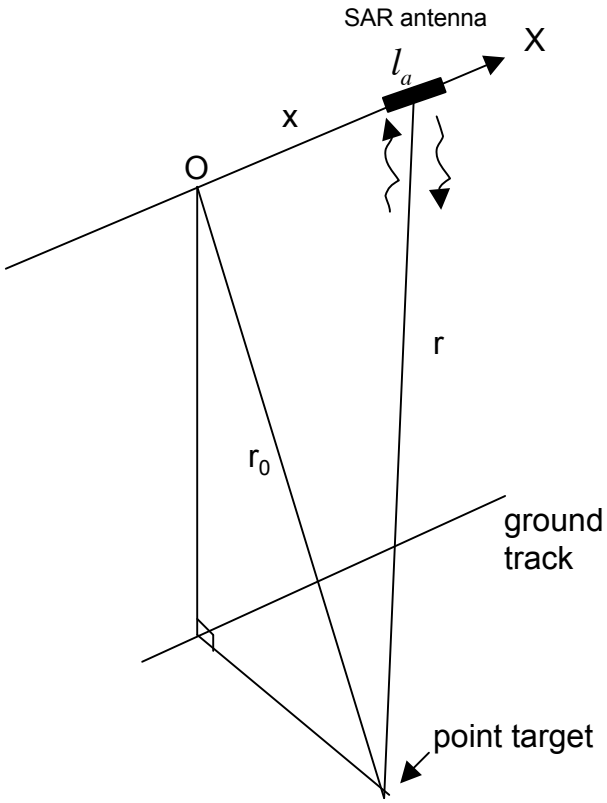

r_0 = range at closest approach

$$r = \left(r_0^2 + x^2\right)^{1/2} = r_0\left(1 + \frac{x^2}{r_0^2}\right)^{1/2} \cong r_0 + \frac{x^2}{2r_0}$$

resolution gain in azimuth direction for ERS: 5 km -> 5 m)

two-way phase of the pulse echoes:

$$\phi(x) = -2kr = -\frac{4\pi}{\lambda} r \cong -\left(\frac{4\pi}{\lambda} r_0 + \frac{2\pi}{\lambda r_0} x^2\right) = \phi_0 - \frac{2\pi}{\lambda r_0} x^2$$

SAR principle: combine the echo sequence coherently, like a long linear array, to get the effect of a large along-track antenna

Two-way phase is function of time, hence Doppler frequency shift f_D is found as:

$$\phi(t) = \phi_0 - \frac{2\pi}{\lambda r_0} v^2 t^2$$

$$f_D(t) = \frac{1}{2\pi}\frac{d\phi}{dt} = -\frac{2v^2}{r_0\lambda} t = -\frac{2v}{r_0\lambda} x$$

If Δx is azimuth target extent at max resolution, the corresponding Doppler bandwidth is:

$$\Delta f = \frac{2v}{r_0\lambda}\Delta x$$

Doppler resolution equals reciprocal of integration time, so:

$$\Delta f = \frac{1}{T} \Rightarrow \frac{2v}{r_0\lambda}\Delta x \approx \frac{v l_a}{r_0\lambda} \Rightarrow \boxed{\Delta x = \frac{l_a}{2}}$$

a smaller real antenna gives higher resolution because it allows a longer synthetic aperture

SAR resolutions and ScanSAR

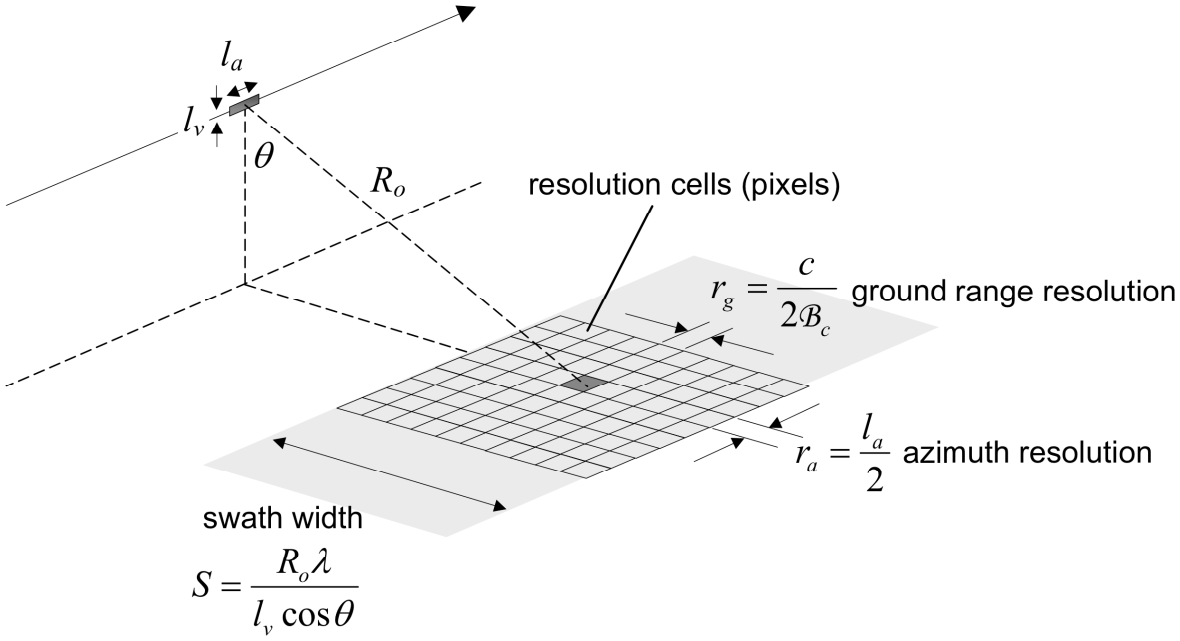

ground range and azimuth resolutions for single-look image

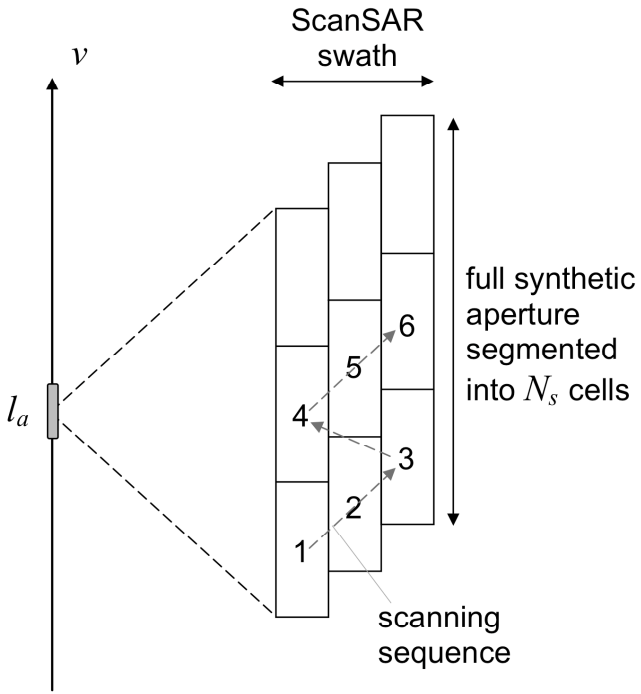

ScanSAR concept

actual azimuth resolution: $r_a = N_L N_S \frac{l_a}{2}$

exploiting multiple SAR images

SAR systems can be multi-temporal, multi-polarisation, multi-frequency:

- **polarimetric images** if the SAR system is polarimetric, i.e. able to transmit/receive EM radiation of different polarisations
- **interferometric images** (coherence, phase), e.g. Envisat ASAR repeat pass
- **multi-polarisation intensity images,** e.g. ASAR dual-pol
- **multi-temporal intensity images**

Multitemporal imaging

example of physical interpretation: dependance of volume scattering on wavelength

- SAR measure the back-scattered signal resulting from surface scattering, volume scattering, multiple volume-surface scattering
- volume scattering in a canopy: main scatterers are the elements with dimension of the order of the wavelength

Austrian pine | **X band** $\lambda = 3$ cm | **L band** $\lambda = 27$ cm | **P band** $\lambda = 70$ cm | **VHF** $\lambda > 3$ m

RADAR POLARIMETRY

The POLARISATION information in the waves backscattered from a given target is strongly related to:

1) its geometrical structure, reflectivity, shape and orientation
2) its properties such as humidity, roughness, …

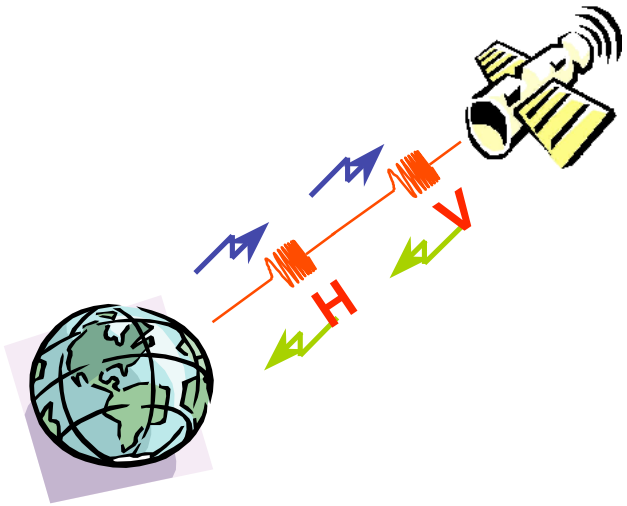

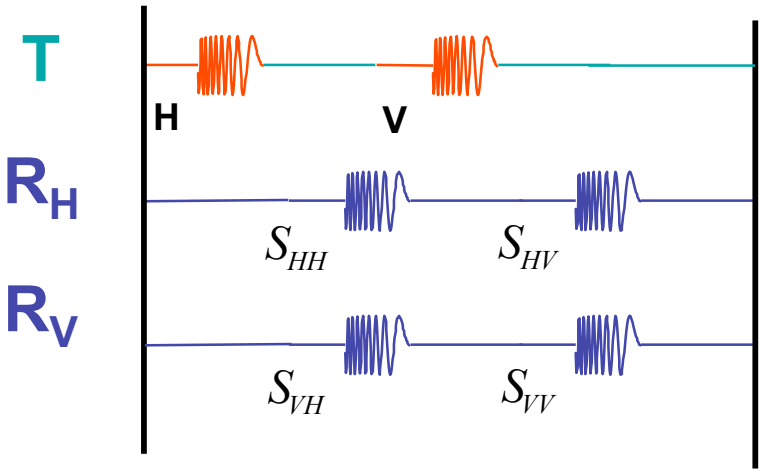

TRANSMITTER: H & V
RECEIVERS: H & V

$$\left\{[S]=\begin{bmatrix} S_{XX} & S_{XY} \\ S_{YX} & S_{YY} \end{bmatrix}\right\}$$

SINCLAIR MATRICES

SCATTERING POLARIMETRY

Polarimetric Interferometric SAR (POL-InSAR)

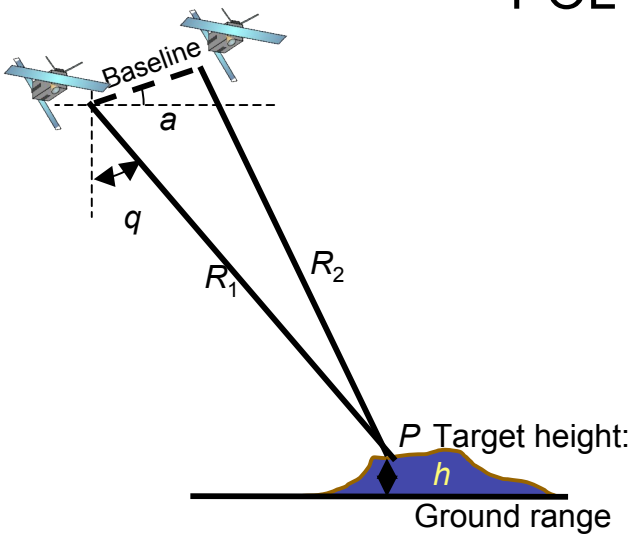

POL-InSAR combines two separate radar technologies

polarimetry + interferometry

Altimetric information associated to each backscattering process

3D structure of canopy

Extraction of important bio and geophysical parameters

The combination of interferometry with polarimetry is **greater** than the sum of its parts: POLInSAR allows to overcome limitations of each technique

POLARIMETRY AND INTERFEROMETRY

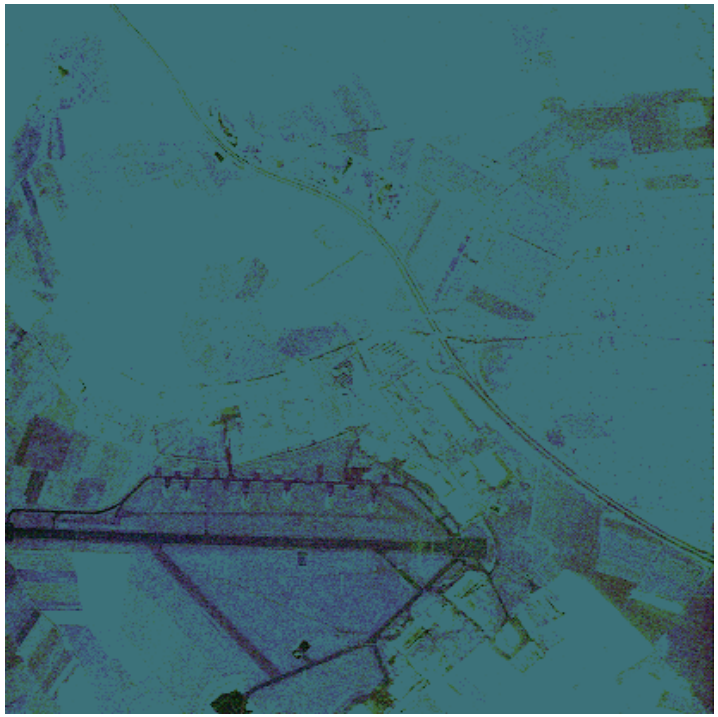

DLR E-SAR L Band
In-Pol SAR (1.5m x 3m) – Baseline 5m

POL-SAR INFORMATION

IN-SAR INFORMATION γ

COMPLEMENTARY INFORMATION

SAR Interferometry to measure small terrain motion

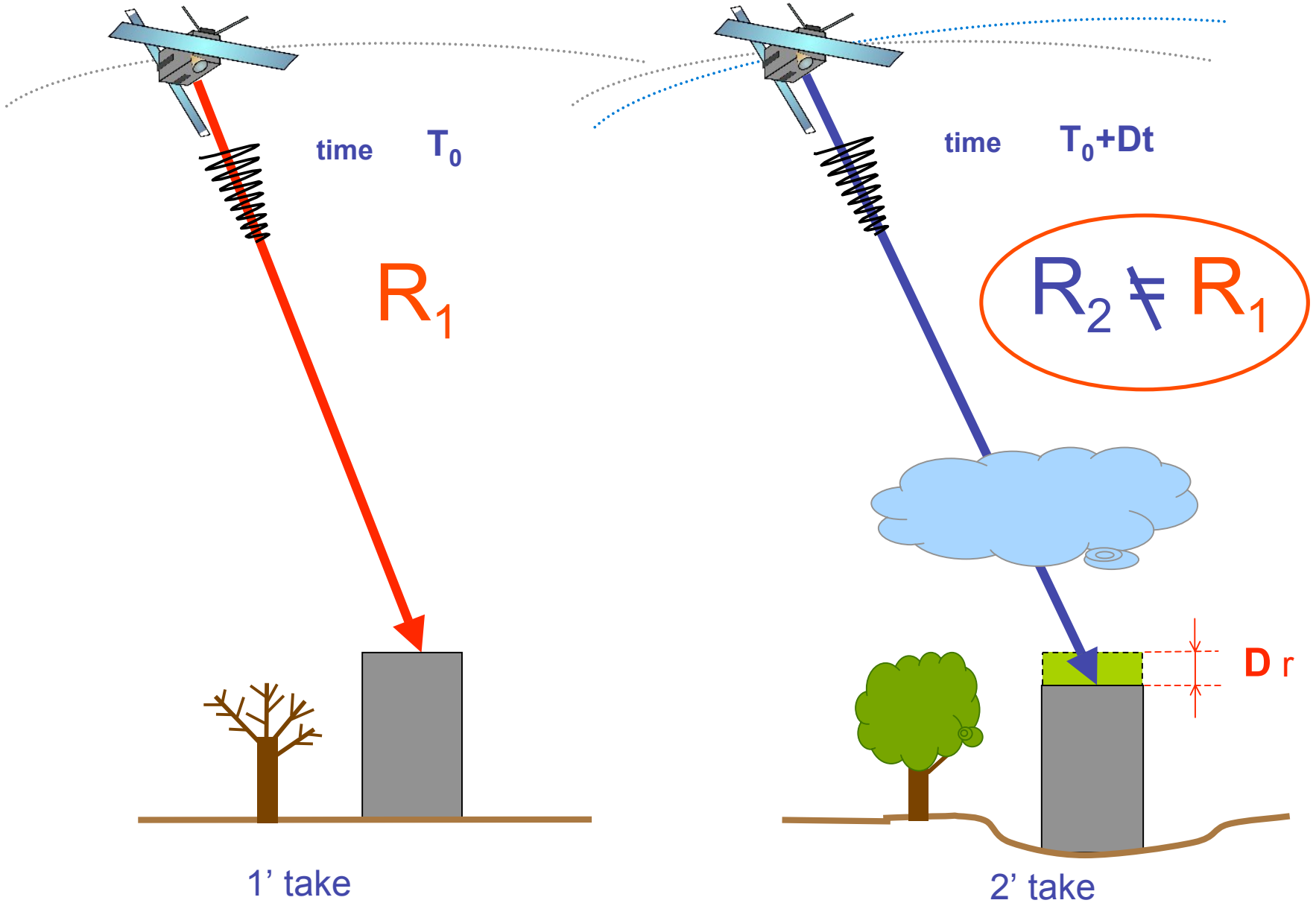

Courtsesy Polimi

SAR Interferometry for Digital Elevation Models

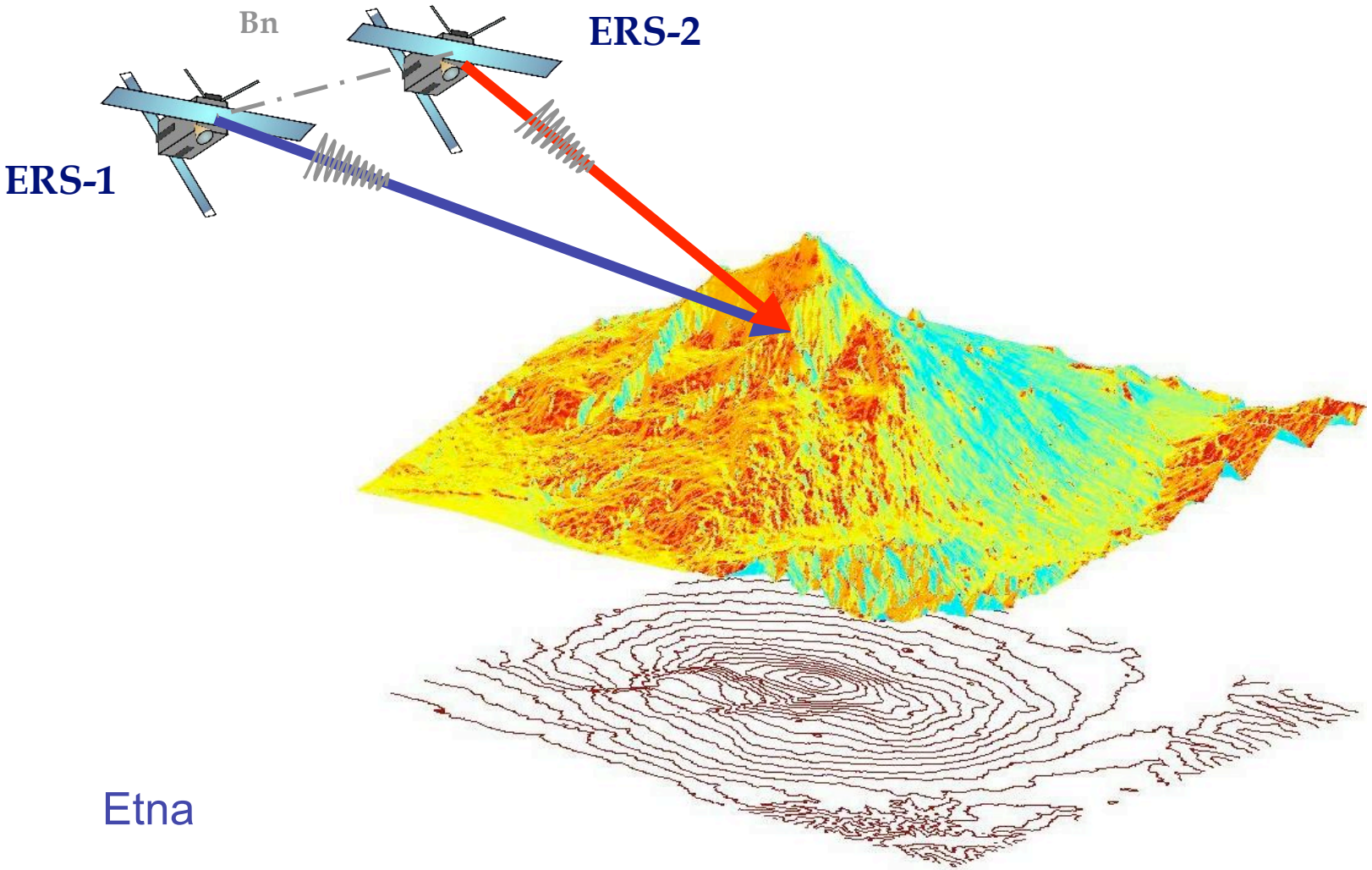

Courtsesy Polimi

some SAR missions

Satellite/SAR	Country	Launch	Res (m)	Band	Polarization
Quill	USA	1964	(>100 m)	X	
Seasat	USA	1978	25	L	HH
SIR A; B	USA	1981; '84	40; ~25	L	HH
SIR C	USA; G, I	1994, '94	~30	L&C; X	Various to quad; HH
Kosmos 1870	USSR	1987	15–30	S	HH
Almaz	USSR	1991	15–30	S	HH
ERS-1	ESA	1991	25	C	VV
J-ERS-1	Japan	1992	30	L	HH
RADARSAT-1	Canada	1995	8, 25, 50, 100	C	HH
ERS-2	ESA	1995	25	C	VV
Priroda	Russia/Ukraine	1996	50	S, L	HH, VV
SRTM	USA; G, I	2000	~30	C, X	HH, VV
ENVISAT	ESA	2002	10, 30, 150,1000	C	VV or HH, dual
IGS-1B	Japan	2003+	1, +	X	Multimode
PALSAR	Japan	2006	2.5–100	L	Various to Quad
JianBing-5	China	2006	3–20	L	Multi-polarimetric
TerraSAR-X	Germany	2007	1, 3, 15	X	Various
RADARSAT-2	Canada	2007	1, 3, 25, 100	C	Various to Quad
COSMO	Italy	2007	1, 3, 25, 100	X	Multi-polarimetric
TecSAR	Israel	2007	1–8	X	Multimode
Kondor-E	Russia	2007	1, +	S	Multimode
HJ-1-C	China	2007	1, +	S	Multimode
SAR-Lupe	Germany	2007	0.12, +	X	Multimode
Arkon-2	Russia	2008	1–50	S, L, P	Multimode
RISAT	India	2008	1–50	C	Various to Quad
Tandem-X	Germany	2009	1, 3, 1	X	Various to Quad
Radarsat-C	Canada	–	1, +	C	Various to Quad
MAPSAR	Brazil/Germany	–	3–20	L	Single, dual, quad
Sentinel-1	ESA	–	5–40	C	Various to Quad

ENVISAT ASAR Antenna

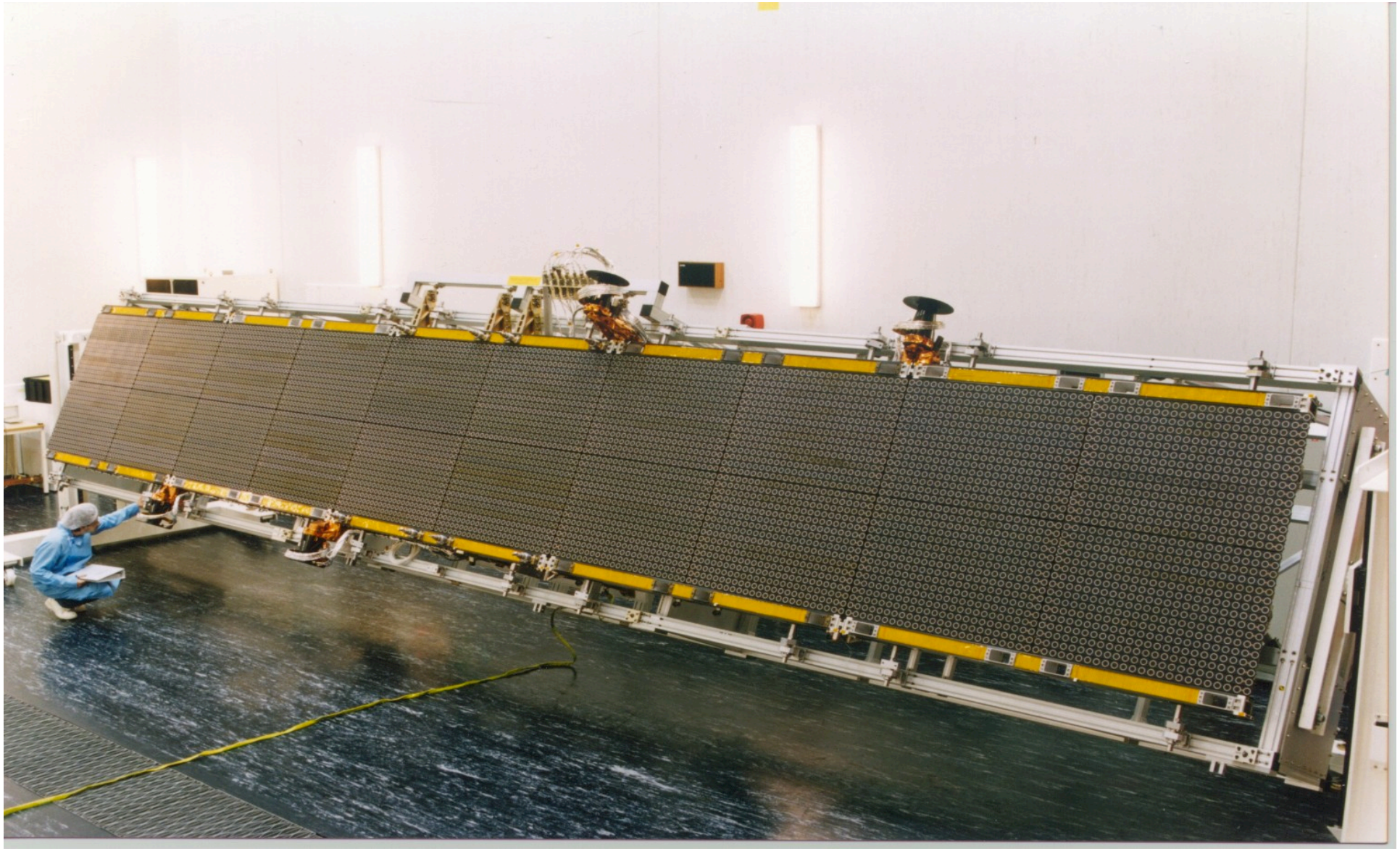

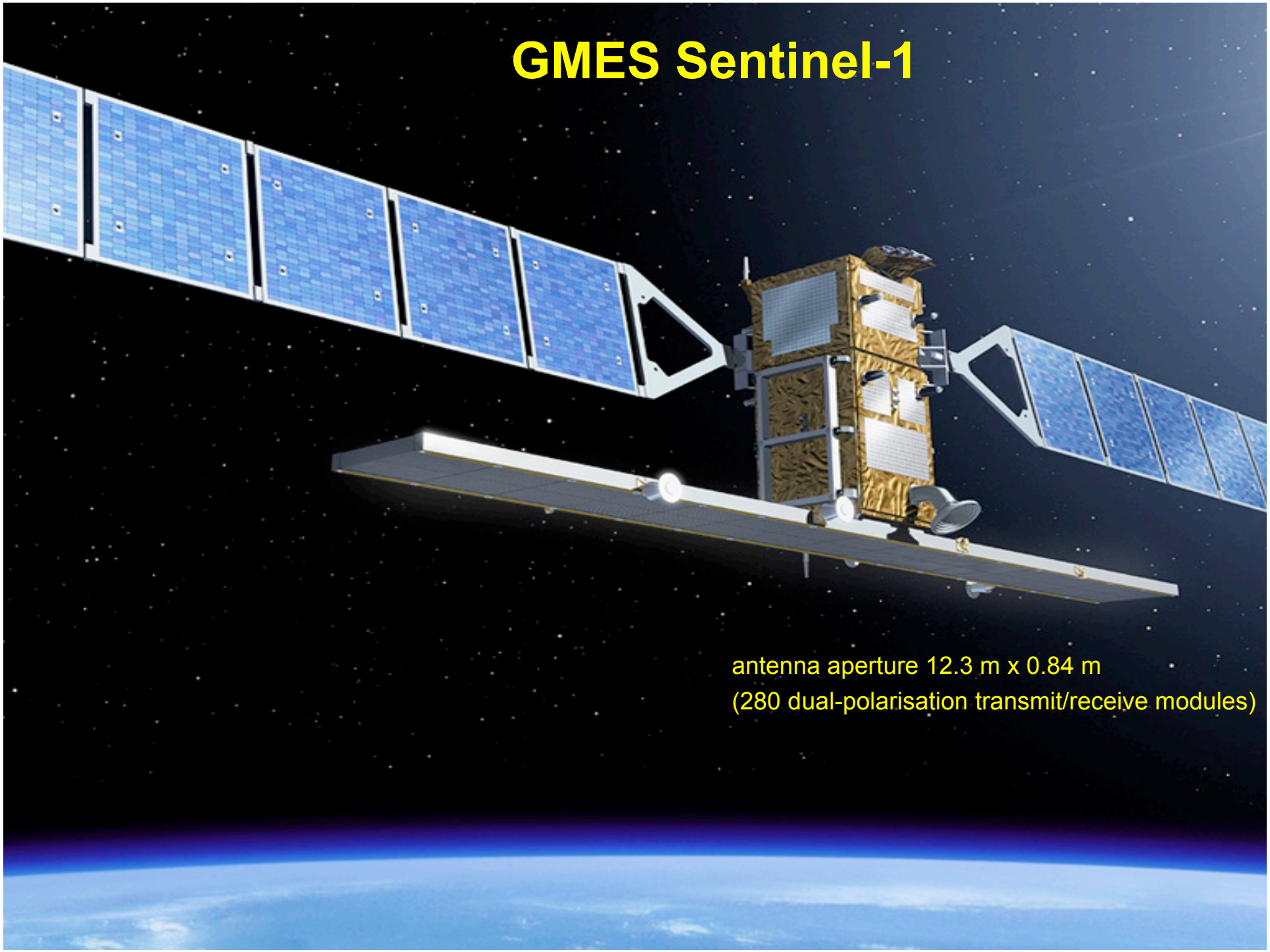
GMES Sentinel-1
antenna aperture 12.3 m x 0.84 m
(280 dual-polarisation transmit/receive modules)

Sentinel-1 key parameters

Mode	*Access Angle*	*Single Look Resolution*	*Swath Width*	*Polarisation*
Interferometric Wide Swath mode	**> 25 deg**	**Range 5 m Azimuth 20 m**	**> 250 km**	**HH+HV or VV+VH**
Wave mode	**23 deg and 36.5 deg**	**Range 5 m Azimuth 5 m**	**> 20 x 20 km Vignettes at 100 km intervals**	**HH or VV**
Strip Map	20-45 deg.	Range 5 m Azimuth 5 m	> 80 km	HH+HV or VV+VH
Extra Wide Swath	> 20 deg.	Range 20 m Azimuth 40 m	> 400 km	HH+HV or VV+VH

Main modes

For All Modes

Radiometric accuracy (3 σ)	**1 dB**
Noise Equivalent Sigma Zero	**-22 dB**
Point Target Ambiguity Ratio	**-25 dB**
Distributed Target Ambiguity Ratio	**-22 dB**

Sentinel-1 SAR Modes

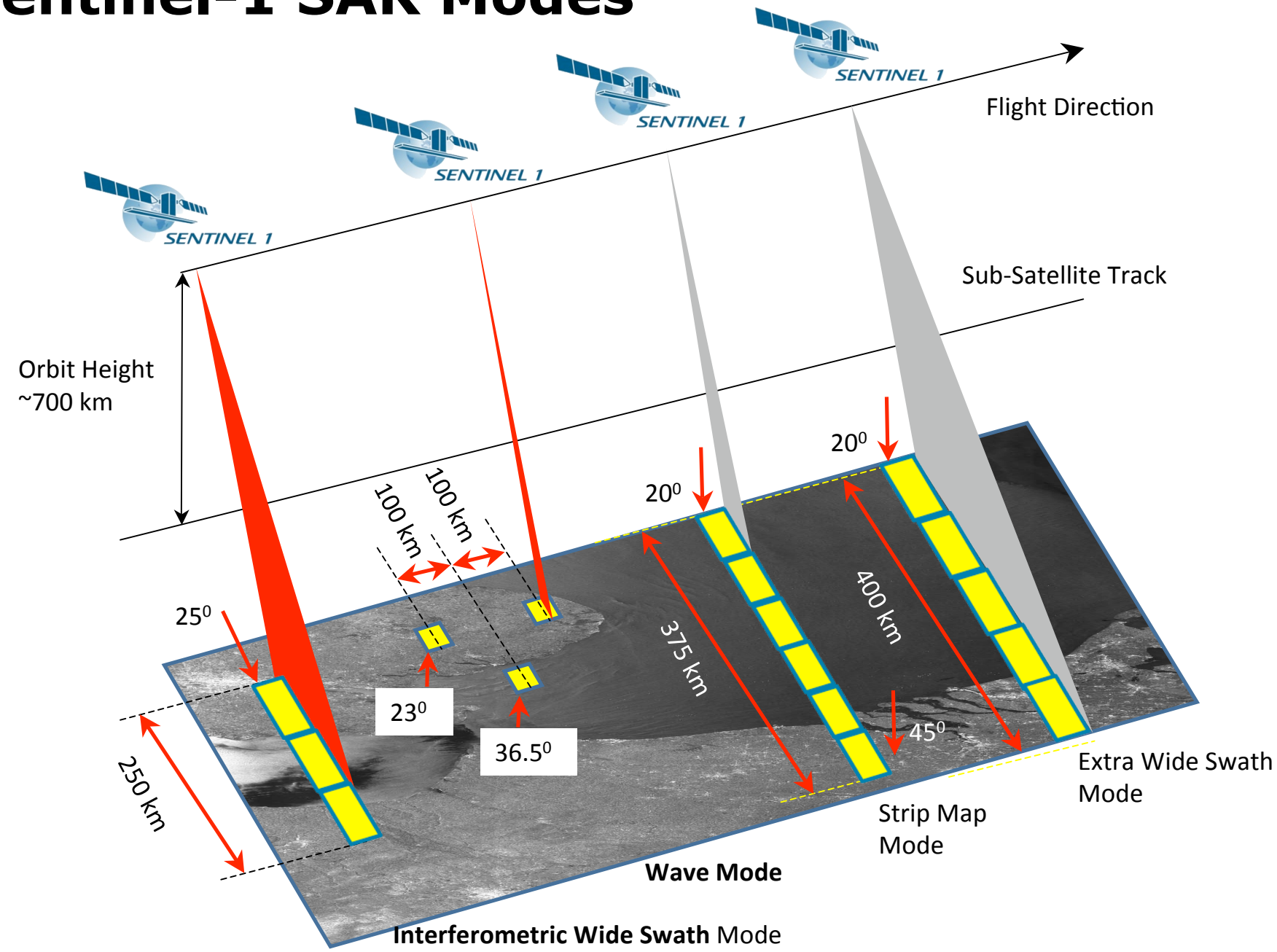

Level 2 product performance prediction

S1 Level-2 Product	Resolution	Performance	Units
Subsidence Rate	5 x 20 m2	1.3	mm/year
Land Cover Classification (2 dB contrast)	30 x 30 m2	75	% correct classification
Forest / Non-Forest Classification	30 x 30 m2	75	% correct classification
Flood Mapping	30 x 30 m2	79 (93)	% correct classification
Snow Cover Classification	30 x 30 m2	75	% correct classification
Ship Detection	5 x 20 m2	20	ship length (m)
Sea Surface Wind Speed	100 x 100 m2	0.4	m/s
Sea Surface Currents	5 Hz	30	cm/s

A SAR of the future : BIOMASS, for global carbon cycle studies

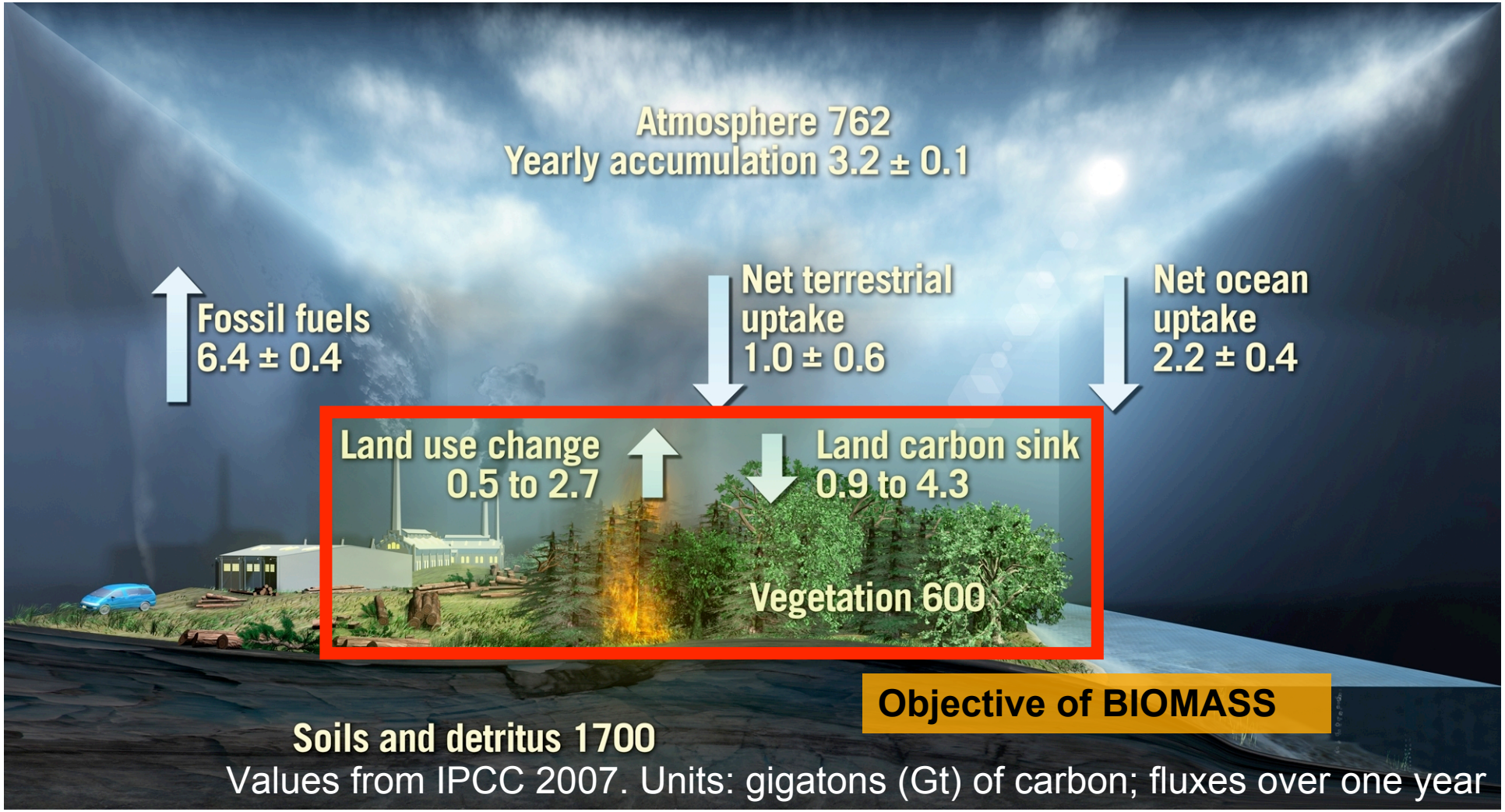

importance of forest biomass in carbon cycle

- Biomass is a proxy for carbon (carbon ~ 0.5 x biomass)
- Forests account for most of the Earth's vegetation biomass
- Changes in forest biomass with time correspond to carbon fluxes
  - Loss = Emissions
  - Growth = Uptake
- Forest biomass is poorly known and a major source of uncertainty in carbon flux estimation

Biomass = dry weight of woody matter + leaves (tons/ha)

Observation concept

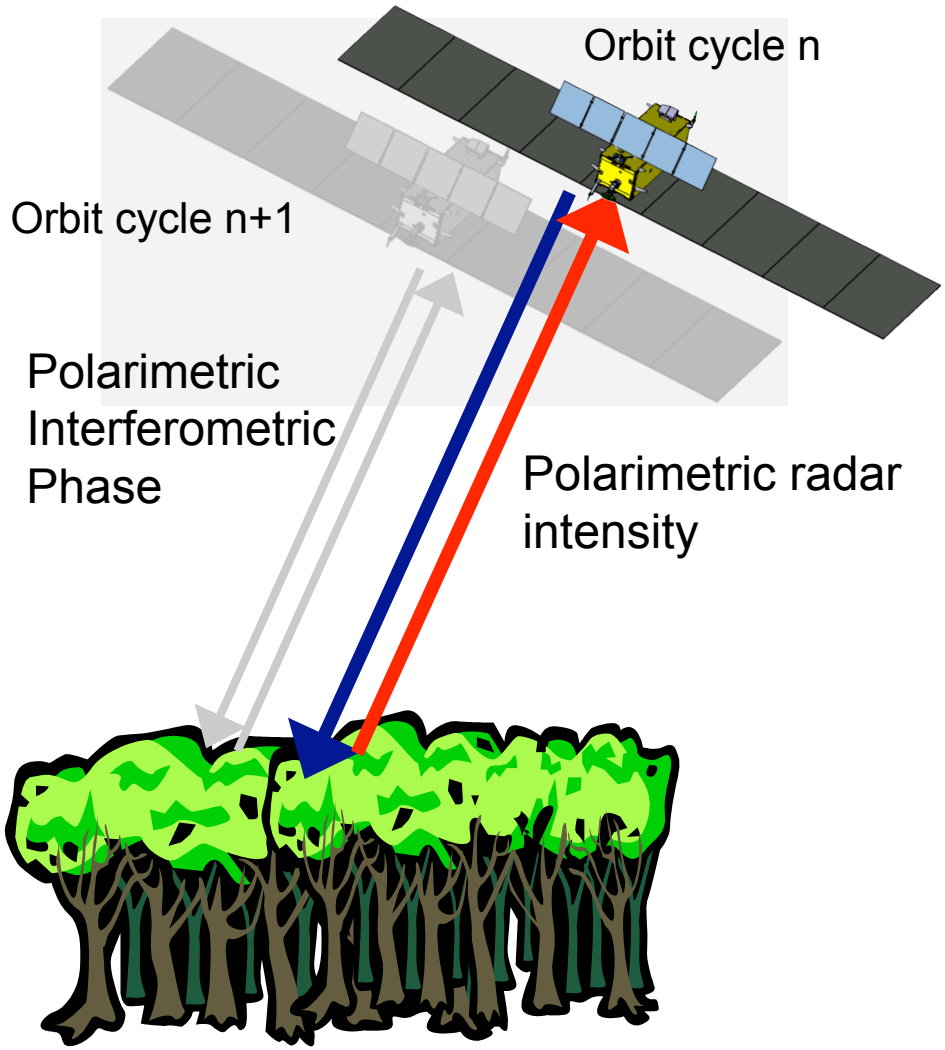

Calibration, Ionospheric correction

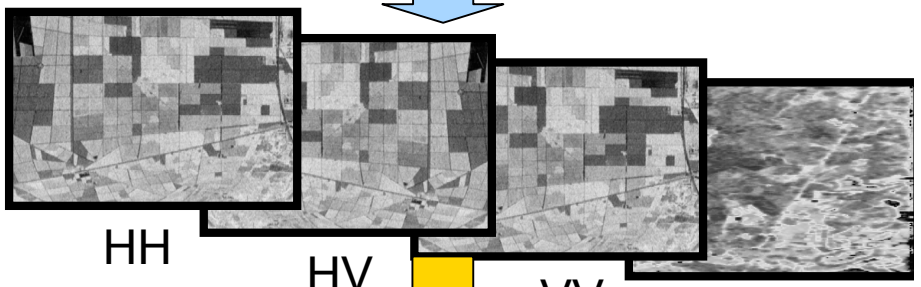

Retrieval algorithm

Geophysical products

- Forest biomass
- Forest height
- Forest biomass temporal change
- Forest disturbance

sensitivity of P-band SAR to forest biomass

- Relationship between P-band backscatter intensity and forest biomass extensively studied using airborne SAR
- Key results:
  - Large dynamic range as function of biomass
  - Robust functional relationship between HV signal and biomass
  - Decrease in sensitivity for high biomass (> 150 tons/ha)

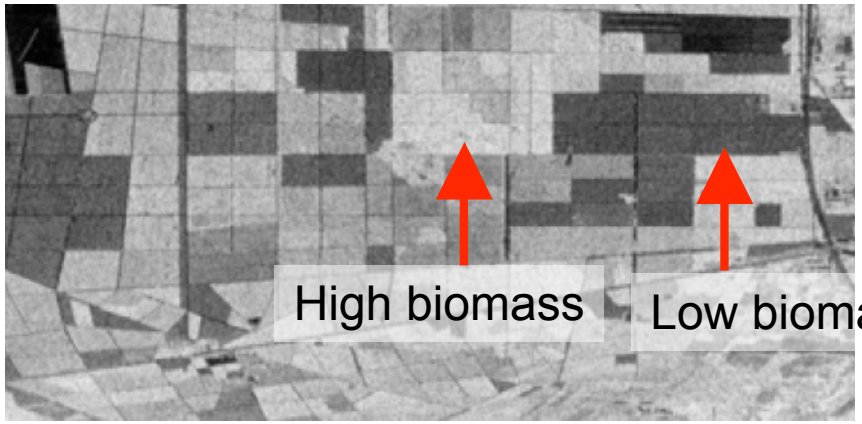

P-Band HV radar intensity

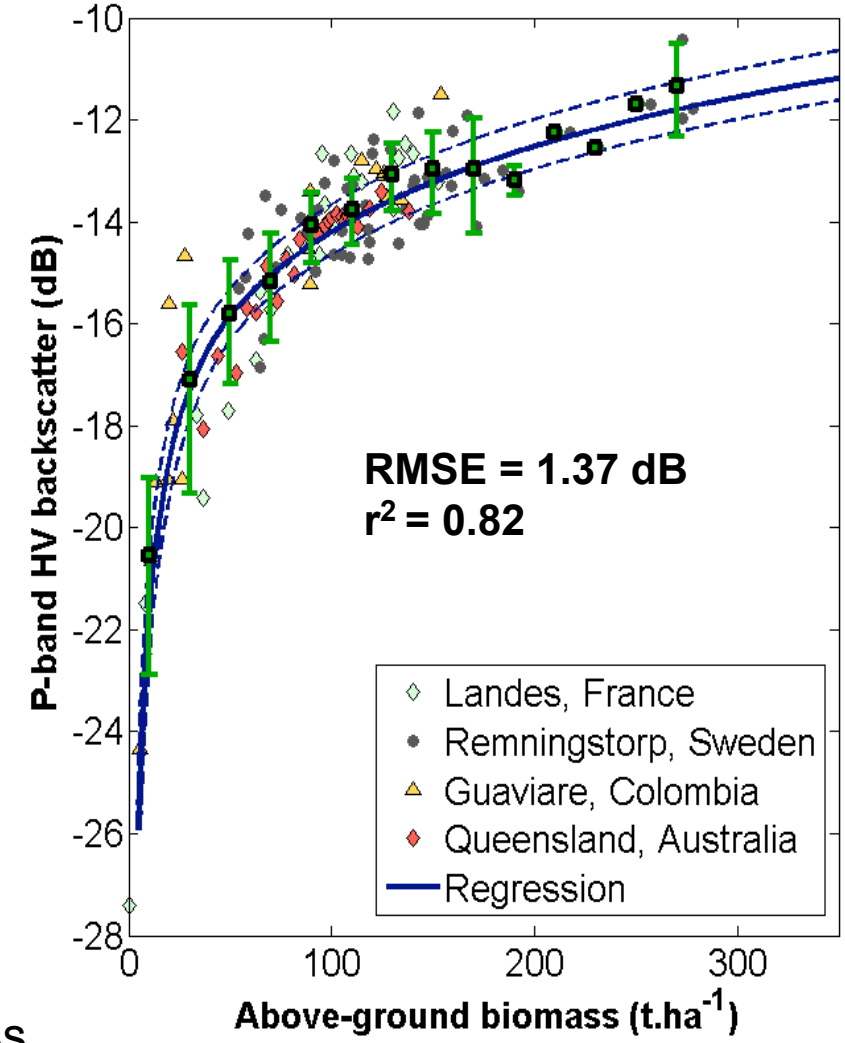

height from Polarimetric SAR Interferometry

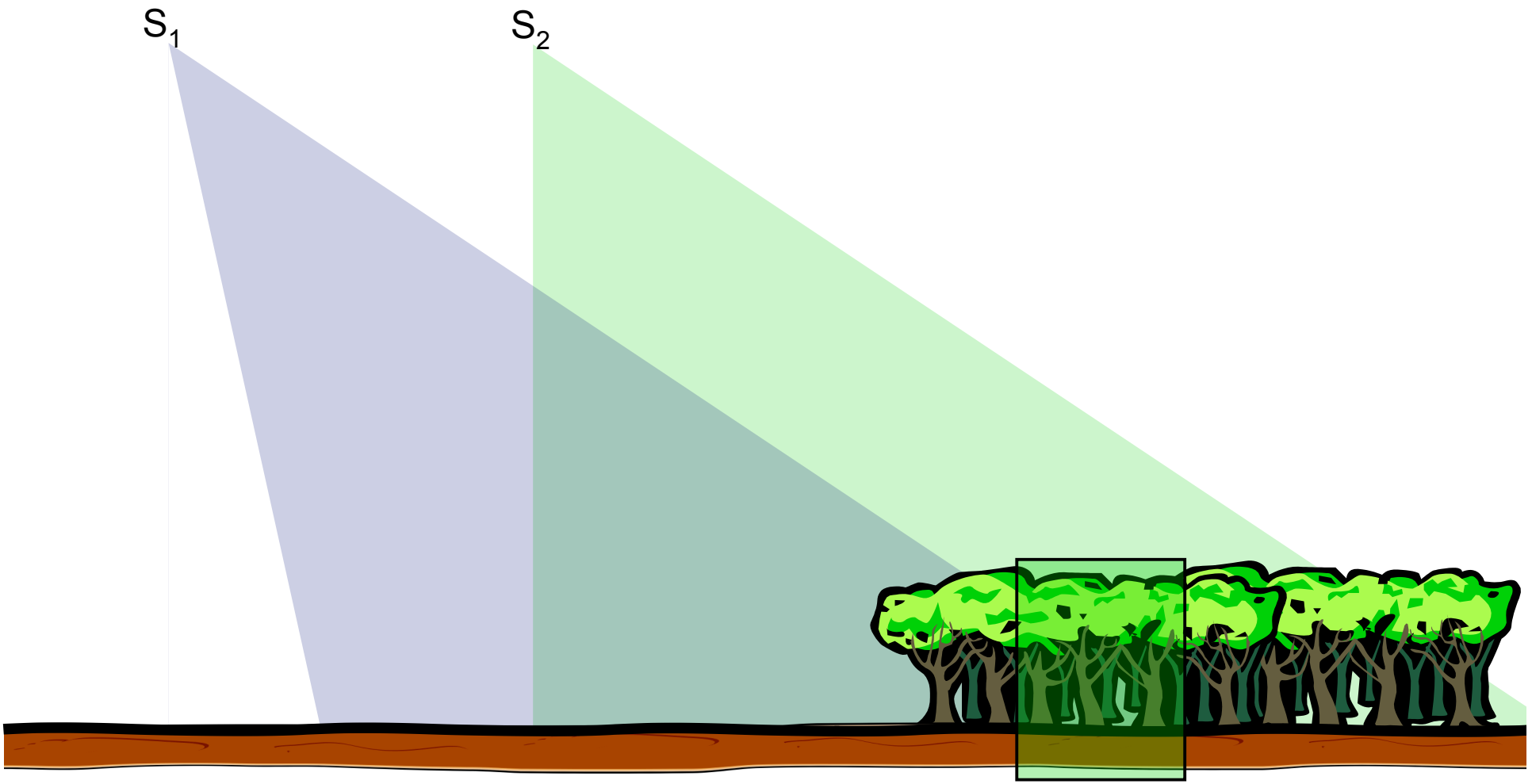

height from Polarimetric SAR Interferometry

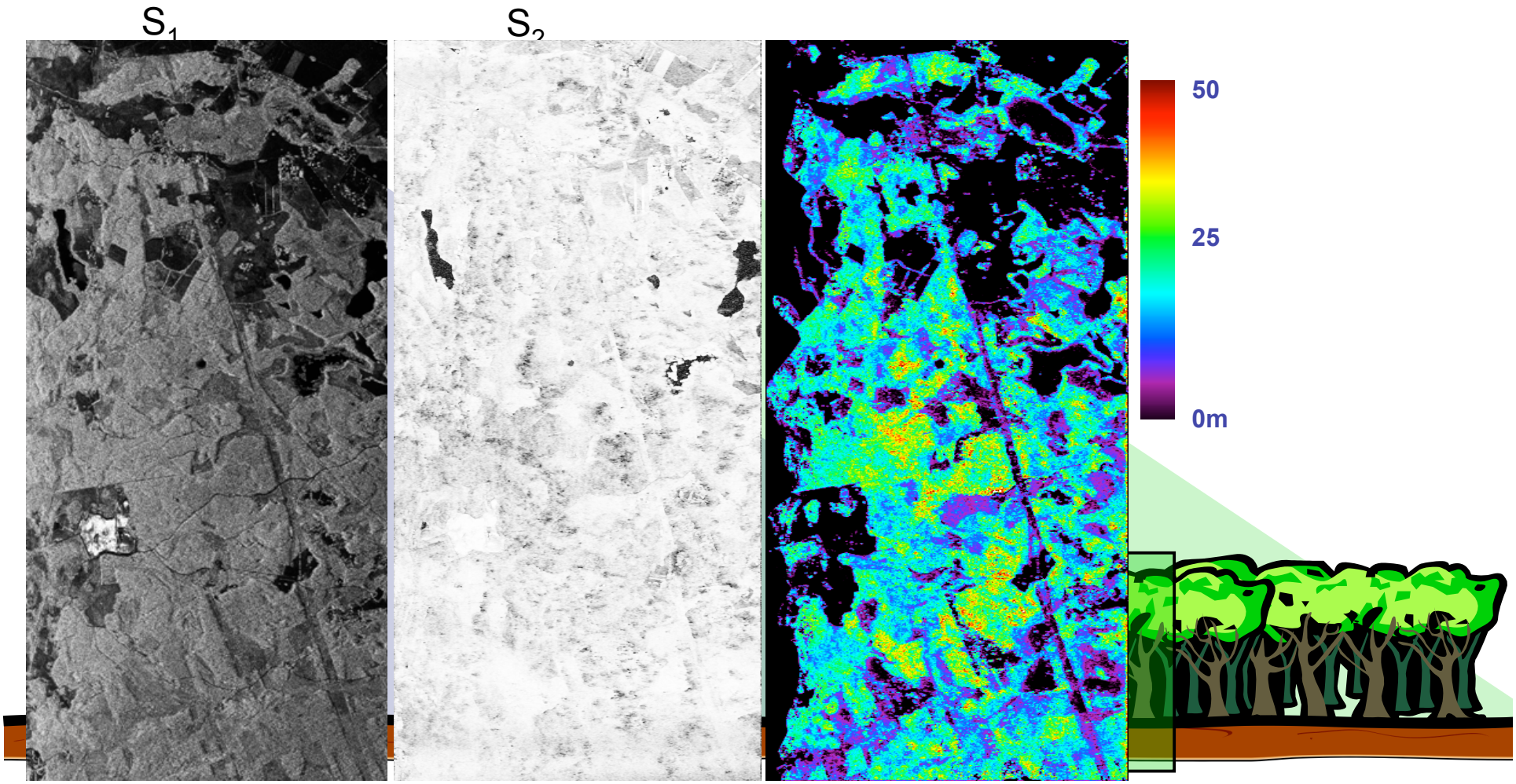

Data Products

Level-2 Product	Properties
Forest biomass	< 20% error; 100 m - 200 m resolution; 2 maps/year; global forest coverage
Forest biomass change	< 20% error;100 - 200 m resolution; annual; global forest coverage
Forest disturbance	Disturbance maps: 90% accuracy; 50 m resolution (major disturbances); 200 m resolution (partial disturbances); 1 per 2 months or seasonal; global forest coverage
Forest height	< 20-30% error; 100 x 100 m resolution; 1 map/year; global forest coverage

BIOMASS options

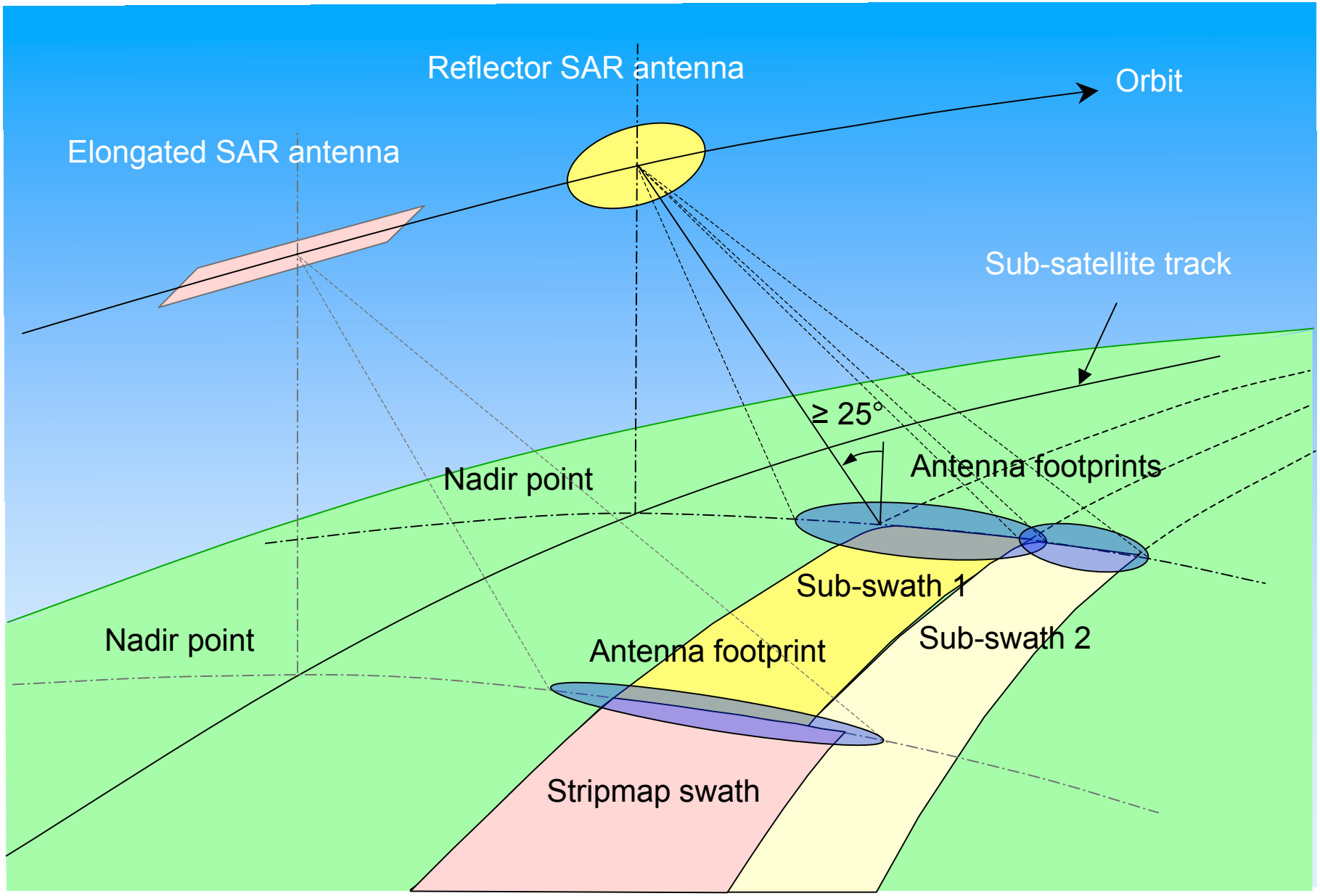

Optical instruments: types

- **Imagers**, using single band or a few bands (<10: multi-spectral; > 10: super-spectral), e.g.:
  - SPOT, Landsat, AVHRR, ALI, AATSR/SLSTR, ASTER, AVNIR, (Venus, Sentinel-2 MSI)..
- **Imaging spectrometers** (“hyper-spectral imagers”: use of dispersing element, in principle >> 10 bands), e.g.:
  - MODIS, MERIS, CHRIS/PROBA, (EnMAP, PRISMA) ..
- **Vertical sounders/spectrometers**, e.g.:
  - IASI, AIRS
- **Limb sounding spectrometers**
  - MIPAS, SCIAMACHY, GOMOS (all on ENVISAT),..
- **Lidars**
  - LITE, GLAS, (ALADIN, ATLID) ..
- **Special spectro-radiometers:**
  - POLDER, (3MI),..

Some definitions

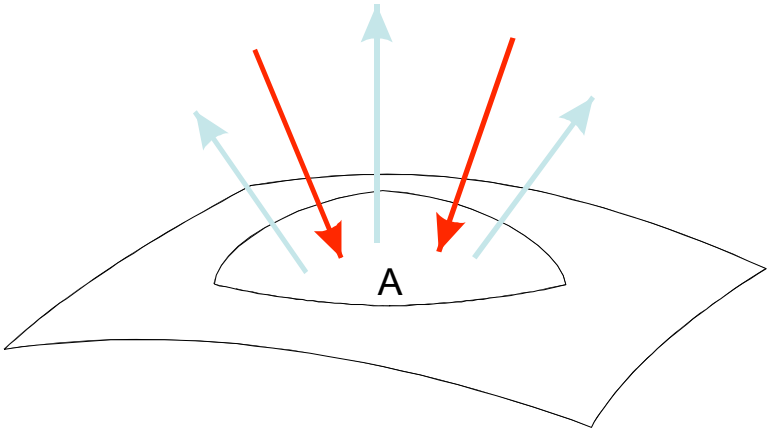

Energy flux (power) through surface A = F (watt, W)

$M = \frac{d\Phi}{dA}$: (radiant emittance) exitance (W/m^2) is the power per unit area

$E = \frac{d\Phi}{dA}$: (radiant) incidance (W/m^2)

or irradiance is the incident power per unit time

$E_\lambda = \frac{d^2\Phi}{dA d\lambda}$: spectral irradiance (often just "irradiance"))

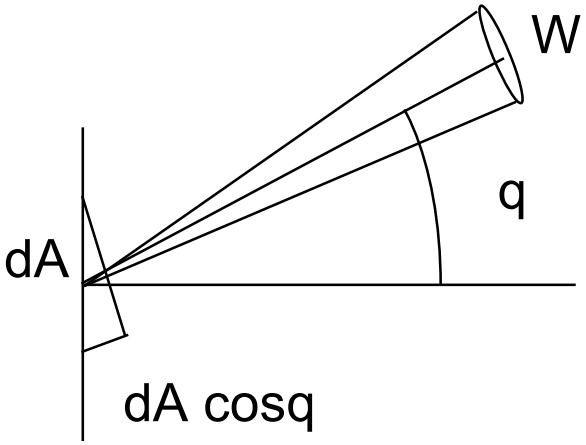

$L = \frac{d^2\Phi}{d\Omega dA \cos q}$: radiance (W/m^{2}sr) is power per unit projected area per unit solid angle

L is conserved in free propagation and through imaging optical systems (under some conditions of good imaging)

for "Lambertian surfaces" radiance is independent of q and: $L = \frac{E}{\pi}$

Some definitions

Bidirectional reflectance distribution function (BRDF) [terminology varying in literature]

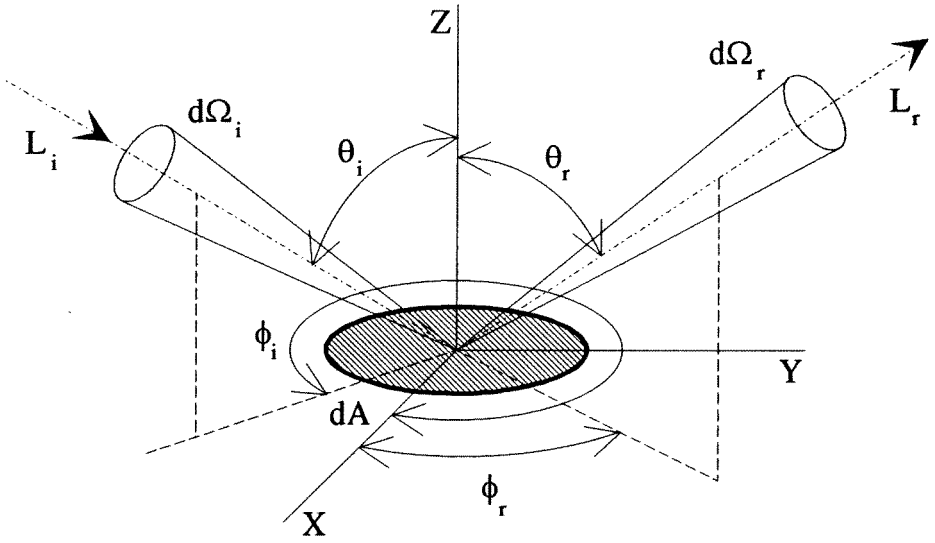

$$BRDF = \frac{dL_r}{L_i \cos\theta_i d\Omega_i} \qquad (\mathrm{sr}^{-1})$$

- For directional radiation (e.g. sun, laser): $BRDF = \frac{L_r}{E_i}$

- Radiance factor, often called “reflectance”, relative to ideal lambertian surface: $\beta = \frac{L_r}{L_{r,ideal}} \qquad L_r = \frac{\beta E_i}{\pi}$

The Solar Spectrum

- solar spectrum can be approximated by blackbody at T = 5780 K
- absorption in solar atmosphere leads to Fraunhofer lines
- in atmosphere, solar radiation is attenuated by scattering and absorption
- strong absorption by O_3, O_2, H_2O and CO_2
- however, in some atmospheric windows the absorption is small

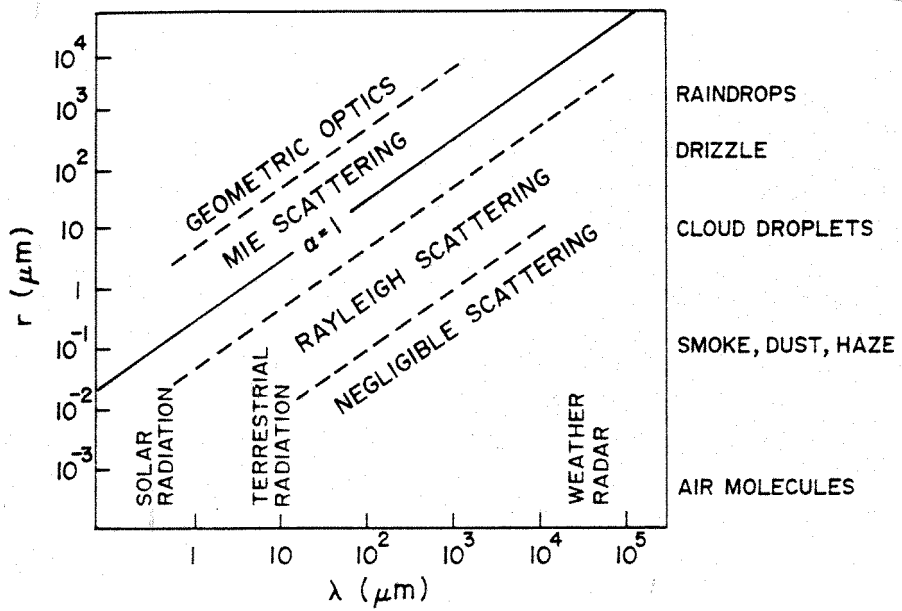

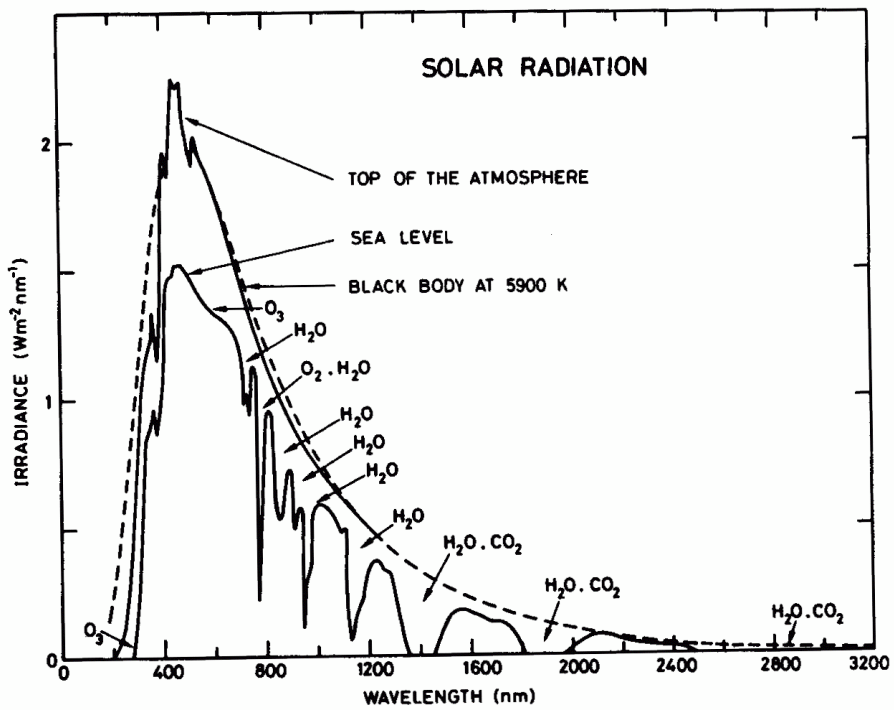

Fig. 4.6. Spectrum of solar radiation (UV, visible, IR) outside the earth's atmosphere and at sea level. (Adapted from Coulson, 1975).

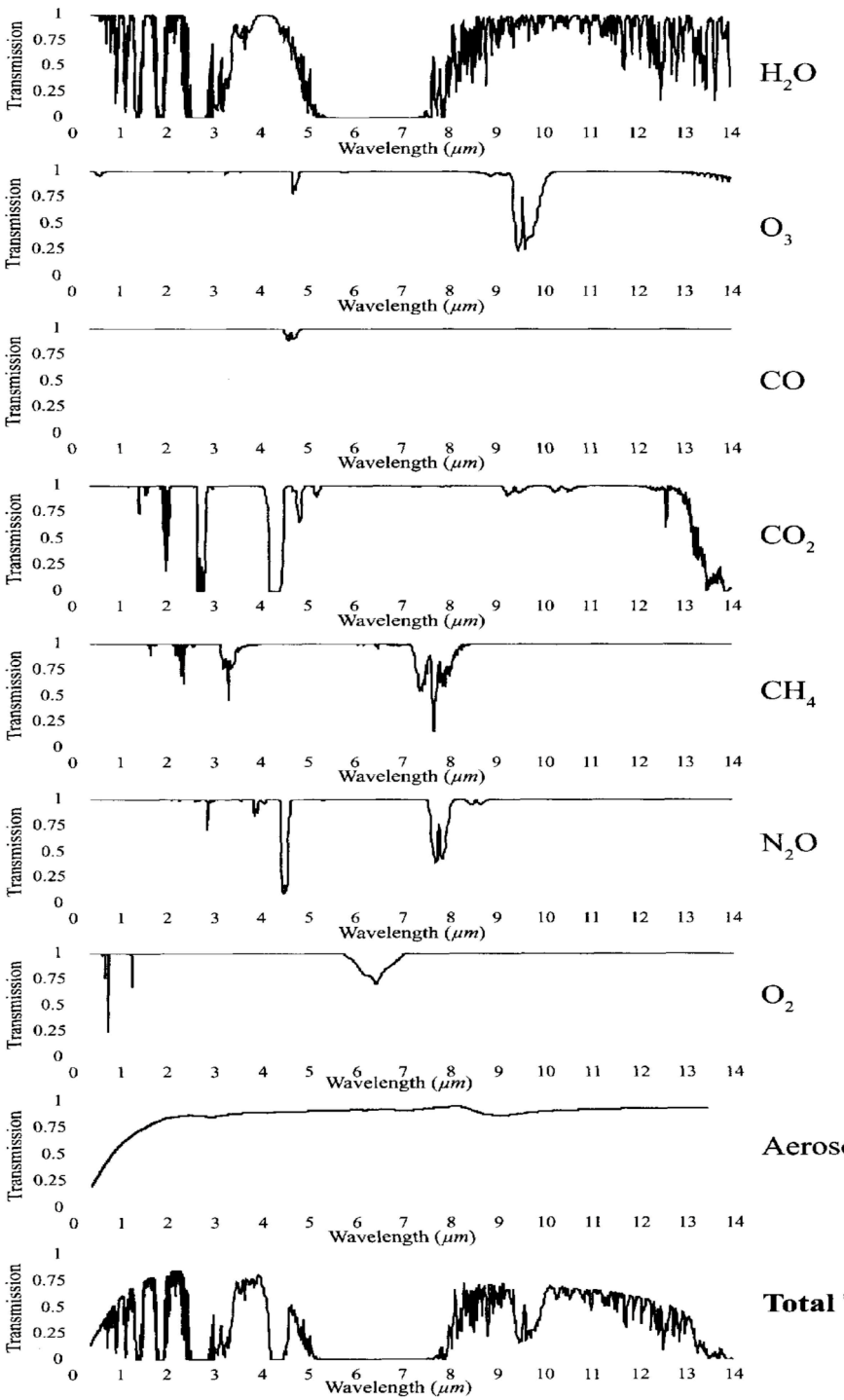

Some of the spectral features as modelled in the MODTRAN code (Berk et al., 1989)

examples of typical surface reflectances

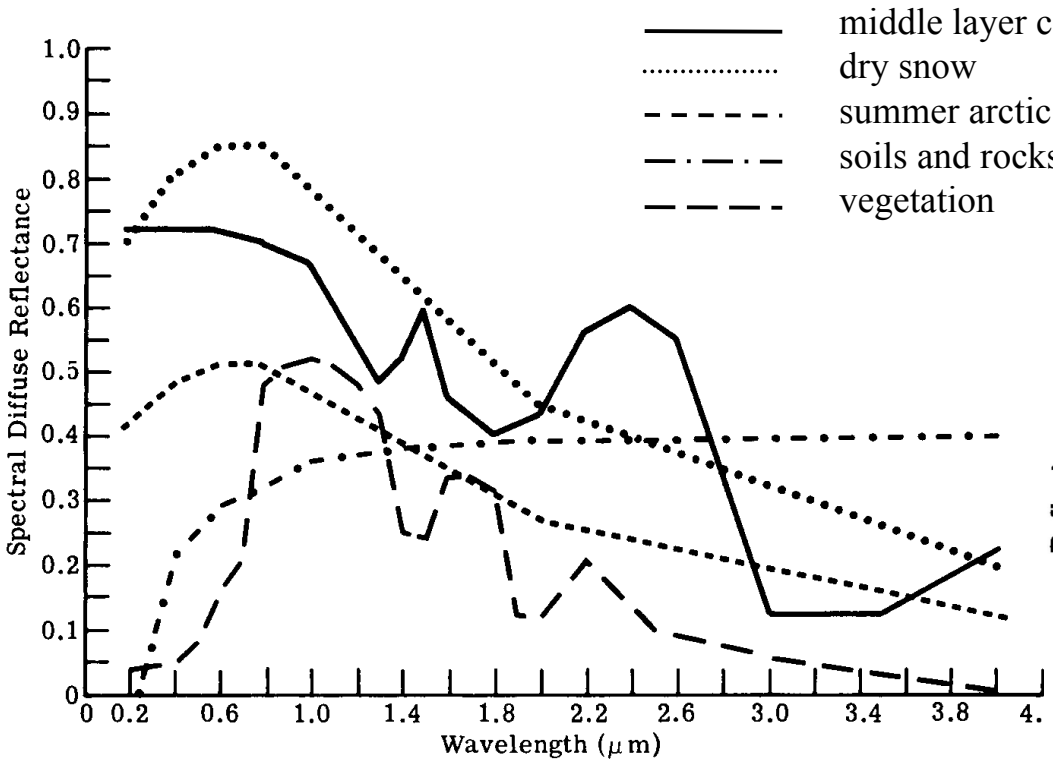

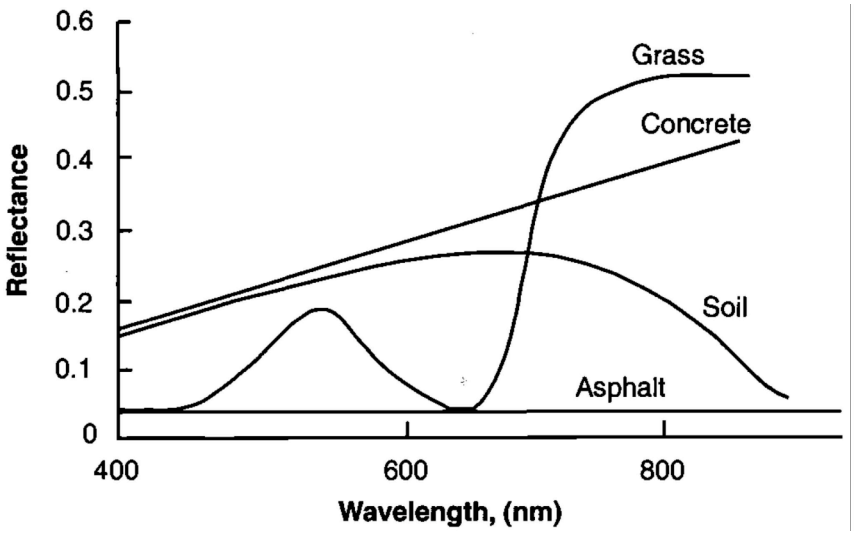

Ref. Infrared handbook, vol.1

Reflectance of water

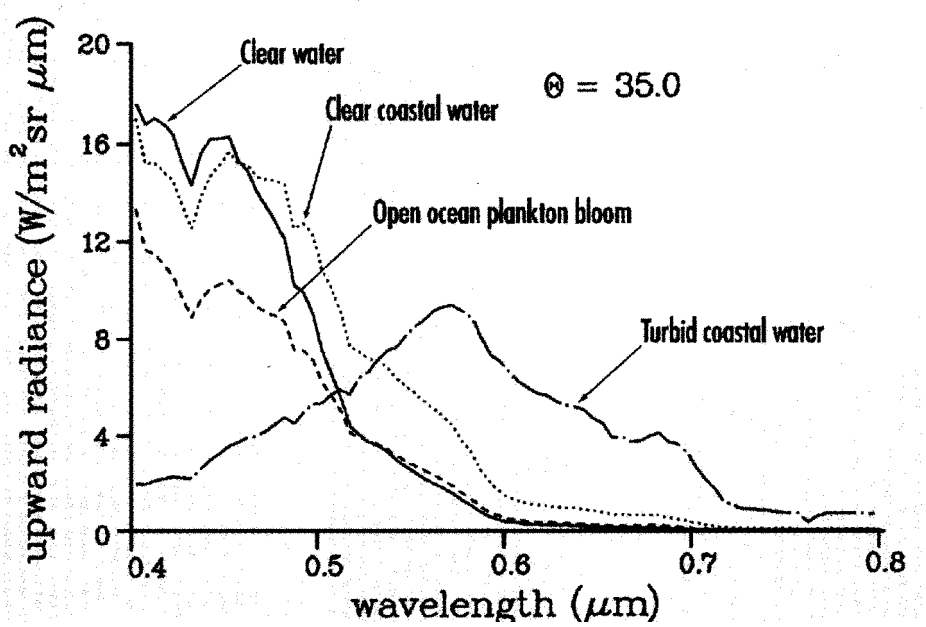

Ref. ESA SP-1184

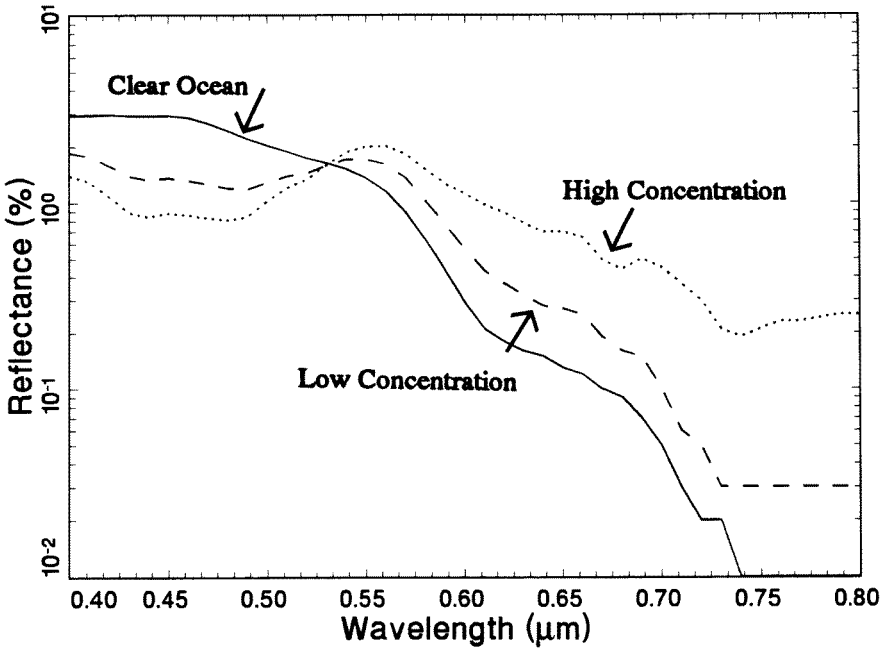

Ref. Infrared handbook, vol.1

Reflectance of snow, ice and clouds

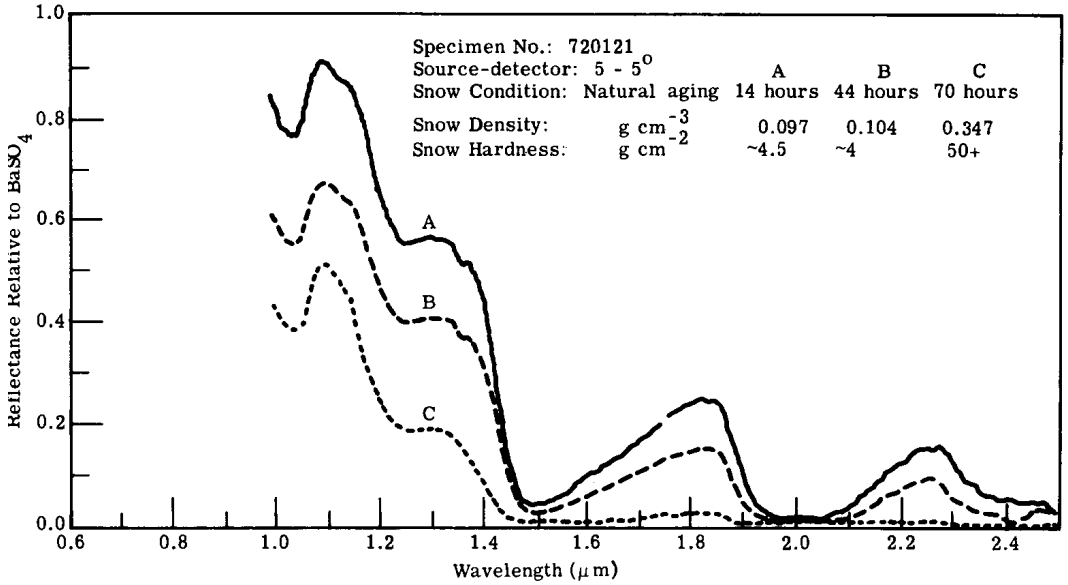

Fig. 3.147 Changes in snow reflectance with natural aging (5–5° source-detector).[126]

Ref. Infrared handbook, vol.1

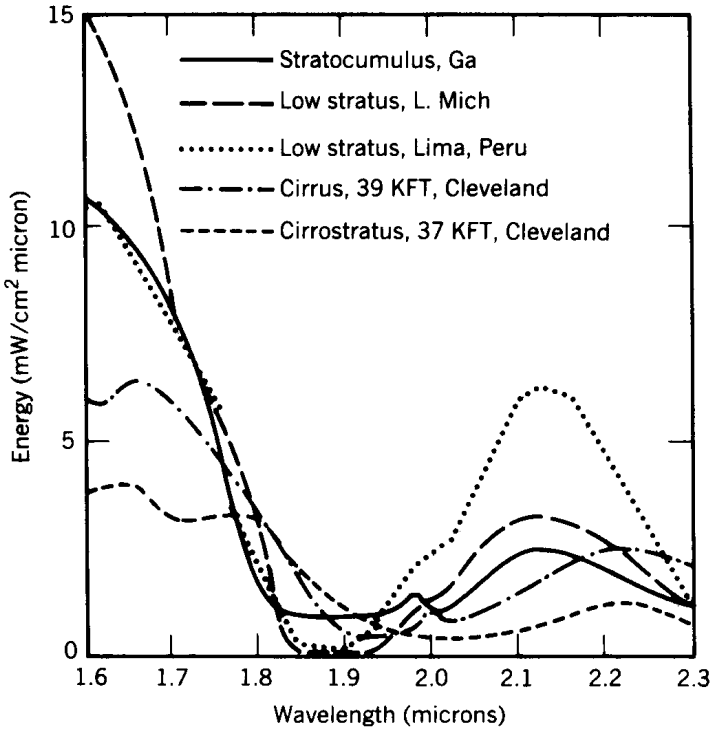

Ref. Szekeldia, satellite monitoring of the Earth

Reflectance of vegetation

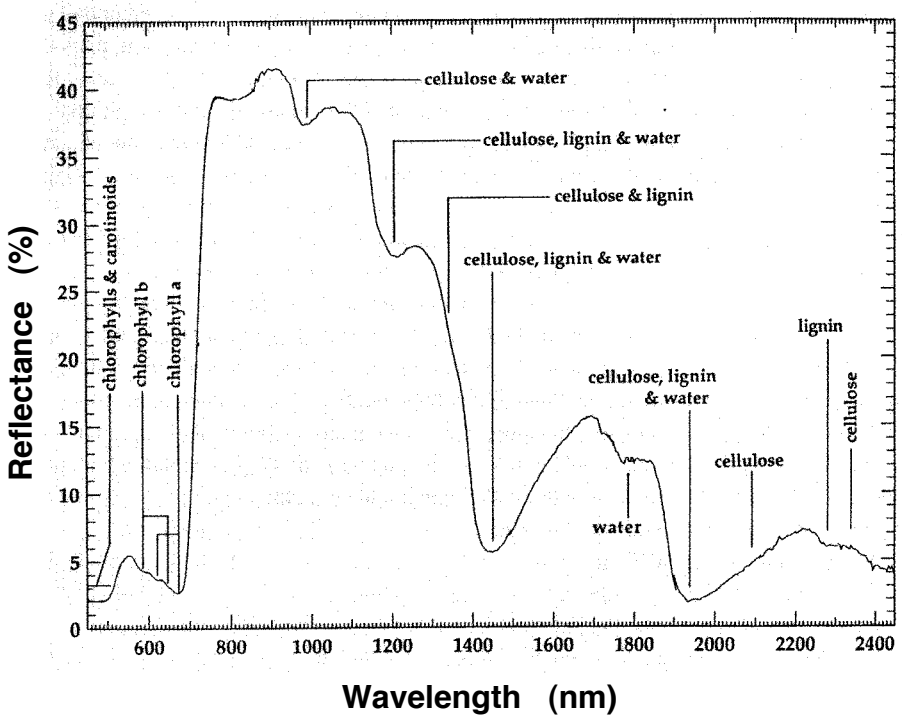

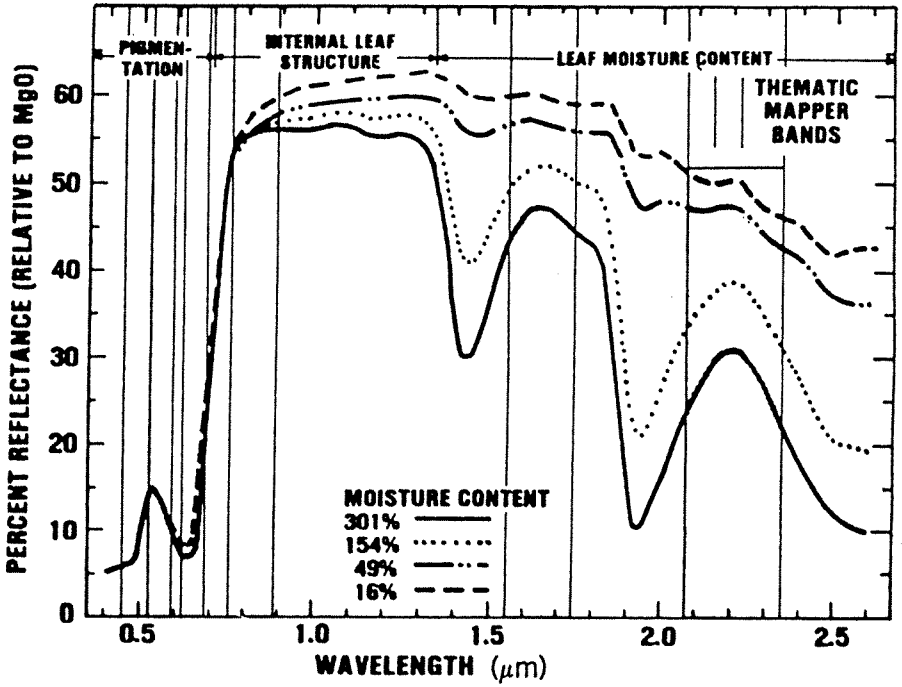

Progressive changes in the spectral response of a sycamore leaf with varying moisture con
(Short, 1982).

Ref. ESA-SP 1144

Reflectance of vegetation

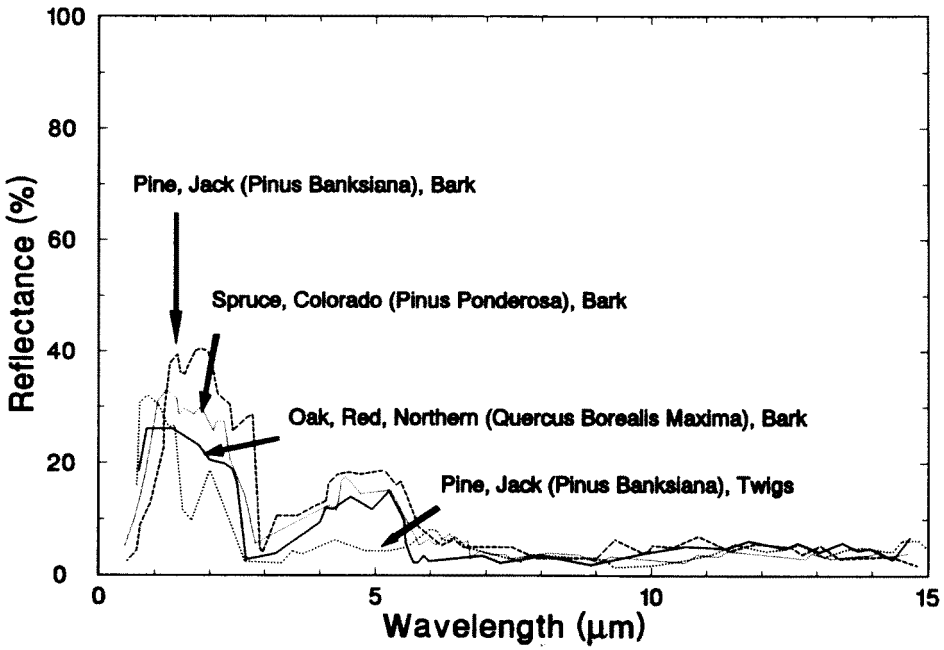

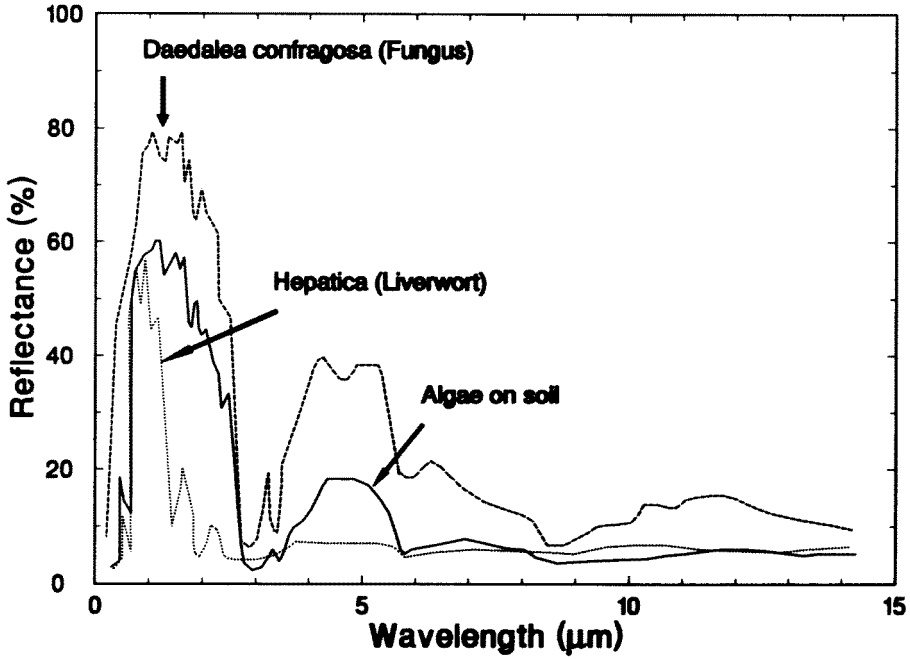

Ref. Infrared handbook, vol.1

imagers: SPOT

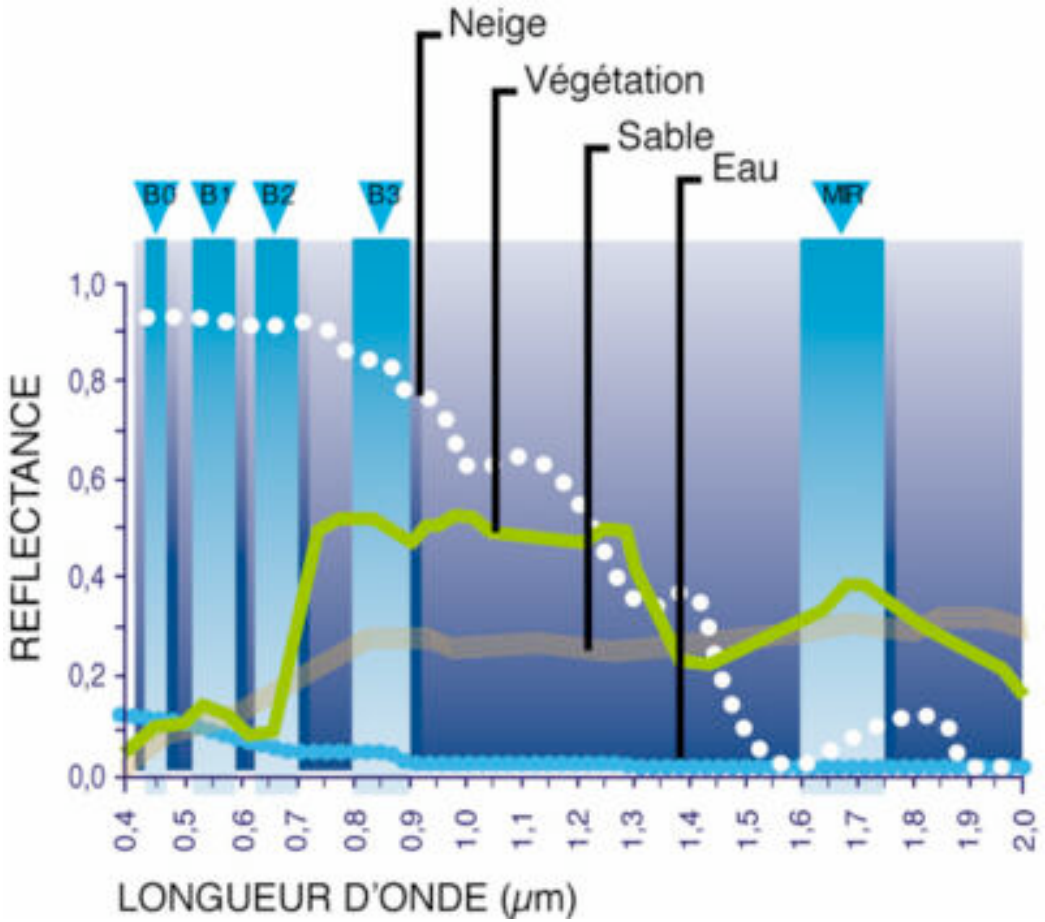

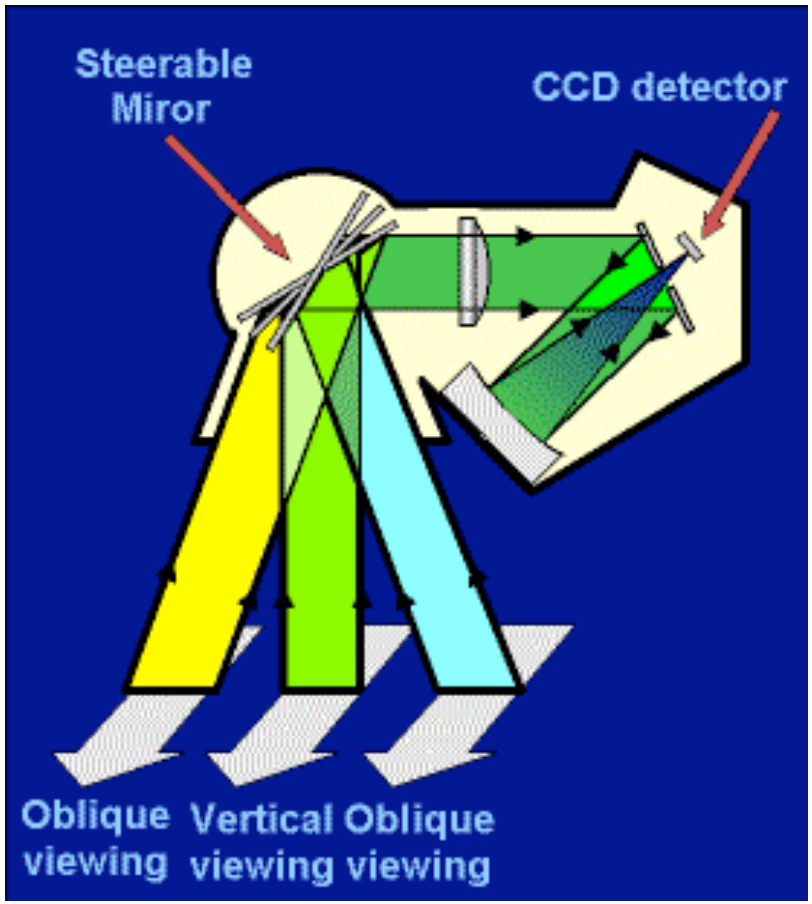

GMES Sentinel-2: enhanced continuity of land optical imagery

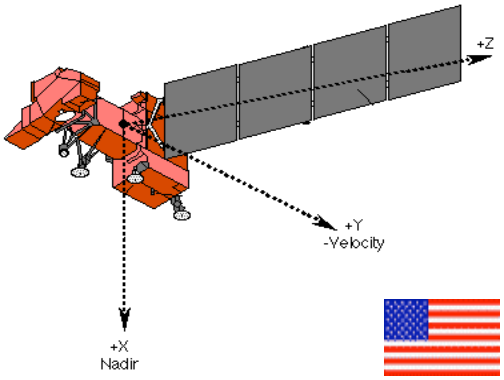

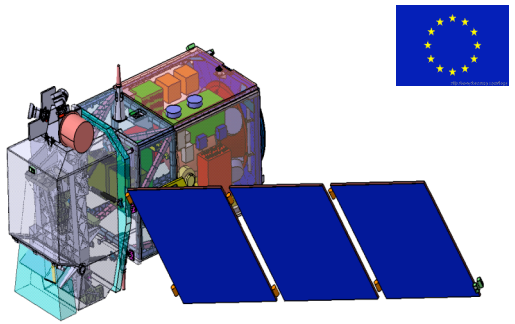

	Landsat	SPOT	Sentinel-2	
Satellites in series	7 + 1*	5	initially 2	
Launch	1972 to 1999*	1986 to 2002	first launch : 2013	
Geometry	scanner	pushbroom	pushbroom	
Global coverage (no clouds)	16	26	5	days
Swath	185	2*60	290	km
Spectral bands	7	4 + 1 (panchromatic)	13	
Spatial sampling distance	30, 60	10, 20	10, 20, 60	m

* LCDM mission from 2012

- operational generation of land cover, land use and change detection maps (e.g. CORINE land cover maps update, soil sealing maps, forest area maps)
- generation of maps of geophysical variables (e.g. leaf chlorophyll content, leaf water content, leaf area index…)

Sentinel-2 Multi-Spectral Instrument (MSI)

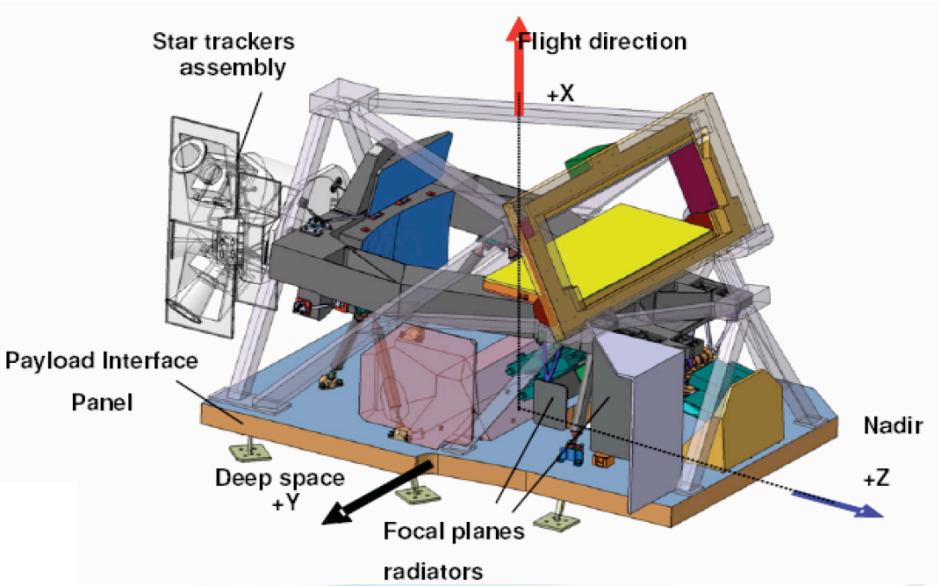

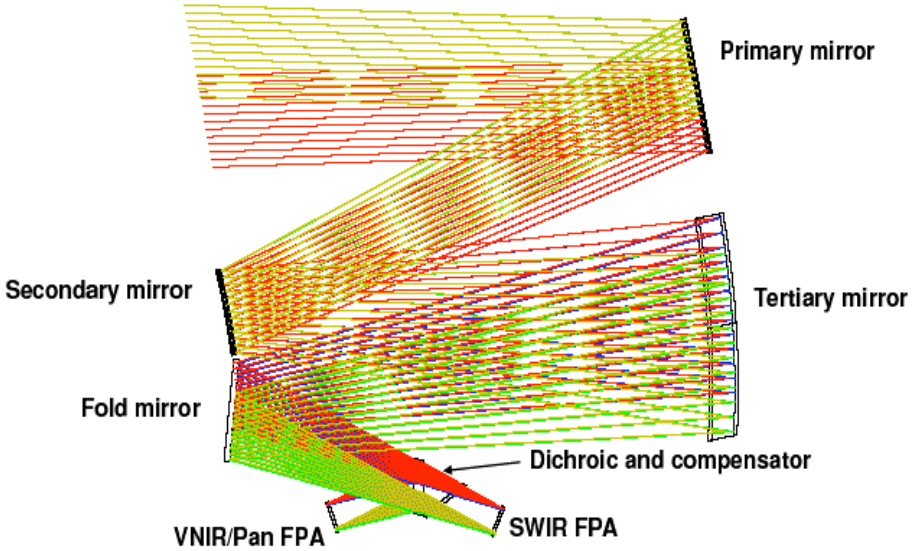

- **Filter based pushbroom imager (280 kg, 1 m^3)**
- **Three mirror anastigmat (TMA) telescope in silicon carbide (structure, mirrors) with 15 cm pupil diameter, with dichroic beam splitter to separate VNIR / SWIR**
- **Focal plane arrays: Si CMOS visible and near-infrared (VNIR) detectors, HgCdTe SWIR detectors passively cooled (190 K)**
- **On-board wavelet compression (~1:3)**
- **Integrated video & compression electronics**
- **Radiometric accuracy: < 5%**

- partial on-board calibration using sun diffuser and vicarious calibration with ground targets to guarantee radiometric performance
- orbit: Sun-synchronous at 786 km (14+3/10 revs per day), with LTDN 10:30 AM
- geographic coverage: systematic, all land & coastal surfaces between -56° & +84° latitude
- lifetime: 7.25 y, consumables for 12 y

Sentinel-2 spectral bands

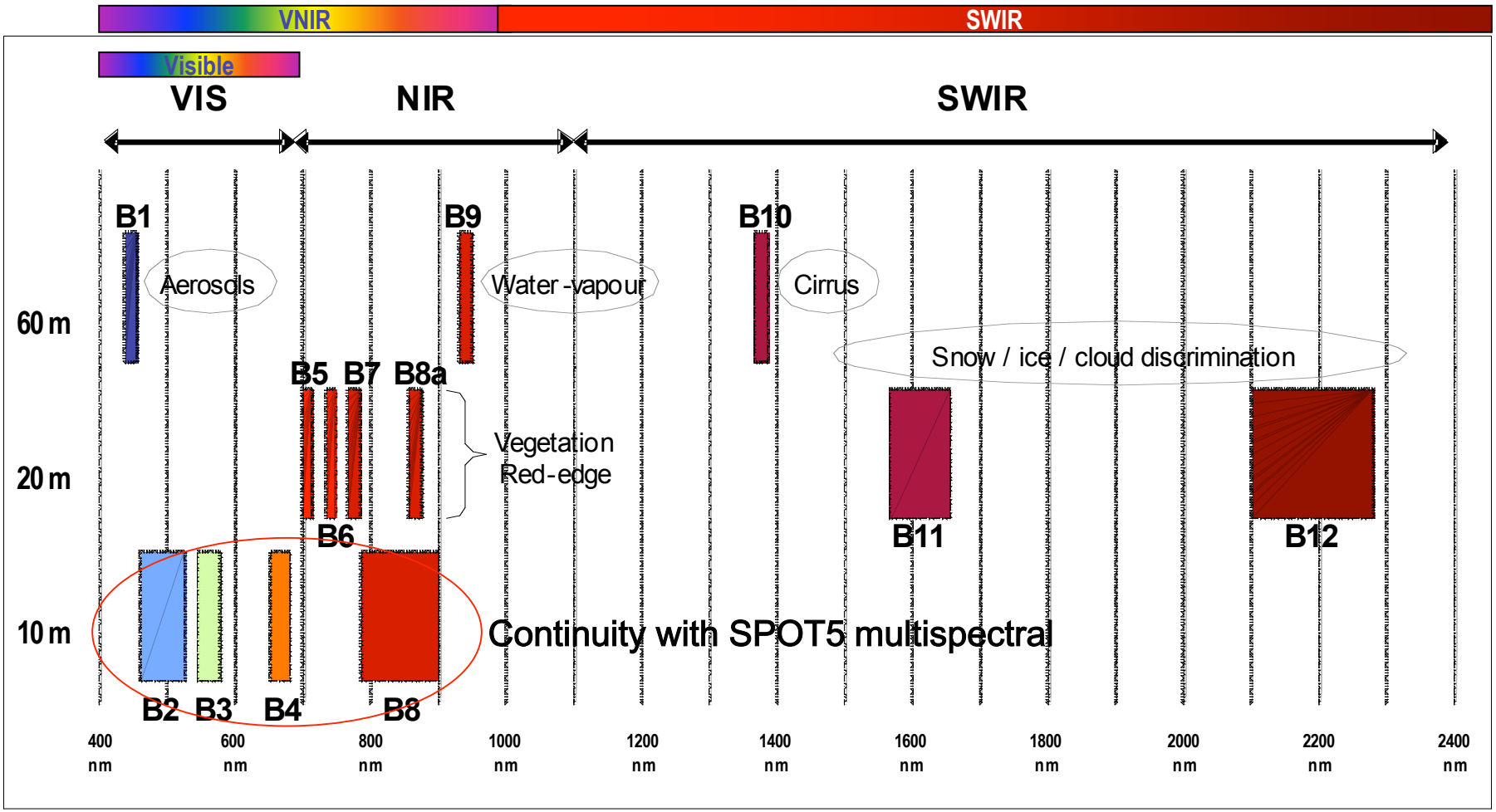

Spectral bands versus spatial resolution

Spectral Bands vs Mission Objectives

MSI spectral bands	Mission objective	Measurement or Calibration
B1(443/20/60) & B12(2190/180/20)	Aerosols correction	Atmospheric correction bands
B8(842/115/10)/B8a(865/20/20), B9(940/20/60)	Water vapour correction	
B10(1375/20/60)	Cirrus detection correction	
B2(490/65/10), B3(560/35/10), B4(665/30/10), B5 (705/15/20), B6(740/15/20), B7(775/20/20), B8(842/115/10)/B8a(865/20/20), B11(1610/90/20), B12(2190/180/20)	Leaf Chlorophyll Content, LAI, fAPAR, Leaf Water Content, Fractional Vegetation Cover, snow/ice/cloud…	Land measurement bands

for each band Bn (Wavelength [nm] / Width [nm] / Spatial Sampling Distance [m])

Sentinel-2 L2b simulated products

Natural color composite (B4, B3, B2)

Visible Near-Infrared composite (B8, B4, B3)

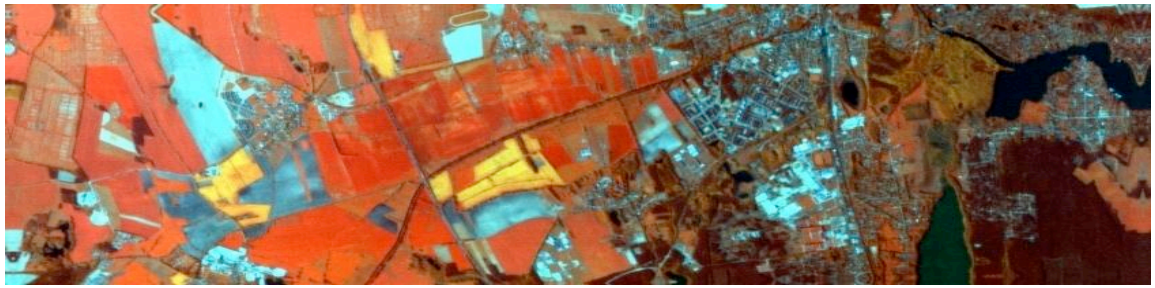

Land Cover Classification (using all bands)

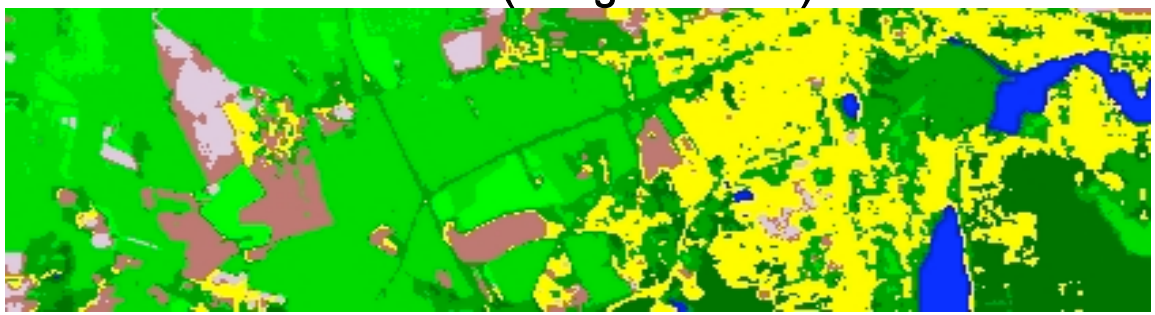

Simulated
Sentinel-2 images

	Urban
	Water
	Forest 1
	Forest 2
	Bare soil 1
	Bare soil 2
	Cultivated field 1
	Cultivated field 2

Level 2b simulated products

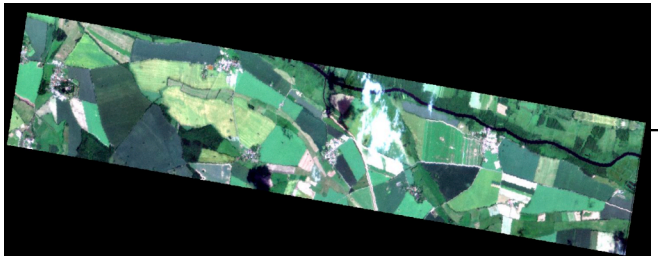

Sentinel-2 simulated Level 1 data

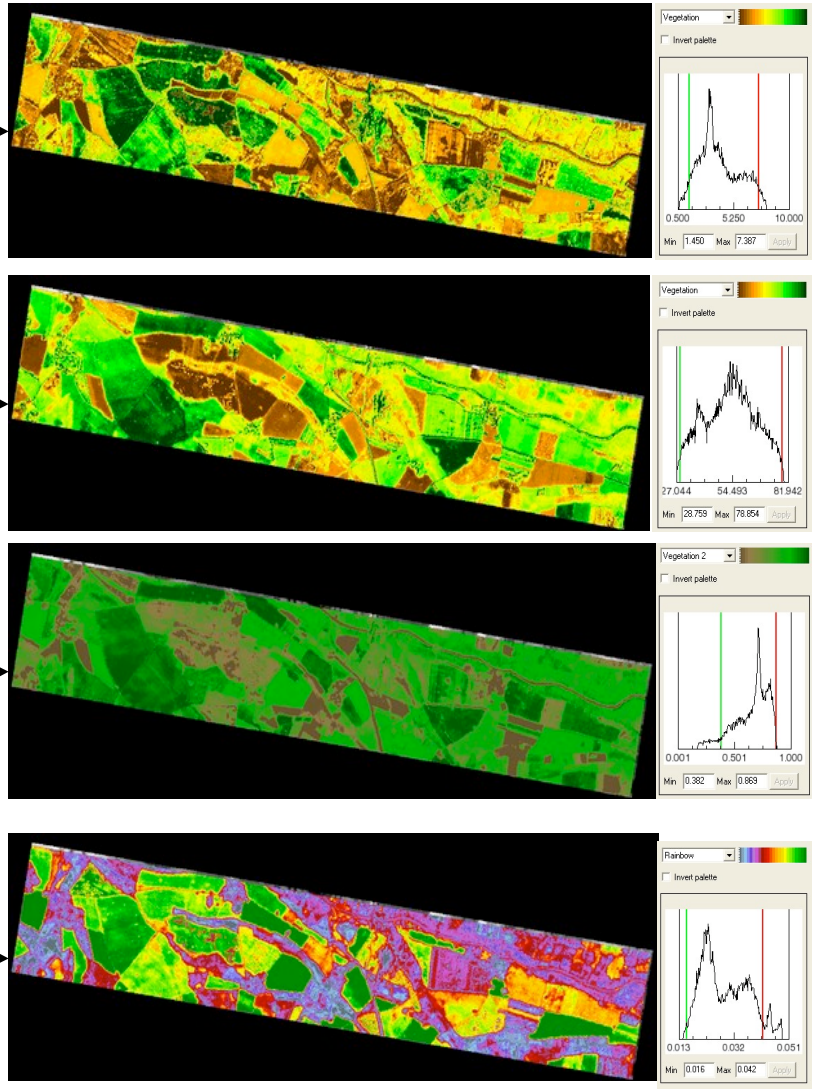

Key Benefits

More accurate classifications exploiting multi-temporal coverage

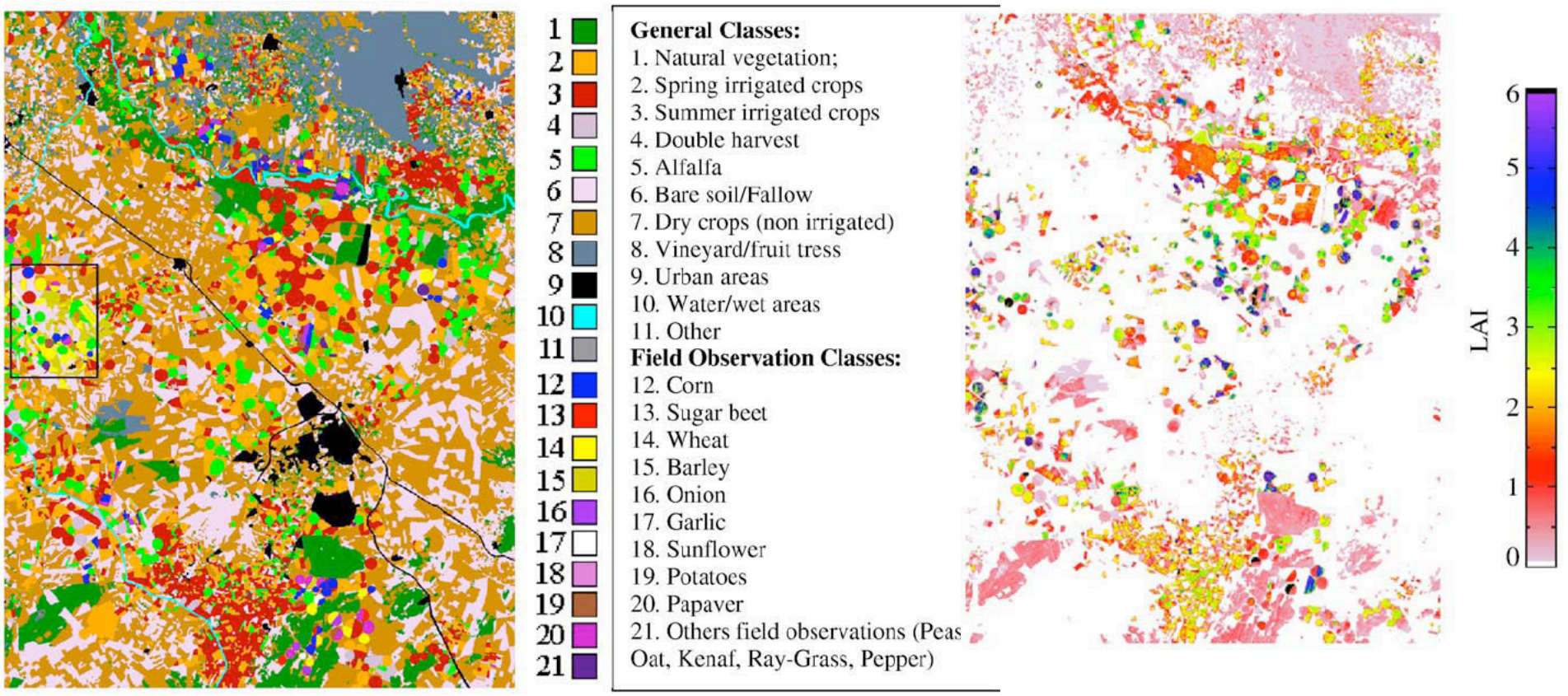

Improved derivation of biophysical parameters

Sentinel-2 will allow application of these methods in a systematic manner

FLEX mission concept for global carbon cycle

- Photosynthesis determines carbon uptake from the atmosphere by terrestrial vegetation.
- FLEX focuses on determination of fluxes rather than pools in the carbon cycle.

NBP: Net Biome Production

NEP: Net Ecosystem Production

NPP: Net Primary Production

GPP: Gross Primary Production

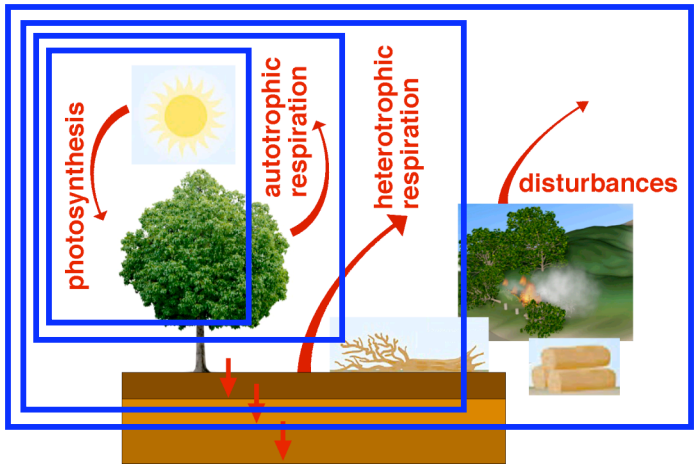

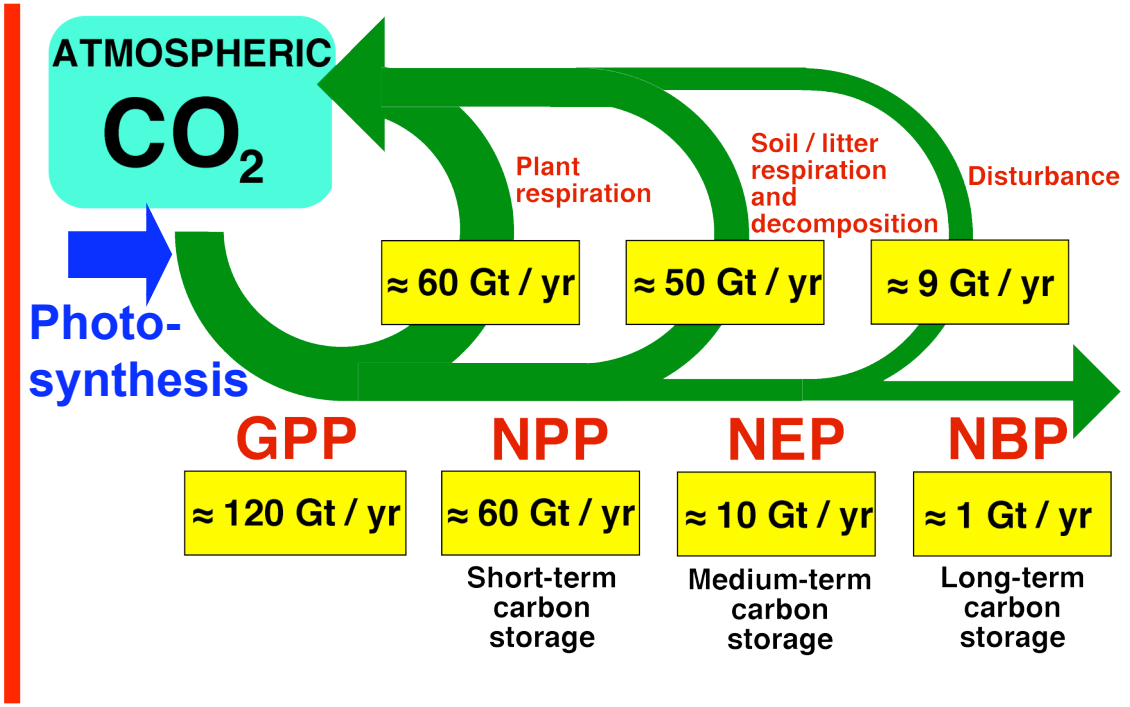

Chlorophyll Fluorescence

- Photosynthesis: absorbed light used for carbon assimilation
- Chlorophyll fluorescence: an indicator for the usage of absorbed light

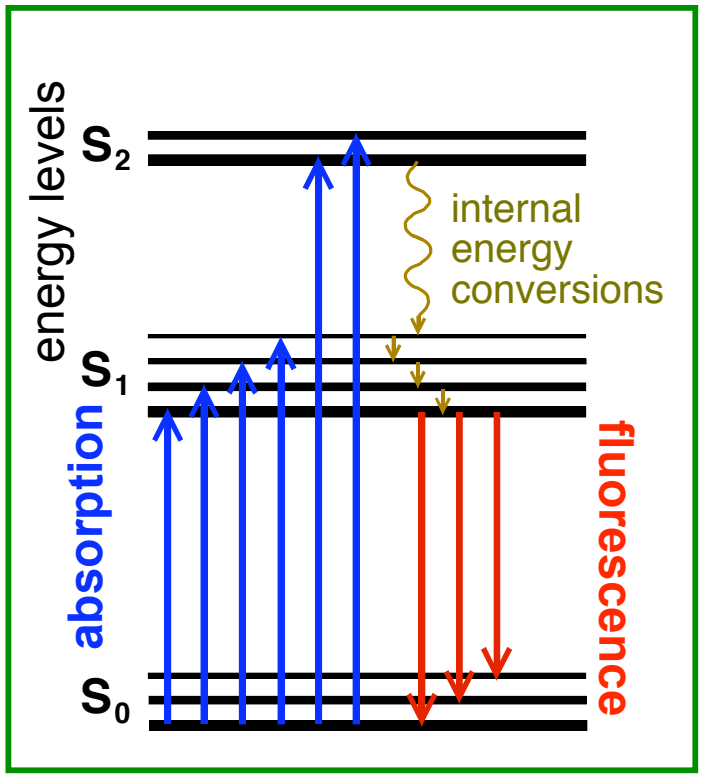

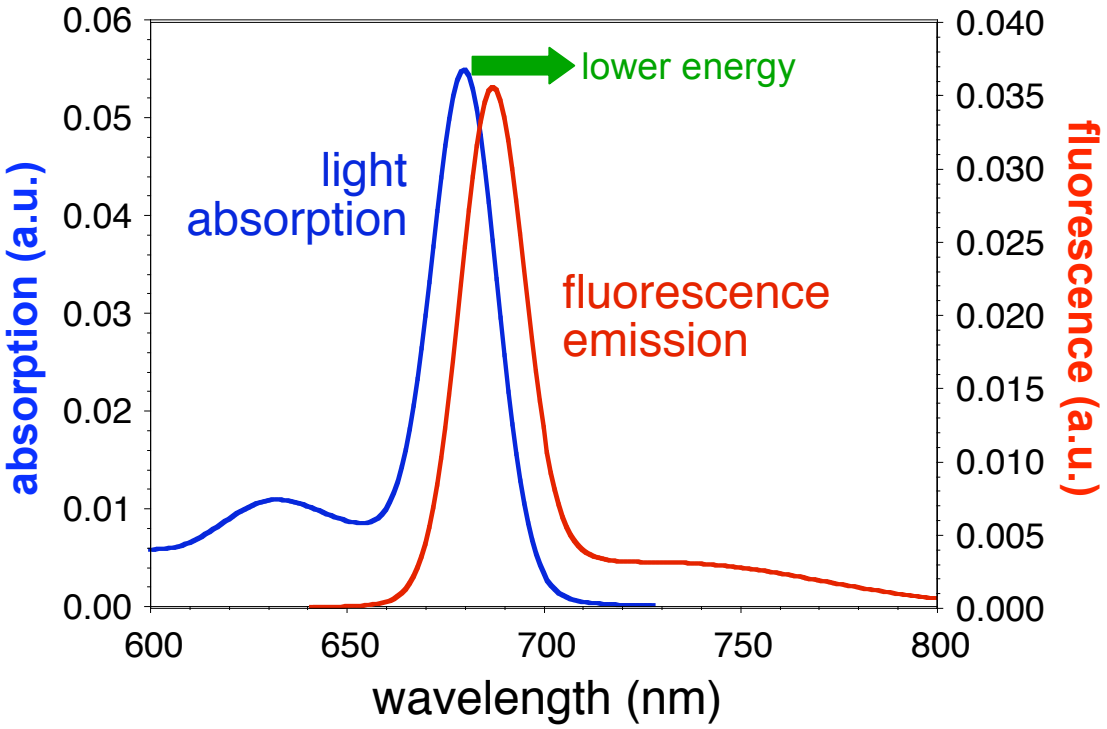

• Down-welling irradiance exhibits strong absorption lines with a certain contrast, while up-welling fluorescence emission exhibits a smooth spectral behaviour.

• Radiation observed by the satellite will exhibit the absorption lines with reduced contrast due to fluorescence dilution.

Retrieval concept

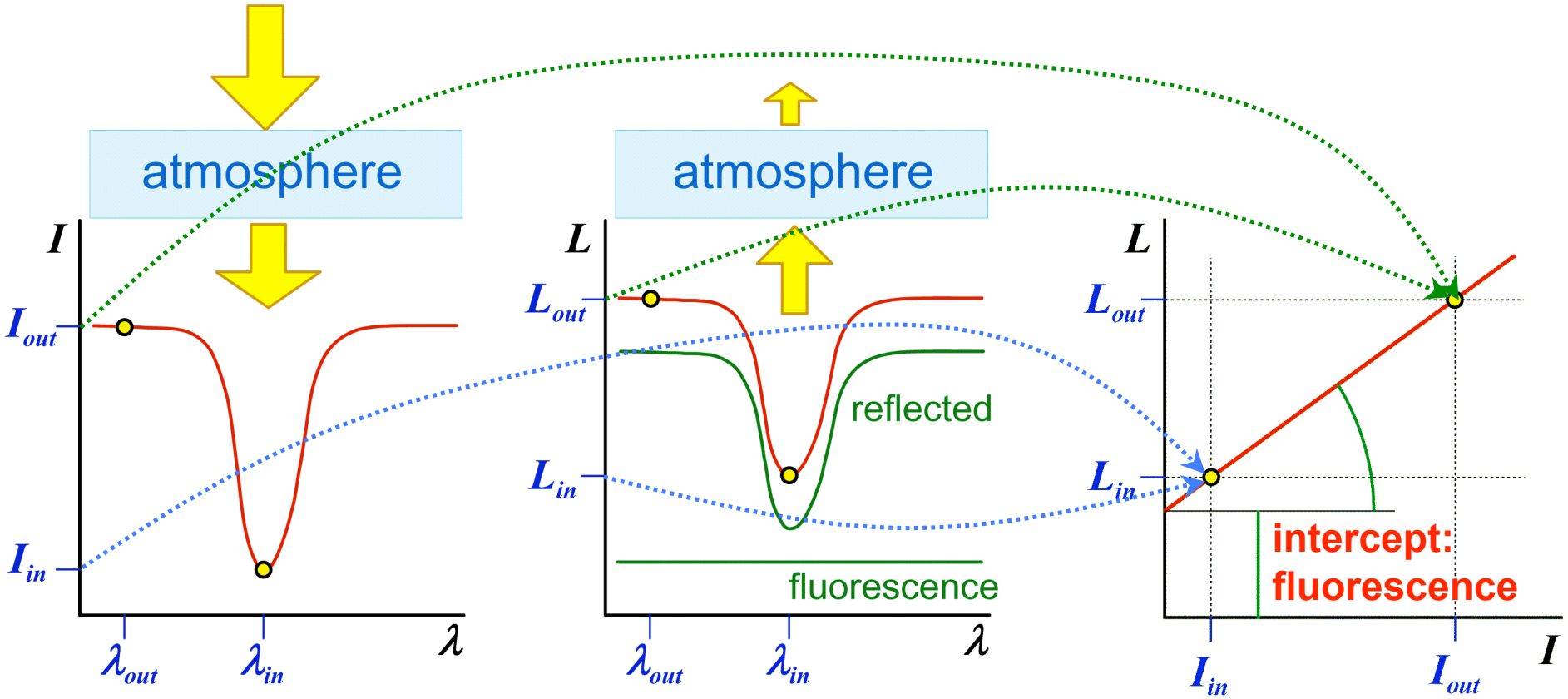

Fluorescence can be retrieved in the relative dark atmospheric absorption bands according to the Fraunhofer Line Depth (FLD) method.

FLEX imaging spectrometry

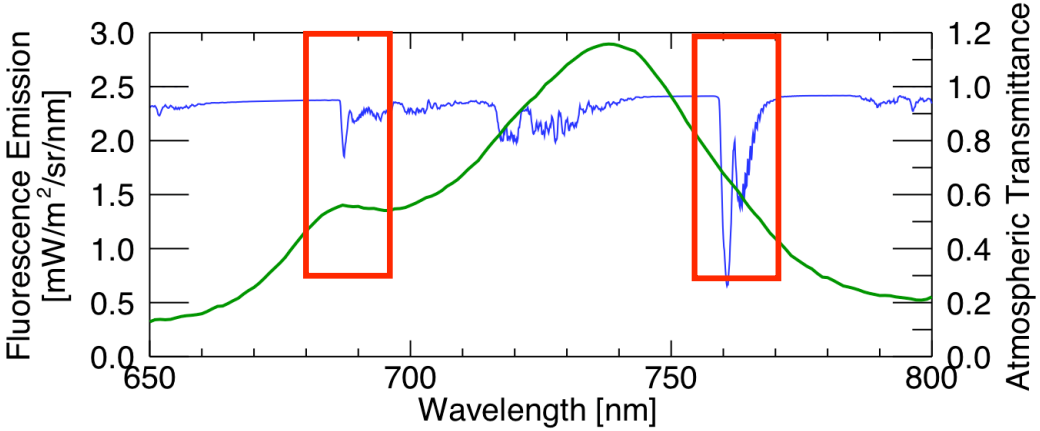

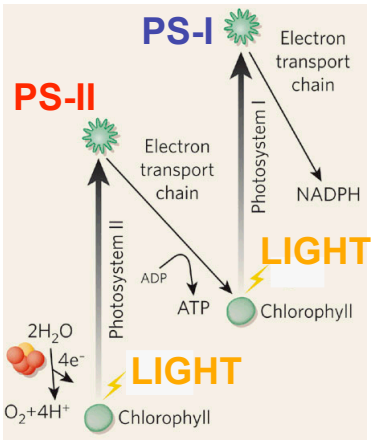

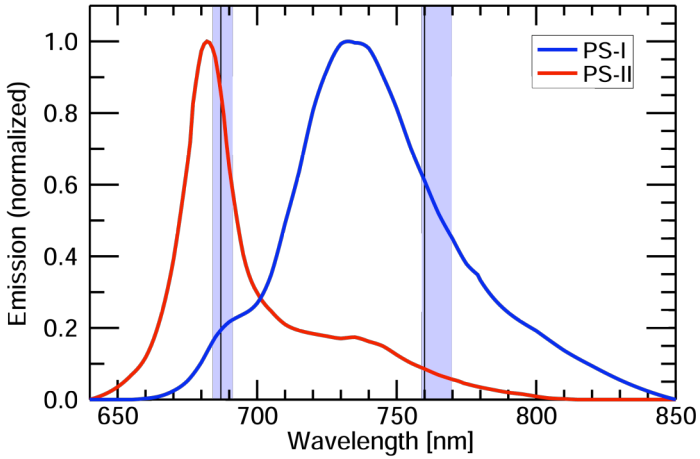

Primary measurements:

- high-performance spectro-radiometry
- Two oxygen absorption bands (O_2-A and O_2-B) are at the right spectral region for fluorescence retrieval
- 20-nm spectral intervals covering the O_2-A and O_2-B bands
- very high spectral resolution (~ 0.1 nm) needed
- Several supporting near-simultaneous measurements needed

Pushbroom Imaging Spectrometer: Concept and Options (1/2)

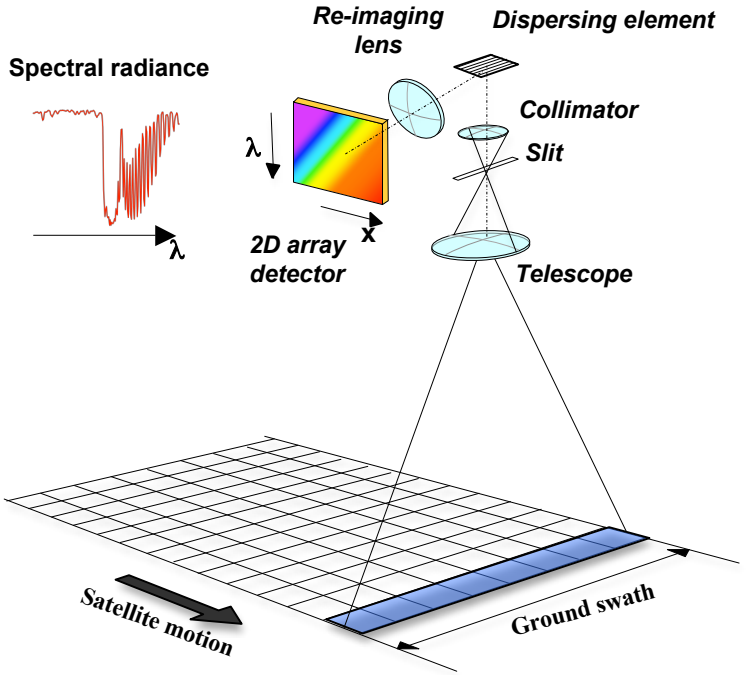

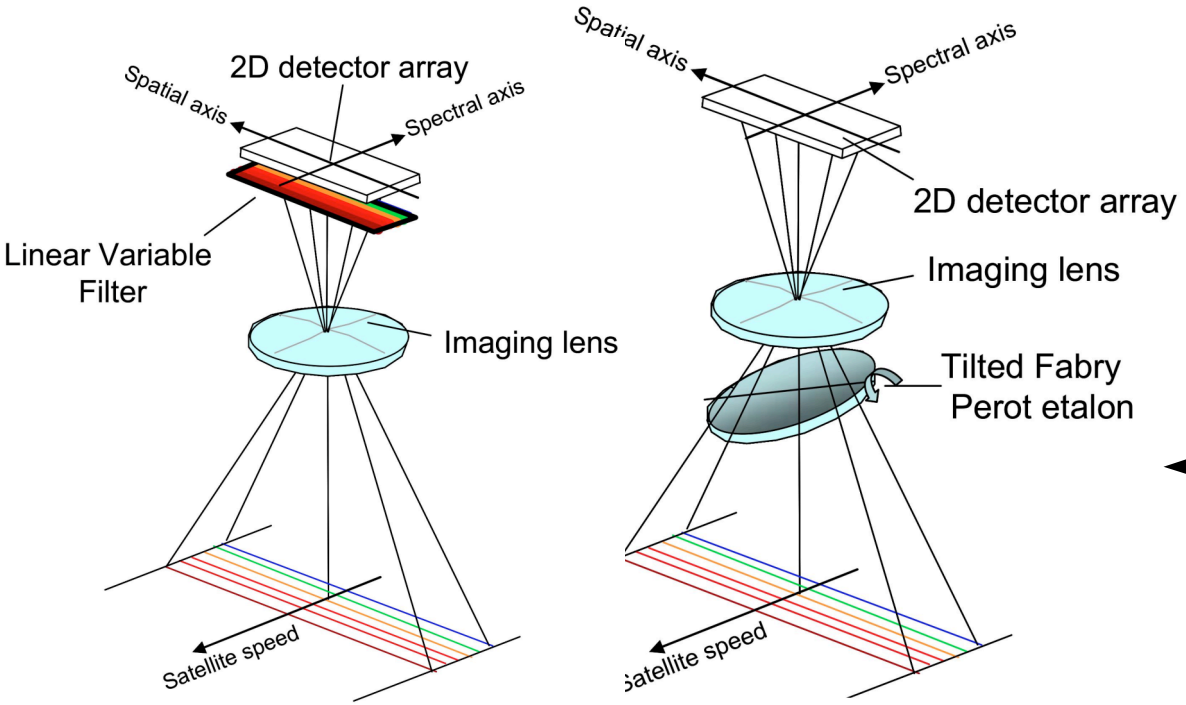

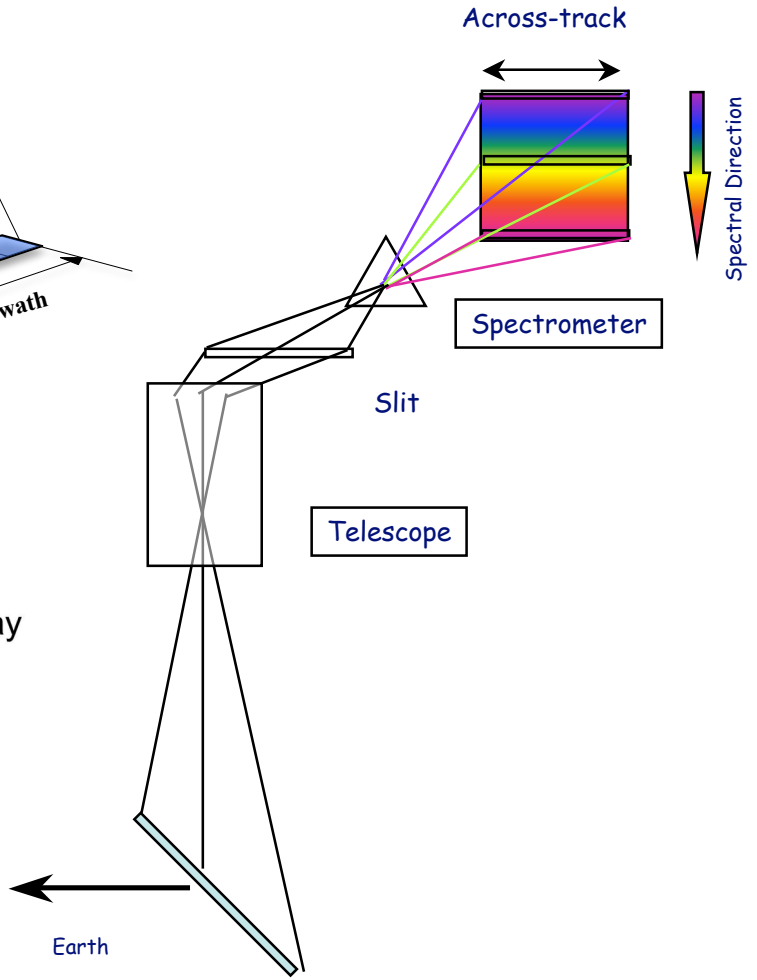

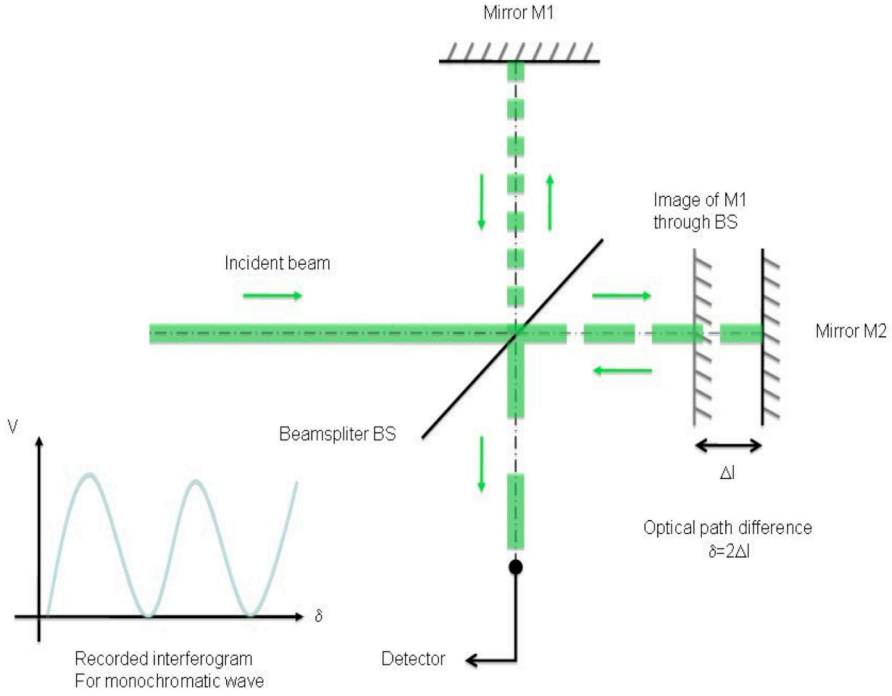

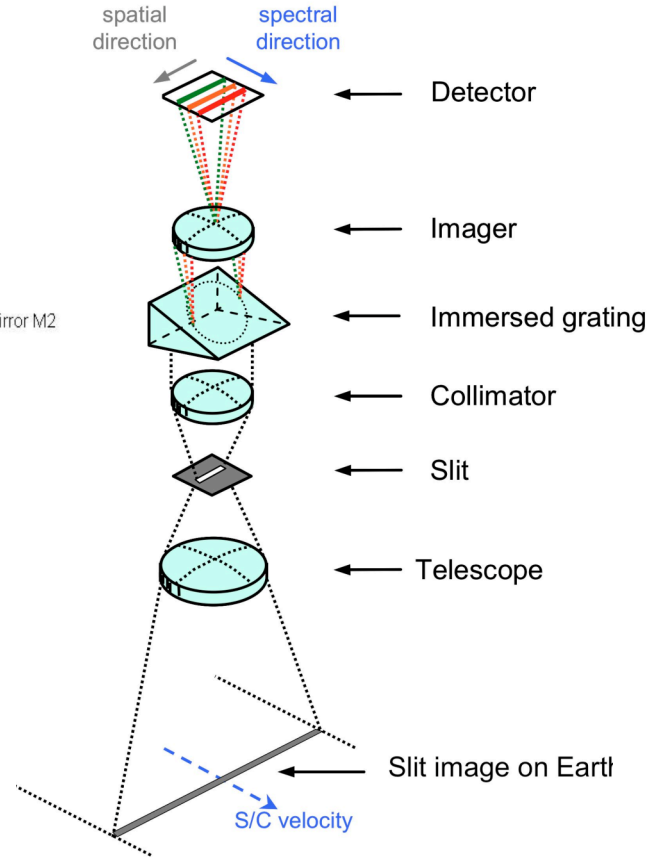

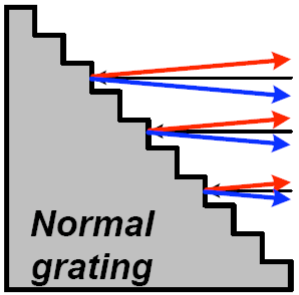

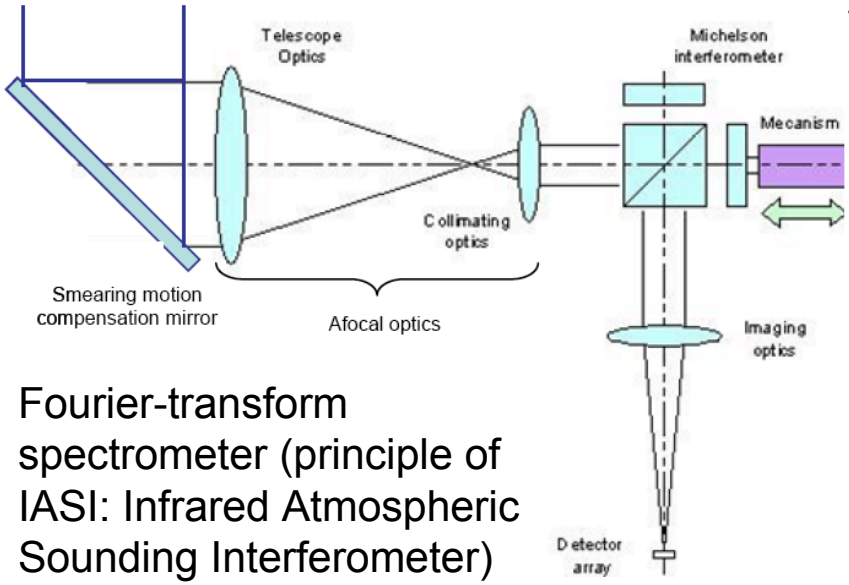

Fourier-transform spectrometer (principle of IASI: Infrared Atmospheric Sounding Interferometer)